

**NRC Report for NOTRUMP Version 38.0 Changes
(Non-Proprietary)**

**R. L. Fittante
A. F. Gagnon
J. J. Hartz
J. Iyengar
W. L. Brown**

June 2000

©2000 Westinghouse Electric Company LLC

Acknowledgements

The following people are acknowledged for their contributions to the generation of this document and the supporting documentation.

J. A. Gresham
T. R. Jurgovan
S. E. Saunders
C. M. Sydorko
R. A. Osterrieder

WESTINGHOUSE ELECTRIC COMPANY LLC

- 1.0 Introduction 1
 - 1.1 Background Information 1
- 2.0 Documentation of NOTRUMP Model Enhancements 4
 - 2.1 Documentation of Bubble Rise Models 4
 - 2.1.1 Derivation of NOTRUMP Evaluation Model Bubble Rise Expression 4
 - 2.1.2 Explicit Bubble Rise Treatment 6
 - 2.1.3 Implicit Bubble Rise Treatment 7
 - 2.2 Documentation of Droplet Fall Models 8
 - 2.2.1 Derivation of NOTRUMP Evaluation Model Droplet Fall Expression 8
 - 2.2.2 Explicit Droplet Fall Treatment 10
 - 2.2.3 Implicit Droplet Fall Treatment 11
 - 2.3 Documentation of Fluid Node Gravitational Head Models 13
 - 2.3.1 Implicit Treatment of Fluid Node Gravitational Head 13
 - 2.4 Documentation of Metal Node Models 17
 - 2.4.1 Implicit versus Explicit Treatment of Interior Metal Nodes 17
 - 2.4.2 NOTRUMP Explicit Formulation 18
 - 2.4.3 NOTRUMP Semi-Implicit Formulation 18
 - 2.5 Documentation of Region Depletion Models 20
 - 2.5.1 Original Region Depletion Model 20
 - 2.5.2 Improved Region Depletion Model (Mixture Level Overshoot) 22
 - 2.5.2.1 Mixture Level Overshoot Logic for Draining Situation 23
 - 2.5.2.2 Mixture Level Overshoot Logic for Filling Situation 26
 - 2.6 References 27
- 3.0 Clarification of Westinghouse Loop Seal Restriction Modeling Methodology 28
 - 3.1 Background Information on Westinghouse Loop Seal Restriction Model 28
 - 3.1.1 WCAP-10054-P-A (NRC Approval 1985) 28
 - 3.1.2 WCAP-11145-P-A (NRC Approval 1986) 30
 - 3.2 Westinghouse Methodology 30
 - 3.3 References 31
- 4.0 Enhanced Model Validation 32
 - 4.1 Separate Effects Validation 32
 - 4.1.1 Validation of Implicit Bubble Rise Model 32
 - 4.1.1.1 Bubble Rise Model Test Case Description 32
 - 4.1.1.2 Comparison of Test Results with Expected Results 33
 - 4.1.1.2.1 Case 1 - Explicit Bubble Rise Model With 0.25 Maximum Time Step Size 33

WESTINGHOUSE ELECTRIC COMPANY LLC

- 4.1.1.2.2 Case 2 - Fully Implicit Model With 0.25 Maximum Time Step Size34
- 4.1.1.2.3 Case 3 - Explicit Bubble Rise Model with 0.1 Time Step Size35
- 4.1.1.2.4 Case 4 - Fully Implicit Model with 0.1 Time Step Size35
- 4.1.1.3 Explicit Formulation Sensitivity Studies35
 - 4.1.1.3.1 Explicit Bubble Rise Model with Constant Dt=0.25 With The Restriction Disabled36
 - 4.1.1.3.2 Explicit Bubble Rise Model with Constant Dt=0.1 With The Restriction Disabled36
 - 4.1.1.4 Bubble Rise Model Simulation Conclusion37
- 4.1.2 Validation of Implicit Droplet Fall Model47
 - 4.1.2.1 Droplet Fall Model Test Case Description47
 - 4.1.2.2 Comparison of Test Results with Expected Results48
 - 4.1.2.2.1 Case 1 - Fully Implicit Model With 0.25 Maximum Time Step Size48
 - 4.1.2.2.2 Case 2 - Explicit Droplet Fall Model With 0.25 Maximum Time Step Size49
 - 4.1.2.2.3 Case 3 - Fully Implicit Model With 0.01 Maximum Time Step Size49
 - 4.1.2.2.4 Case 4 - Explicit Droplet Fall Model With 0.01 Maximum Time Step Size50
 - 4.1.2.3 Explicit Formulation Sensitivity Studies50
 - 4.1.2.3.1 Case 1 - Explicit Droplet Fall Model With 0.25 Time Step With The Restriction Disabled50
 - 4.1.2.3.2 Case 2 - Explicit Droplet Fall Model With 0.01 Time Step With The Restriction Disabled51
 - 4.1.2.4 Droplet Fall Model Simulation Conclusions51
- 4.1.3 Validation of Implicit Fluid Node Gravitational Head Model65
 - 4.1.3.1 Description of Test Cases65
 - 4.1.3.2 Comparison of Test Results with Expected Results67
 - 4.1.3.3 Implicit Fluid Node Gravitational Head Model Conclusions69
- 4.1.4 Validation of Semi-implicit Metal Node Model95
 - 4.1.4.1 NOTRUMP Simulation - Metal Node Model Description95
 - 4.1.4.1.1 Test Cases96
 - 4.1.4.2 Comparison of Test Results with Expected Results97
 - 4.1.4.2.1 Explicit vs. Semi-implicit Metal Node Model with Standard EM Time Step Size97
 - 4.1.4.2.2 Explicit vs. Semi-implicit Metal Node Model with Reduced Time Step Size98

WESTINGHOUSE ELECTRIC COMPANY LLC

4.1.4.3 Additional Discussion98

4.1.4.4 Semi-Implicit Metal Node Model Conclusions99

4.1.5 Validation of Improved Region Depletion Model 116

4.1.5.1 Description of Test Cases 116

4.1.5.2 Comparison of Test Results with Expected Results 117

4.1.5.3 Improved Region Depletion Model Conclusions 118

4.2 Integral Effects Validation 122

4.2.1 Sample Plant - Small Break LOCA Simulation122

4.2.1.1 Cases Analyzed122

4.2.1.2 NOTRUMP Simulation122

4.2.1.3 Discussion of Results123

4.2.1.3.1 6-inch Cold Leg Break, AFW=200 gpm123

4.2.1.3.2 3-inch Cold Leg Break, AFW=0 gpm124

4.2.1.4 Conclusion124

4.3 References132

1.0 Introduction

The purpose of this document is to inform the USNRC of the changes being made to the NOTRUMP Evaluation Model (EM) beginning with NOTRUMP Version 38.0. The changes being implemented are a direct result of errors/inconsistencies in the NOTRUMP EM which needed to be addressed. As a result, several features of the AP600 NOTRUMP EM are being introduced into the standard NOTRUMP EM to address these deficiencies. A summary of the models being introduced is as follows:

1. Implicit Bubble Rise Model Formulation
2. Implicit Droplet Fall Model Formulation
3. Implicit Fluid Node Gravitational Head Formulation
4. Semi-Implicit Metal Node Formulation
5. Improved Region Depletion Model Formulation ("Mixture Level Overshoot")

The enclosed documentation presents details on the model derivations as well as details regarding separate effect and integral effect model validation cases performed. The 10 CFR 50.46 reporting information regarding the NOTRUMP Version 38.0 code is being compiled and will be sent via separate correspondence.

In addition to the changes being implemented, clarification of the Westinghouse methodology concerning the application of and subsequent removal of the loop seal restriction model is being provided as well.

1.1 Background Information

The NOTRUMP small break LOCA EM contains a mixture level tracking model which is utilized when fluid nodes are grouped together into fluid node stacks. These stacks are utilized to track a single mixture level within the defined fluid node stacks. During the review of several plant analysis results, it was discovered that the NOTRUMP code could predict non-physical mixture level hangs to occur at fluid node boundaries in a stack of fluid nodes. When this occurs, the local mass and energy of a fluid node can be perturbed by flows being reset from the matrix solution value resulting from the mixture level hang. As a result of this observation, an internal Non-conformance Report (NR) was opened while this error was investigated.

In general, the occurrence of mixture level hangs, while not desirable, is generally conservative since it can result in the restriction of flow in the affected fluid node/flow link depending on the location of the mixture level hang. Should the level hang occur downstream of the core fluid nodes, any restriction to flow could result in a conservative core level depression since it acts as a secondary loop seal restriction. Figure 1-1 represents the NOTRUMP EM noding diagram with fluid nodes 3 through 6 representing the core fluid node region of the model. If the level hang occurs in the core node stack, a

WESTINGHOUSE ELECTRIC COMPANY LLC

non-conservative result could be obtained depending on the direction of the level movement. Should the level hang occur during the core draining/uncovery process, it would result in a predicted mixture level above what would be expected and a non-conservative Peak Cladding Temperature (PCT) would be calculated. If the level hang were to occur during the core refill process, the core uncovery period would be extended beyond what would be expected and a conservative PCT would be calculated. All plant analyses performed by Westinghouse were reviewed for non-conservative core mixture level hangs. As result of this investigation all Analysis Of Record (AOR) grade analyses were found to be in compliance.

To improve the level tracking behavior, several models developed during the AP600 program were introduced/validated during the error investigation phase. It was determined that the implementation of these models significantly improved the mixture level response over that observed during the initial investigation phase.

In addition, the Westinghouse methodology regarding the loop seal restriction model application/removal is being clarified in this document to address concerns raised by several utilities with respect to this issue. The concern stemmed from the fact that the Westinghouse analysts are given the flexibility to remove the artificial loop seal restriction for certain break sizes under certain conditions. The utilities felt that the documentation was not sufficiently clear as to the Westinghouse methodology involving the removal of the loop seal restriction model and to the understanding which the NRC may have had regarding this issue. The documentation included herein is intended to clarify the Westinghouse position on this matter and resolve the utility concerns.

a,c

Figure 1-1 NOTRUMP Evaluation Model Noding Diagram For Westinghouse PWRs

2.0 Documentation of NOTRUMP Model Enhancements

This section documents the details of the model enhancements that are being made to the new NOTRUMP Evaluation Model (EM) beginning with NOTRUMP Version 38.0, which are:

1. Implicit Bubble Rise Model.
2. Implicit Droplet Fall Model.
3. Implicit Fluid Node Gravitational Head Model.
4. Semi-Implicit Metal Node Model.
5. Improved Region Depletion Model (Mixture Level Overshoot).

2.1 Documentation of Bubble Rise Models

The bubble rise model accounts for the physical separation of the gas (or vapor) phase from the two-phase mixture. The bubble rise model in NOTRUMP is used to calculate the steam bubble escape rate from the lower (i.e., mixture) region of a stratified interior fluid node.

2.1.1 Derivation of NOTRUMP Evaluation Model Bubble Rise Expression

The bubble rise mass flow rate is expressed in Appendix H of Reference 1 as the net gas phase mass flow rate passing through the interface between the mixture and vapor regions of a fluid node. This net gas phase mass flow rate can be obtained from the relative velocity of liquid and vapor phases across the interface, along with the density and interfacial area associated with the gas phase. The resulting expression is given by:

$$W_{BR} = (\rho_g \cdot A_g)_M \cdot \langle\langle V_{relative} \rangle\rangle$$

where subscript M refers to the interface between the upper (i.e., vapor) region and lower (i.e., mixture) region. Recasting the interfacial gas area (A_g) in terms of total interfacial area (i.e., $A_g = (\alpha \cdot A)$) and expanding the relative velocity in terms of averaged vapor and liquid velocity components results in the following:

$$W_{BR} = (\alpha \cdot \rho_g \cdot A)_M (\langle\langle V_g \rangle\rangle - \langle\langle V_f \rangle\rangle)$$

Since the regions within each fluid node are treated as homogeneous in NOTRUMP, the above equation can be rewritten as:

$$W_{BR} = \alpha_M \cdot \rho_g \cdot A_{MV} (\langle\langle V_g \rangle\rangle - \langle\langle V_f \rangle\rangle)$$

where A_{MV} is the mixture-vapor region interfacial area. From Appendix H of Reference 1, the average gas phase velocity at the interface is expressed as:

$$\langle\langle V_g \rangle\rangle = C_0 \langle j \rangle_M + \langle\langle V_{gj} \rangle\rangle$$

where the mixture velocity $\langle j \rangle_M$ (i.e., volumetric flux) is defined as:

$$\langle j \rangle_M = \alpha_M \langle\langle V_g \rangle\rangle + (1 - \alpha_M) \langle\langle V_f \rangle\rangle$$

where $\langle \rangle$ indicates a quantity averaged over cross-sectional area and $\langle\langle \rangle\rangle$ indicates a weighted mean quantity.

Combining the previous two equations, the following expression is obtained for the relative velocity that can be used in the bubble rise mass flow rate equation:

$$\langle\langle V_g \rangle\rangle - \langle\langle V_f \rangle\rangle = \frac{\langle\langle V_{gj} \rangle\rangle + \langle\langle V_f \rangle\rangle (C_0 - 1)}{1 - \alpha_M \cdot C_0}$$

In Reference 1 (Appendix H), it is [

] ^{a,c} leads to the following form, which is consistent with Appendix H of Reference 1:

$$[\quad \quad \quad]^{a,c}$$

Using the above expression for the relative velocity in the bubble rise mass flow rate equation results in the following form [

$$[\quad \quad \quad]^{a,c}$$

where in the above expression for bubble rise mass flow rate, the correlations for $\langle\langle V_{gj} \rangle\rangle$ and C_0 are provided in Appendix G of Reference 1.

$$[\quad \quad \quad]^{a,c}$$

$$[\quad \quad \quad]^{a,c}$$

WESTINGHOUSE ELECTRIC COMPANY LLC

This is the NOTRUMP EM bubble rise expression, as contained in Appendix H of Reference 1, including several modifications described in Section 2.9 of Reference 2, as previously reported.

The explicit and implicit treatments of the bubble rise mass flow rate expression are discussed in Sections 2.1.2 and 2.1.3, respectively.

2.1.2 Explicit Bubble Rise Treatment

The previous NOTRUMP EM treats the bubble rise mass flow rate expression explicitly. In the explicit treatment, the code calculates each node's bubble rise mass flow rate at the beginning of each time step from the final expression in Section 2.1.1, using the known properties of the node. The code then holds this bubble rise mass flow rate constant throughout the time step. This explicit implementation of bubble rise can lead to an instability if the model convects more vapor mass out of a mixture region during a time step than exists in that region. This is a violation of the material Courant limit. The bubble rise material Courant limit becomes prohibitively restrictive as mixture levels approach and cross node boundaries. A traditional approach to help alleviate this problem would be the incorporation of time step size controller logic, which would limit the time step size to prevent violation of the material Courant limit caused by the explicit bubble rise treatment. However, this approach is not employed in NOTRUMP. Instead, the explicit bubble rise treatment in NOTRUMP applies the following restriction in an attempt to prevent the bubble rise from depleting the current vapor mass in the mixture region of the node in a given time step:

$$W_{BR(N)} = \min \left[W_{BR(N)}, \frac{XMFN(N) \cdot TMMFN(N)}{DELTEXP} \right]$$

where:

- XMFN(N) = quality in mixture region of fluid node N at the beginning of the time step
- TMMFN(N) = total mass in mixture region of fluid node N at the beginning of the time step
- DELTEXP = $\min[\Delta t \cdot FRACEXP \cdot FMARGIN, DELTMAX]$
- Δt = current time step
- FRACEXP = user input maximum factor by which the time step can be increased
- FMARGIN = 1.01
- DELTMAX = user input maximum time step size

The intent of this restriction is to prevent the material Courant limit from being violated by limiting the explicit bubble rise mass flow rate, instead of limiting the time step size, as the mixture region is depleted. Although it would appear that applying this restriction would be beneficial, validation described in Section 4.1.1 indicates that this restriction is not performing as intended, and in fact does not prevent the material Courant limit from being violated. This is the case because the restriction uses the vapor mass that exists in the mixture region at the beginning of the time step in its limit expression, instead of using either a predicted average value that applies over the time step, or a predicted end-of-time step value. Both predicted values would be smaller than the vapor mass value at the beginning of the time step during mixture region depletion. As such, the restriction adversely affects the

code's solution for the node's mixture region total energy central unknown variable, and thereafter the mixture region calculated thermodynamic properties, as the mixture region is depleted. Instead of the bubble rise mass flow rate exhibiting the traditional instabilities and oscillatory behavior which would accompany mixture region depletion had such a restriction not been applied, the problem manifests itself in the abnormal solution of the mixture region energy with the restriction applied. To circumvent these problems, an option was provided to treat the bubble rise model implicitly in NOTRUMP, as described in Section 2.1.3.

2.1.3 Implicit Bubble Rise Treatment

The new NOTRUMP EM treats the bubble rise mass flow rate expression implicitly. The implicit bubble rise treatment estimates the change in the bubble rise mass flow rate corresponding to the change in the fluid node's central variables during each time step. In the implicit treatment, the bubble rise mass flow rate in a fluid node is linearized as follows:

$$W_{BR}(t + \Delta t) = W_{BR}(t) + \frac{\partial W_{BR}}{\partial U_M} \cdot \Delta U_M + \frac{\partial W_{BR}}{\partial M_M} \cdot \Delta M_M + \frac{\partial W_{BR}}{\partial U_V} \cdot \Delta U_V + \frac{\partial W_{BR}}{\partial M_V} \cdot \Delta M_V$$

where:

W_{BR}	= bubble rise mass flow rate
t	= time at beginning of time step
Δt	= time step size
U_M, U_V	= mixture and vapor region total internal energy
$\Delta U_M, \Delta U_V$	= change in mixture and vapor region total internal energy during time step
M_M, M_V	= mixture and vapor region mass
$\Delta M_M, \Delta M_V$	= change in mixture and vapor region mass during time step

The above expression for $W_{BR}(t+\Delta t)$ is applied accordingly in the fluid node's net mass and energy exchange rates between the mixture and vapor regions, and thus affects the central matrix solution (i.e., $W_{BR}(t+\Delta t)$ in the implicit formulation replaces $W_{BR}(t)$ in the explicit formulation). In the above, $W_{BR}(t)$ is calculated at the beginning of each time step from the final expression in Section 2.1.1, analogous to what is done in the explicit treatment. In addition, the following partial derivatives of the bubble rise mass flow rate are calculated (at the beginning of the time step) in the implicit formulation by differentiating the W_{BR} expression with respect to the nodal central variables:

$$\frac{\partial W_{BR}}{\partial U_M}, \frac{\partial W_{BR}}{\partial M_M}, \frac{\partial W_{BR}}{\partial U_V}, \frac{\partial W_{BR}}{\partial M_V}$$

Note that when the bubble rise is treated explicitly, these derivatives are not needed and are set to zero.

2.2 Documentation of Droplet Fall Models

The droplet fall model accounts for the physical separation of the liquid phase from a vapor region. The droplet fall model contained in NOTRUMP is used to calculate the liquid droplet fallback rate from the upper (i.e., vapor) region to the lower (i.e., mixture) region of a stratified interior fluid node.

2.2.1 Derivation of NOTRUMP Evaluation Model Droplet Fall Expression

The droplet fall mass flow rate can be expressed as the net liquid phase mass flow rate passing across the interface between the mixture and vapor regions of a fluid node:

$$W_{DF} = ((1 - \alpha) \rho_f A)_V (\langle\langle V_f \rangle\rangle - \langle\langle V_g \rangle\rangle)$$

where: subscript V refers to the interface between the upper (i.e., vapor) region and lower (i.e., mixture) region.

Since the regions within each fluid node are treated as homogeneous in NOTRUMP, the above equation can be rewritten as:

$$W_{DF} = (1 - \alpha_V) \rho_f A_{MV} (\langle\langle V_f \rangle\rangle - \langle\langle V_g \rangle\rangle)$$

where A_{MV} is the mixture-vapor region interfacial area. The liquid phase velocity at the interface can be expressed as follows (analogous to Equation G-17 of Reference 1):

$$\langle\langle V_f \rangle\rangle = C_0 \langle j \rangle_V + \langle\langle V_{ff} \rangle\rangle$$

where the mixture velocity $\langle j \rangle_V$ (i.e., volumetric flux) is defined as:

$$\langle j \rangle_V = \alpha_V \langle\langle V_g \rangle\rangle + (1 - \alpha_V) \langle\langle V_f \rangle\rangle$$

Combining the previous two equations, the following expression for relative velocity is obtained:

$$\langle\langle V_f \rangle\rangle - \langle\langle V_g \rangle\rangle = \frac{\langle\langle V_{ff} \rangle\rangle + \langle\langle V_g \rangle\rangle (C_0 - 1)}{(1 - (1 - \alpha_V) C_0)}$$

[]^{a,c}

[]^{a,c}

WESTINGHOUSE ELECTRIC COMPANY LLC

Using the above expression for the relative velocity in the droplet fall mass flow rate equation results in the following form:

$$\left[\dots \right]^{a,c}$$

where in the above expression for droplet mass flow rate, the correlations for $\langle\langle V_f \rangle\rangle$ and C_0 are given by the following:

$$\left[\dots \right]^{a,c}$$

Note that the same result can be obtained from the bubble rise formulation if one makes the following substitutions in the bubble rise mass flow rate expression and obtains an appropriate relation for the relative velocity $\langle\langle V_g \rangle\rangle \rightarrow \langle\langle V_f \rangle\rangle$:

$$W_{BR} \Rightarrow W_{DF}$$

$$\alpha_M \Rightarrow (1 - \alpha_V)$$

$$\rho_g \Rightarrow \rho_f$$

From this exercise, an effective $\langle\langle V_{gj} \rangle\rangle$ can be obtained such that:

$$\left[\dots \right]^{a,c}$$

Substituting the following expressions

$$\left[\dots \right]^{a,c} \text{ and } \left[\dots \right]^{a,c}$$

one obtains:

$$\left[\dots \right]^{a,c}$$

Note that this is similar to Equation G-58 of Reference 1 for $n=1$ in general droplet flow.

Returning to the above droplet fall mass flow rate expression, substitution of the expressions

$$\left[\dots \right]^{a,c}$$

$$\left[\dots \right]^{a,c}$$

$$\left[\dots \right]^{a,c}$$

results in the following final form of the droplet fall mass flow rate in the NOTRUMP Evaluation Model (EM):

$$\left[\dots \right]^{a,c}$$

The explicit and implicit treatments of the droplet fall mass flow rate expression are discussed in Sections 2.2.2 and 2.2.3, respectively.

2.2.2 Explicit Droplet Fall Treatment

The previous NOTRUMP EM treats the droplet fall mass flow rate expression explicitly. In the explicit treatment, the code calculates each node's droplet fall mass flow rate at the beginning of each time step from the final expression in Section 2.2.1, using the known properties of the node. The code then holds this droplet fall mass flow rate constant throughout the time step. This explicit implementation of droplet fall can lead to an instability if the model convects more liquid mass out of a vapor region during a time step than exists in that region. This is a violation of the material Courant limit. The droplet fall material Courant limit becomes prohibitively restrictive as mixture levels approach and cross node boundaries. A traditional approach to help alleviate this problem would be the incorporation of time step size controller logic, which would limit the time step size to prevent violation of the material Courant limit caused by the explicit droplet fall treatment. However, this approach is not employed in NOTRUMP. Instead, the explicit droplet fall treatment in NOTRUMP applies the following restriction in an attempt to prevent the droplet fall from depleting the current liquid mass in the vapor region of the node in a given time step:

$$W_{DF(N)} = \min \left[W_{DF(N)}, \frac{(1 - X_{VFN}(N)) \cdot T_{MVFN}(N)}{DELTEXP} \right]$$

where:

- X_{VFN}(N) = quality in vapor region of fluid node N at the beginning of the time step
- T_{MVFN}(N) = total mass in vapor region of fluid node N at the beginning of the time step
- DELTEXP = min[Δt·FRACEXP·FMARGIN, DELTMAX]
- Δt = current time step size
- FRACEXP = user input maximum factor by which the time step size can be increased

FMARGIN = 1.01
 DELTMAX = user input maximum time step size

The intent of this restriction is to prevent the material Courant limit from being violated by limiting the explicit droplet fall mass flow rate, instead of limiting the time step size, as the vapor region is depleted. Although it would appear that applying this restriction would be beneficial, validation described in Section 4.1.2 indicates that this restriction is not performing as intended, and in fact does not prevent the material Courant limit from being violated. This is the case because the restriction uses the liquid mass that exists in the vapor region at the beginning of the time step in its limit expression, instead of using either a predicted average value that applies over the time step, or a predicted end-of-time step value. Both predicted values would be smaller than the liquid mass value at the beginning of the time step during vapor region depletion. As such, the restriction adversely affects the code's solution for the node's vapor region total energy central unknown variable, and thereafter the vapor region calculated thermodynamic properties, as the vapor region is depleted. Instead of the droplet fall mass flow rate exhibiting the traditional instabilities and oscillatory behavior which would accompany vapor region depletion had such a restriction not been applied, the problem manifests itself in the abnormal solution of the vapor region energy with the restriction applied. To circumvent these problems, an option was provided to treat the droplet fall model implicitly in NOTRUMP, as described in Section 2.2.3.

2.2.3 Implicit Droplet Fall Treatment

The new NOTRUMP EM treats the droplet fall mass flow rate expression implicitly. The implicit droplet fall treatment estimates the change in the droplet fall mass flow rate corresponding to the change in the fluid node's central variables during each time step. In the implicit treatment, the droplet fall mass flow rate in a fluid node is linearized as follows:

$$W_{DF}(t + \Delta t) = W_{DF}(t) + \frac{\partial W_{DF}}{\partial U_M} \cdot \Delta U_M + \frac{\partial W_{DF}}{\partial M_M} \cdot \Delta M_M + \frac{\partial W_{DF}}{\partial U_V} \cdot \Delta U_V + \frac{\partial W_{DF}}{\partial M_V} \cdot \Delta M_V$$

where:

W_{DF} = droplet fall mass flow rate
 t = time at beginning of time step
 Δt = time step size
 U_M, U_V = mixture and vapor region total internal energy
 $\Delta U_M, \Delta U_V$ = change in mixture and vapor region total internal energy during time step
 M_M, M_V = mixture and vapor region mass
 $\Delta M_M, \Delta M_V$ = change in mixture and vapor region mass during time step

The above expression for $W_{DF}(t+\Delta t)$ is applied accordingly in the fluid node's net mass and energy exchange rates between the mixture and vapor regions, and thus affects the central matrix solution (i.e., $W_{DF}(t+\Delta t)$ in the implicit formulation replaces $W_{DF}(t)$ in the explicit formulation). In the above, $W_{DF}(t)$ is calculated at the beginning of each time step from the final expression in Section 2.2.1, analogous to what is done in the explicit treatment. In addition, the following partial derivatives of the droplet fall mass flow rate are calculated (at

WESTINGHOUSE ELECTRIC COMPANY LLC

the beginning of the time step) in the implicit formulation by differentiating the W_{DF} expression with respect to the nodal central variables:

$$\frac{\partial W_{DF}}{\partial U_M}, \frac{\partial W_{DF}}{\partial M_M}, \frac{\partial W_{DF}}{\partial U_V}, \frac{\partial W_{DF}}{\partial M_V}$$

Note that when the droplet fall is treated explicitly, these derivatives are not needed and are set to zero.

2.3 Documentation of Fluid Node Gravitational Head Models

The gravitational head in NOTRUMP is accounted for within both fluid nodes and flow links, as described in Section 5 of Reference 1. Within fluid nodes, the pressure calculated from the known state variables is assumed to apply to the top of the fluid node. Using this convention, the code calculates the pressure at the end of any flow link connected to a fluid node as the sum of the pressure at the top of the fluid node plus the gravitational head from the top of the fluid node to the center of the flow link-fluid node connection. Within flow links (either non-critical or critical), the code calculates a gravitational head term from the elevation difference between the upstream and downstream ends of the flow link, using the density of the fluid within the flow link. The formulation of the gravitational head terms is setup to conserve the total integrated force on the flow link cross-section by calculating an effective pressure that gives the same force when multiplied by the total area.

In the previous NOTRUMP Evaluation Model (EM), in the gravitational head model that is documented in Section 5 of Reference 1, both the fluid node and flow link contributions to the gravitational head were treated explicitly. When treated explicitly, the gravitational head is calculated at the beginning of each time step and then held constant throughout the time step. This implementation, however, can lead to flow instabilities when the density of the fluid within the fluid node or flow link changes rapidly. To circumvent this problem, an option was provided to treat the fluid node contribution to the gravitational head implicitly, as described in Section 2.3.1. Although the flow link contribution to the gravitational head is still treated explicitly, any adverse effects that it may have can typically be minimized or even eliminated entirely with input modeling modifications to the flow link-fluid node network connections (by minimizing the elevation difference between the upstream and downstream ends of each flow link).

2.3.1 Implicit Treatment of Fluid Node Gravitational Head

The new NOTRUMP EM treats the fluid node gravitational head model implicitly. The implicit treatment estimates the change in the gravitational head corresponding to the change in the fluid node's central variables during each time step, and applies to the upstream and downstream fluid nodes of non-critical flow links.

For non-critical flow links, the gravitational head terms in the $(P_u)_k$ and $(P_d)_k$ are the pressures at the center of the upstream and downstream ends, respectively, of flow link k . From Reference 1 (Equation 5-5), the pressure at the center of the upstream end of the flow link $(P_u)_k$ is expressed as:

$$\begin{aligned}
 (P_u)_k = \frac{1}{\pi R^2} \left\{ \left[[P(R)]_i + \frac{g}{144 g_c} \cdot \frac{R - (y_u)_k}{(v_v)_i} + \frac{g}{144 g_c} \cdot \frac{(y_u)_k}{(v_M)_i} \right] \cdot \int_{-R}^{(y_u)_k} dA(y) \right. \\
 - \left[\frac{g}{144 g_c} \cdot \frac{1}{(v_M)_i} \right] \cdot \int_{-R}^{(y_u)_k} y dA(y) + \left[[P(R)]_i + \frac{g}{144 g_c} \cdot \frac{R}{(v_v)_i} \right] \cdot \int_{(y_u)_k}^R dA(y) \\
 \left. - \left[\frac{g}{144 g_c} \cdot \frac{1}{(v_v)_i} \right] \cdot \int_{(y_u)_k}^R y dA(y) \right\}
 \end{aligned}$$

where subscript i refers to the fluid node at the upstream end of flow link k.

Recall that the pressure at the center of the downstream end of flow link k is analogous (refer to Equation 5-6 of Reference 1), and therefore will not be developed here.

From Equation 5-3 of Reference 1, $[P(R)]_i$ is the pressure at the top of the upstream end of flow link k (i.e., at the elevation of the center of the upstream end of the flow link plus the radius of the flow link, $(E_u)_k + R$), and is defined as follows:

$$[P(R)]_i = P_i + \frac{g}{144 g_c} \left[\frac{(E_{top})_i - \max[(E_{mix})_i, (E_u)_k + R]}{(v_v)_i} + \frac{\max[(E_{mix})_i, (E_u)_k + R] - [(E_u)_k + R]}{(v_M)_i} \right]$$

From Equation 5-7 of Reference 1:

$$(y_u)_k = \min\{\max[(E_{mix})_i - (E_u)_k, -R] + R\}$$

Using Equations O-5 and O-6 of Reference 1 and expanding the integrals in Equation 5-5 of Reference 1, $(P_u)_k$ can be expressed in the following form:

[

]a, c

WESTINGHOUSE ELECTRIC COMPANY LLC

At the limits of $(y_u)_k$, this expression for $(P_u)_k$ reduces to the following forms:

- At the upper limit of $(y_u)_k=R$:

$$[\quad]^{a,c}$$

Substituting in the expression for $[(P(R))_i]$ and recalling that the mixture elevation is at or above the top of the flow link when $(y_u)_k=R$ yields the following:

$$[\quad]^{a,c}$$

$$[\quad]^{a,c}$$

Substituting in the expression for $[P(R)]_i$ and recalling that the mixture elevation is at or below the bottom of the flow link when $(y_u)_k=-R$ yields the following:

$$[\quad]^{a,c}$$

The above expressions for $(P_u)_k$ may be generally written as:

$$(P_u)_k = P_i + GHV + GHM$$

where GHV and GHM are the fluid node gravitational head term contributions from the vapor and mixture regions, respectively, and are generally expressed as functions of the mixture elevation in the fluid node as follows:

$$GHV = \frac{GV((E_{mix})_i)}{(v_v)_i}$$

and

$$GHM = \frac{GM((E_{mix})_i)}{(v_M)_i}$$

In the implicit treatment of fluid node gravitational head, GHV and GHM are linearized as follows:

$$GHV(t + \Delta t) = GHV(t) + \frac{\partial GHV}{\partial X} \cdot \Delta X$$

and

$$GHM(t + \Delta t) = GHM(t) + \frac{\partial GHM}{\partial X} \cdot \Delta X$$

where X denotes each of the four fluid node central variables $((U_M)_i, (M_M)_i, (U_V)_i, \text{ and } (M_V)_i)$. The partial derivatives of GHV and GHM are given by the following (where the subscript i on the fluid node terms is dropped for brevity):

$$\frac{\partial(GHV)}{\partial X} = \frac{1}{v_V} \cdot \left[\frac{\partial(GV)}{\partial(E_{mix})} \cdot \frac{\partial(E_{mix})}{\partial V_M} \cdot \frac{\partial V_M}{\partial X} - GHV \cdot \frac{\partial v_V}{\partial X} \right]$$

and

$$\frac{\partial(GHM)}{\partial X} = \frac{1}{v_M} \cdot \left[\frac{\partial(GM)}{\partial(E_{mix})} \cdot \frac{\partial(E_{mix})}{\partial V_M} \cdot \frac{\partial V_M}{\partial X} - GHM \cdot \frac{\partial v_M}{\partial X} \right]$$

The above expressions for GHV(t+Δt) and GHM(t+Δt) are applied accordingly in the flow link's pressure drop terms, and thus affect the central matrix. Note that when the fluid node gravitational head is treated explicitly, these derivatives are not needed and are set to zero.

2.4 Documentation of Metal Node Models

There are two types of metal node models in NOTRUMP, interior metal nodes and boundary metal nodes.

An interior metal node is defined as a fixed control volume containing metal at thermodynamic equilibrium and having associated with it one conservation equation for total internal energy expressed in terms of metal node temperature. An interior metal node may be connected to fluid nodes via heat links. Heat links serve as paths for the flow of energy. The energy conservation equation for an interior metal node in NOTRUMP is expressed as Equation (2-31) of Reference 1.

A boundary metal node is defined as a control volume containing metal at a specified temperature T . As with interior metal nodes, a boundary metal node may be connected to fluid nodes via heat links. The metal temperature for boundary metal nodes is specified as a function of time as expressed in Equation (2-32) of Reference 1.

2.4.1 Implicit versus Explicit Treatment of Interior Metal Nodes

The treatment or meaning of implicit versus explicit interior metal nodes in Reference 1 is somewhat unclear. A fully implicit treatment of interior metal nodes is presented in Reference 1 (refer to Appendix E for details). A fully implicit treatment of interior metal node temperature associated with the energy equations can be seen in a central matrix equation (Equation E-5 of Reference 1), which would have the following form:

$$\begin{bmatrix}
 \underline{A}_{=WW} & \underline{A}_{=WU_M} & \underline{A}_{=WM_M} & \underline{A}_{=WU_V} & \underline{A}_{=WM_V} & \underline{0}_{=WT} \\
 \underline{A}_{=U_M W} & \underline{D}_{=U_M U_M} & \hat{\underline{D}}_{=U_M M_M} & \hat{\underline{D}}_{=U_M U_V} & \hat{\underline{D}}_{=U_M M_V} & \underline{A}_{=U_M T} \\
 \underline{A}_{=M_M W} & \hat{\underline{D}}_{=M_M U_M} & \underline{D}_{=M_M M_M} & \hat{\underline{D}}_{=M_M U_V} & \hat{\underline{D}}_{=M_M M_V} & \underline{0}_{=M_M T} \\
 \underline{A}_{=U_M W} & \hat{\underline{D}}_{=U_V U_M} & \hat{\underline{D}}_{=U_V M_M} & \underline{D}_{=U_V U_V} & \hat{\underline{D}}_{=U_V M_V} & \underline{A}_{=U_V T} \\
 \underline{A}_{=M_V W} & \hat{\underline{D}}_{=M_V U_M} & \hat{\underline{D}}_{=M_V M_M} & \hat{\underline{D}}_{=M_V U_V} & \underline{D}_{=M_V M_V} & \underline{0}_{=M_V T} \\
 \underline{0}_{=TW} & \underline{A}_{=TU_M} & \underline{A}_{=TM_M} & \underline{A}_{=TU_V} & \underline{A}_{=TM_V} & \underline{D}_{=TT}
 \end{bmatrix} \cdot \begin{bmatrix} \underline{\Delta W} \\ \underline{\Delta U}_M \\ \underline{\Delta M}_M \\ \underline{\Delta U}_V \\ \underline{\Delta M}_V \\ \underline{\Delta T} \end{bmatrix} = \begin{bmatrix} \underline{B}_W \\ \underline{B}_{U_M} \\ \underline{B}_{M_M} \\ \underline{B}_{U_V} \\ \underline{B}_{M_V} \\ \underline{B}_T \end{bmatrix} \quad (1)$$

However, this form of the central matrix equation that addresses the fully implicit treatment of interior metal nodes was not implemented in NOTRUMP, as described on pages E-22 and E-23 of Reference 1. Instead, an explicit treatment and a semi-implicit treatment of interior metal nodes are implemented in NOTRUMP, and the highlights are briefly explained below for clarification.

2.4.2 NOTRUMP Explicit Formulation

The previous NOTRUMP Evaluation Model (EM) uses an explicit interior metal node treatment. By explicit, it is meant that all linearization with respect to interior metal node temperature (in both the interior fluid node energy conservation equations and the interior metal node energy conservation equations) is omitted. Linearization of the interior metal node energy conservation equations with respect to all other unknowns is retained however.

For the explicit interior metal node treatment, the fully implicit central matrix Equation 1 reduces to Equation 2 (which is Equation E-148 of Reference 1), where \underline{I} is the identity submatrix:

$$\begin{bmatrix}
 \underline{A}_{=WW} & \underline{A}_{=WU_M} & \underline{A}_{=WM_M} & \underline{A}_{=WU_V} & \underline{A}_{=WM_V} & \underline{0}_{=WT} \\
 \underline{A}_{=U_M W} & \underline{D}_{=U_M U_M} & \hat{\underline{D}}_{=U_M M_M} & \hat{\underline{D}}_{=U_M U_V} & \hat{\underline{D}}_{=U_M M_V} & \underline{0}_{=U_M T} \\
 \underline{A}_{=M_M W} & \hat{\underline{D}}_{=M_M U_M} & \underline{D}_{=M_M M_M} & \hat{\underline{D}}_{=M_M U_V} & \hat{\underline{D}}_{=M_M M_V} & \underline{0}_{=M_M T} \\
 \underline{A}_{=U_V W} & \hat{\underline{D}}_{=U_V U_M} & \hat{\underline{D}}_{=U_V M_M} & \underline{D}_{=U_V U_V} & \hat{\underline{D}}_{=U_V M_V} & \underline{0}_{=U_V T} \\
 \underline{A}_{=M_V W} & \hat{\underline{D}}_{=M_V U_M} & \hat{\underline{D}}_{=M_V M_M} & \hat{\underline{D}}_{=M_V U_V} & \underline{D}_{=M_V M_V} & \underline{0}_{=M_V T} \\
 \underline{0}_{=TW} & \underline{A}_{=TU_M} & \underline{A}_{=TM_M} & \underline{A}_{=TU_V} & \underline{A}_{=TM_V} & \underline{I}
 \end{bmatrix} \cdot \begin{bmatrix} \underline{\Delta W} \\ \underline{\Delta U}_M \\ \underline{\Delta M}_M \\ \underline{\Delta U}_V \\ \underline{\Delta M}_V \\ \underline{\Delta T} \end{bmatrix} = \begin{bmatrix} \underline{B}_W \\ \underline{B}_{U_M} \\ \underline{B}_{M_M} \\ \underline{B}_{U_V} \\ \underline{B}_{M_V} \\ \underline{B}_T \end{bmatrix} \quad (2)$$

Note that for the explicit interior metal node treatment, all terms involving derivatives with respect to the interior metal node temperature are omitted, so that $\underline{A}_{=U_M T}$ and $\underline{A}_{=U_V T}$ reduce to zero submatrices, and \underline{D}_{TT} reduces to the identity submatrix.

2.4.3 NOTRUMP Semi-Implicit Formulation

The new NOTRUMP EM uses a semi-implicit interior metal node treatment. By semi-implicit, it is meant that linearization with respect to interior metal node temperature is retained in the interior metal node energy conservation equations, but omitted in the interior fluid node energy conservation equations.

For the semi-implicit treatment, the fully implicit central matrix Equation 1 reduces to Equation 3:

Westinghouse Proprietary Class 2
WESTINGHOUSE ELECTRIC COMPANY LLC

$$\begin{bmatrix}
 \underline{A}_{WW} & \underline{A}_{WU_M} & \underline{A}_{WM_M} & \underline{A}_{WU_V} & \underline{A}_{WM_V} & \underline{0}_{WT} \\
 \underline{A}_{U_M W} & \underline{D}_{U_M U_M} & \hat{\underline{D}}_{U_M M_M} & \hat{\underline{D}}_{U_M U_V} & \hat{\underline{D}}_{U_M M_V} & \underline{0}_{U_M T} \\
 \underline{A}_{M_M W} & \hat{\underline{D}}_{M_M U_M} & \underline{D}_{M_M M_M} & \hat{\underline{D}}_{M_M U_V} & \hat{\underline{D}}_{M_M M_V} & \underline{0}_{M_M T} \\
 \underline{A}_{U_V W} & \hat{\underline{D}}_{U_V U_M} & \hat{\underline{D}}_{U_V M_M} & \underline{D}_{U_V U_V} & \hat{\underline{D}}_{U_V M_V} & \underline{0}_{U_V T} \\
 \underline{A}_{M_V W} & \hat{\underline{D}}_{M_V U_M} & \hat{\underline{D}}_{M_V M_M} & \hat{\underline{D}}_{M_V U_V} & \underline{D}_{M_V M_V} & \underline{0}_{M_V T} \\
 \underline{0}_{TW} & \underline{A}_{TU_M} & \underline{A}_{TM_M} & \underline{A}_{TU_V} & \underline{A}_{TM_V} & \underline{D}_{TT}
 \end{bmatrix} \cdot \begin{bmatrix} \underline{\Delta W} \\ \underline{\Delta U}_M \\ \underline{\Delta M}_M \\ \underline{\Delta U}_V \\ \underline{\Delta M}_V \\ \underline{\Delta T} \end{bmatrix} = \begin{bmatrix} \underline{B}_W \\ \underline{B}_{U_M} \\ \underline{B}_{M_M} \\ \underline{B}_{U_V} \\ \underline{B}_{M_V} \\ \underline{B}_T \end{bmatrix} \quad (3)$$

Note that for the semi-implicit interior metal node treatment, $\underline{A}_{U_M T}$ and $\underline{A}_{U_V T}$ reduce to zero submatrices, but \underline{D}_{TT} is retained.

2.5 Documentation of Region Depletion Models

In the NOTRUMP sequence of calculations, once the central matrix solution for time step Δt^{n+1} has been completed and the central unknowns $\Delta(U_M)_i^{n+1}$, $\Delta(M_M)_i^{n+1}$, $\Delta(U_V)_i^{n+1}$, and $\Delta(M_V)_i^{n+1}$ for each interior fluid node “i” have been calculated, updating of the central variables for each interior fluid node “i” is performed as follows:

$$(U_M)_i^{n+1} = (U_M)_i^n + \Delta(U_M)_i^{n+1}$$

$$(M_M)_i^{n+1} = (M_M)_i^n + \Delta(M_M)_i^{n+1}$$

$$(U_V)_i^{n+1} = (U_V)_i^n + \Delta(U_V)_i^{n+1}$$

and

$$(M_V)_i^{n+1} = (M_V)_i^n + \Delta(M_V)_i^{n+1}$$

At this point, “region depletion” logic is performed for each interior fluid node “i”, if the mass or energy of either region of interior fluid node “i” is non-positive following the aforementioned updating process.

The original region depletion model and an improved region depletion model (mixture level overshoot) are described in Sections 2.5.1 and 2.5.2, respectively.

2.5.1 Original Region Depletion Model

The previous NOTRUMP Evaluation Model (EM) employs the original region depletion model that is described at the end of Section 10 of Reference 1. In this model, if either the mass or energy of a region of interior fluid node “i” is non-positive, both the mass and energy of that region are set to zero, and the mass and energy of the other region are adjusted so that the total mass and energy of interior fluid node “i” remain the same. The same logic is performed for each interior fluid node, independent of whether or not the interior fluid node is in a stack of interior fluid nodes. Thus, within a stack, this model forces the mixture level to stop exactly at the interior fluid node boundaries at the end of the time step in which region depletion occurs.

Consider the draining of interior fluid node “i” where the mixture region is depleted from the node, such that either $(M_M)_i^{n+1} \leq 0$ or $(U_M)_i^{n+1} \leq 0$ (or both) is true. In the original region depletion model, the mixture region mass and energy of interior fluid node “i” are added to the vapor region mass and energy, respectively, of the same interior fluid node “i”, and both the mass and energy of the mixture region of interior fluid node “i” are set to zero (keeping the total mass and energy of interior fluid node “i” the same), as follows:

First, the vapor region mass and energy of interior fluid node "i" are adjusted:

$$(M_V)_i^{n+1,adjusted} = (M_V)_i^{n+1} + (M_M)_i^{n+1}$$

and

$$(U_V)_i^{n+1,adjusted} = (U_V)_i^{n+1} + (U_M)_i^{n+1}$$

For consistency, the vapor region mass and energy unknowns of interior fluid node "i" are also adjusted:

$$\Delta(M_V)_i^{n+1,adjusted} = \Delta(M_V)_i^{n+1} + (M_M)_i^{n+1}$$

and

$$\Delta(U_V)_i^{n+1,adjusted} = \Delta(U_V)_i^{n+1} + (U_M)_i^{n+1}$$

Next, the mixture region mass and energy unknowns of interior fluid node "i" are adjusted:

$$\Delta(M_M)_i^{n+1,adjusted} = \Delta(M_M)_i^{n+1} - (M_M)_i^{n+1}$$

And

$$\Delta(U_M)_i^{n+1,adjusted} = \Delta(U_M)_i^{n+1} - (U_M)_i^{n+1}$$

Finally, the mixture region mass and energy of interior fluid node "i" are adjusted (set to zero):

$$(M_M)_i^{n+1,adjusted} = 0$$

and

$$(U_M)_i^{n+1,adjusted} = 0$$

Similarly, consider the filling of interior fluid node "i" where the vapor region is depleted from the node, such that either $(M_V)_i^{n+1} \leq 0$ or $(U_V)_i^{n+1} \leq 0$ (or both) is true. In the original region depletion model, the vapor region mass and energy of interior fluid node "i" are added to the mixture region mass and energy, respectively, of the same interior fluid node "i", and both the mass and energy of the vapor region of interior fluid node "i" are set to zero (keeping the total mass and energy of interior fluid node "i" the same) as follows:

First, the mixture region mass and energy of interior fluid node "i" are adjusted:

$$(M_M)_i^{n+1,adjusted} = (M_M)_i^{n+1} + (M_V)_i^{n+1}$$

and

$$(U_M)_i^{n+1,adjusted} = (U_M)_i^{n+1} + (U_V)_i^{n+1}$$

For consistency, the mixture region mass and energy unknowns of interior fluid node “i” are also adjusted:

$$\Delta(M_M)_i^{n+1,adjusted} = \Delta(M_M)_i^{n+1} + (M_V)_i^{n+1}$$

and

$$\Delta(U_M)_i^{n+1,adjusted} = \Delta(U_M)_i^{n+1} + (U_V)_i^{n+1}$$

Next, the vapor region mass and energy unknowns of interior fluid node i are adjusted:

$$\Delta(M_V)_i^{n+1,adjusted} = \Delta(M_V)_i^{n+1} - (M_V)_i^{n+1}$$

and

$$\Delta(U_V)_i^{n+1,adjusted} = \Delta(U_V)_i^{n+1} - (U_V)_i^{n+1}$$

Finally, the vapor region mass and energy of interior fluid node “i” are adjusted (set to zero):

$$(M_V)_i^{n+1,adjusted} = 0$$

and

$$(U_V)_i^{n+1,adjusted} = 0$$

Adjustments to the temperature unknown and temperature central variable of interior metal nodes that are connected (via non-critical heat links) to interior fluid node “i”, due to the adjustments of the interior fluid node “i” central described above, are subsequently performed.

The original region depletion model described above is not capable of reliably predicting a natural crossing of the mixture level over the node boundaries in a stack of interior fluid nodes, whether the stack is draining or filling. By its method of forcing the mixture level to stop exactly at the interior node boundaries within a stack, the original region depletion model can result in unrealistic “level hangs”. Also, the addition of the non-positive mass and energy of the depleted region of a node to the mass and energy of the other region of the node can result in a non-positive mass and/or energy in other (non-depleted) region. This can also result in the calculation of a non-physical temperature and/or pressure.

2.5.2 Improved Region Depletion Model (Mixture Level Overshoot)

The new NOTRUMP EM employs an improved region depletion model, known as the mixture level overshoot model, for the interior fluid nodes within a stack. The mixture level

overshoot model improves the code's ability to pass a mixture level across fluid node boundaries in a stack, in both draining and filling situations. The mixture level overshoot logic passes the mixture elevation out of a node in the four steps as described below.

In a draining situation, if either the mass or energy of the mixture region of a fluid node in the stack is non-positive, the mixture level overshoot logic first estimates the volume of the vapor region that should have formed in the lower node. Second, it adds the upper-node mixture region mass and energy to the lower node's mixture region. Third, it takes a volume-weighted fraction of the mass and energy of the upper node's vapor region and places it into the lower node's vapor region. However, if the newly formed vapor region is superheated, its mass and energy are reset to the values for saturated steam, adding or subtracting mass and energy from the upper node's vapor region as necessary to conserve mass and energy. Fourth, it zeroes the upper-node mixture region mass and energy. An analogous situation exists in a node filling event and is handled in a similar way, except that newly formed mixture regions are allowed to be subcooled.

2.5.2.1 Mixture Level Overshoot Logic for Draining Situation

The logic presented below is for the situation in which the mixture level drains out of interior fluid node N into the interior fluid node below it in the stack, NBELOW. An estimate for what would be the change in volume of the mixture region of interior fluid node N, $\Delta(V_M)_N^{n+1}$, is given by DELVM:

$$DELVM = \left(\frac{\partial(V_M)_N}{\partial(U_M)_N} \right)^n \cdot \Delta(U_M)_N^{n+1} + \left(\frac{\partial(V_M)_N}{\partial(M_M)_N} \right)^n \cdot \Delta(M_M)_N^{n+1} + \left(\frac{\partial(V_M)_N}{\partial(U_V)_N} \right)^n \cdot \Delta(U_V)_N^{n+1} + \left(\frac{\partial(V_M)_N}{\partial(M_V)_N} \right)^n \cdot \Delta(M_V)_N^{n+1}$$

An estimate for what would be the new mixture region volume of interior fluid node N, $(V_M)_N^{n+1}$, is given by ESTVM:

$$ESTVM = (V_M)_N^n + DELVM$$

For the regular case of the mixture region in interior fluid node N being completely depleted (ESTVM<0):

An estimate for the new time pressure in interior fluid node NBELOW, P_{NBELOW}^{n+1} , for use in the following calculations is given by PBELOW:

$$PBELOW = P_{NBELOW}^n + \left(\frac{\partial P_{NBELOW}}{\partial(U_M)_{NBELOW}} \right)^n \cdot \Delta(U_M)_{NBELOW}^{n+1} + \left(\frac{\partial P_{NBELOW}}{\partial(M_M)_{NBELOW}} \right)^n \cdot \Delta(M_M)_{NBELOW}^{n+1} + \left(\frac{\partial P_{NBELOW}}{\partial(U_V)_{NBELOW}} \right)^n \cdot \Delta(U_V)_{NBELOW}^{n+1} + \left(\frac{\partial P_{NBELOW}}{\partial(M_V)_{NBELOW}} \right)^n \cdot \Delta(M_V)_{NBELOW}^{n+1}$$

$$PBELOW = \min\{\max[PBELOW, 0.2], 3000.0\}$$

An estimate for what would be the new time volume of the vapor region of interior fluid node N, $(V_V)_N^{n+1}$, is given by ESTVV:

$$ESTVV = (V_V)_N^n - DELVM$$

Step 1 – Reset the interior fluid node N vapor region mass and energy based upon ESTVV (to fill the volume of interior fluid N, V_N):

$$(M_V)_N^{n+1,adjusted} = (M_V)_N^{n+1} \cdot \frac{V_N}{ESTVV}$$

$$\Delta(M_V)_N^{n+1,adjusted} = \Delta(M_V)_N^{n+1} + ((M_V)_N^{n+1,adjusted} - (M_V)_N^{n+1})$$

$$(U_V)_N^{n+1,adjusted} = (M_V)_N^{n+1,adjusted} \cdot \frac{(U_V)_N^{n+1}}{(M_V)_N^{n+1}}$$

$$\Delta(U_V)_N^{n+1,adjusted} = \Delta(U_V)_N^n + ((U_V)_N^{n+1,adjusted} - (U_V)_N^{n+1})$$

Step 2 – Add the negative (i.e., non-positive) mixture region mass and/or energy of interior fluid node N to the mixture region mass and/or energy of interior fluid node NBELOW, and reset those of interior fluid node N to zero:

$$(M_M)_{NBELOW}^{n+1,adjusted} = (M_M)_{NBELOW}^{n+1} + (M_M)_N^{n+1}$$

$$\Delta(M_M)_{NBELOW}^{n+1,adjusted} = \Delta(M_M)_{NBELOW}^{n+1} + (M_M)_N^{n+1}$$

$$\Delta(M_M)_N^{n+1,adjusted} = \Delta(M_M)_N^{n+1} - (M_M)_N^{n+1}$$

$$(M_M)_N^{n+1,adjusted} = 0$$

$$(U_M)_{NBELOW}^{n+1,adjusted} = (U_M)_{NBELOW}^{n+1} + (U_M)_N^{n+1}$$

$$\Delta(U_M)_{NBELOW}^{n+1,adjusted} = \Delta(U_M)_{NBELOW}^{n+1} + (U_M)_N^{n+1}$$

$$\Delta(U_M)_N^{n+1,adjusted} = \Delta(U_M)_N^{n+1} - (U_M)_N^{n+1}$$

$$(U_M)_N^{n+1,adjusted} = 0$$

Step 3 – Add the mass and energy that was removed from the vapor region of interior fluid node N to the vapor region of interior fluid node NBELOW, creating a new vapor region in interior fluid node NBELOW (if one didn't already exist):

WESTINGHOUSE ELECTRIC COMPANY LLC

$$(M_V)_{NBELOW}^{n+1,adjusted} = (M_V)_{NBELOW}^{n+1} + ((M_V)_N^{n+1} - (M_V)_N^{n+1,adjusted})$$

$$\Delta(M_V)_{NBELOW}^{n+1,adjusted} = \Delta(M_V)_{NBELOW}^{n+1} + ((M_V)_N^{n+1} - (M_V)_N^{n+1,adjusted})$$

$$(U_V)_{NBELOW}^{n+1,adjusted} = (U_V)_{NBELOW}^{n+1} + ((U_V)_N^{n+1} - (U_V)_N^{n+1,adjusted})$$

$$\Delta(U_V)_{NBELOW}^{n+1,adjusted} = \Delta(U_V)_{NBELOW}^{n+1} + ((U_V)_N^{n+1} - (U_V)_N^{n+1,adjusted})$$

Step 4 - Check if the newly created vapor region in the interior fluid node NBELOW is superheated, and if so, reset it to saturated vapor.

Employ NOTRUMP internal steam tables to calculate $h_g(PBELOW)$ and $v_g(PBELOW)$

$$UGBELOW = h_g(BELOW) - 0.18511 \cdot PBELOW \cdot v_g(PBELOW)$$

Perform the following only if $(M_V)_{NBELOW}^{n+1,adjusted} \neq 0$:

Check if $\frac{(U_V)_{NBELOW}^{n+1,adjusted}}{(M_V)_{NBELOW}^{n+1,adjusted}} > UGBELOW$ and perform the following if so:

$$(M_V)_{NBELOW}^{n+1,adjusted\ again} = \frac{(ESTVV - V_N)}{v_g(PBELOW)}$$

$$\Delta(M_V)_{NBELOW}^{n+1,adjusted\ again} = \Delta(M_V)_{NBELOW}^{n+1,adjusted} + ((M_V)_{NBELOW}^{n+1,adjusted\ again} - (M_V)_{NBELOW}^{n+1,adjusted})$$

$$(M_V)_N^{n+1,adjusted\ again} = (M_V)_N^{n+1,adjusted} - ((M_V)_{NBELOW}^{n+1,adjusted\ again} - (M_V)_{NBELOW}^{n+1,adjusted})$$

$$\Delta(M_V)_N^{n+1,adjusted\ again} = \Delta(M_V)_N^{n+1,adjusted} - ((M_V)_{NBELOW}^{n+1,adjusted\ again} - (M_V)_{NBELOW}^{n+1,adjusted})$$

$$(U_V)_{NBELOW}^{n+1,adjusted\ again} = (M_V)_{NBELOW}^{n+1,adjusted\ again} \cdot UGBELOW$$

$$\Delta(U_V)_{NBELOW}^{n+1,adjusted\ again} = \Delta(U_V)_{NBELOW}^{n+1,adjusted} + ((U_V)_{NBELOW}^{n+1,adjusted\ again} - (U_V)_{NBELOW}^{n+1,adjusted})$$

$$(U_V)_N^{n+1,adjusted\ again} = (U_V)_N^{n+1,adjusted} - ((U_V)_{NBELOW}^{n+1,adjusted\ again} - (U_V)_{NBELOW}^{n+1,adjusted})$$

$$\Delta(U_V)_N^{n+1,adjusted\ again} = \Delta(U_V)_N^{n+1,adjusted} - ((U_V)_{NBELOW}^{n+1,adjusted\ again} - (U_V)_{NBELOW}^{n+1,adjusted})$$

For the special case of the mixture region in interior fluid node N not being completely depleted (in the event that $ESTVM \geq 0$, due to round-off for example):

WESTINGHOUSE ELECTRIC COMPANY LLC

In this case, the mixture region mass and energy of interior fluid node N is mixed with the mixture region mass and energy of interior fluid node NBELOW, then this combined mass and energy is redistributed between the mixture regions of both interior fluid nodes based upon volume weighting:

$$TEMPMM = (M_M)_{NBELOW}^{n+1} + (M_M)_N^{n+1}$$

$$TEMPUM = (U_M)_{NBELOW}^{n+1} + (U_M)_N^{n+1}$$

$$(M_M)_N^{n+1,adjusted} = TEMPMM \cdot \left(\frac{ESTVM}{(V_M)_{NBELOW} + ESTVM} \right)$$

$$\Delta(M_M)_N^{n+1,adjusted} = \Delta(M_M)_N^{n+1} + ((M_M)_N^{n+1,adjusted} - (M_M)_N^{n+1})$$

$$(U_M)_N^{n+1,adjusted} = (M_M)_N^{n+1,adjusted} \cdot \left(\frac{TEMPUM}{TEMPMM} \right)$$

$$\Delta(U_M)_N^{n+1,adjusted} = \Delta(U_M)_N^{n+1} + ((U_M)_N^{n+1,adjusted} - (U_M)_N^{n+1})$$

$$(M_M)_{NBELOW}^{n+1,adjusted} = TEMPMM - (M_M)_N^{n+1,adjusted}$$

$$\Delta(M_M)_{NBELOW}^{n+1,adjusted} = \Delta(M_M)_{NBELOW}^{n+1} + ((M_M)_{NBELOW}^{n+1,adjusted} - (M_M)_{NBELOW}^{n+1})$$

$$(U_M)_{NBELOW}^{n+1,adjusted} = TEMPUM - (U_M)_N^{n+1,adjusted}$$

$$\Delta(U_M)_{NBELOW}^{n+1,adjusted} = \Delta(U_M)_{NBELOW}^{n+1} + ((U_M)_{NBELOW}^{n+1,adjusted} - (U_M)_{NBELOW}^{n+1})$$

Finally, adjustments to the temperature unknown and temperature central variable of interior metal nodes that are connected (via non-critical heat links) to either interior fluid node N or NBELOW, due to the adjustments of the interior fluid node N and NBELOW central variables described above, are subsequently performed.

Note that in the case of a mixture level draining out of the bottom interior fluid node of a stack, the original region depletion model described in Section 2.5.1 is employed.

2.5.2.2 Mixture Level Overshoot Logic for Filling Situation

This logic applies to the situation in which the mixture level fills up out of interior fluid node N into the interior fluid node above it in the stack, NABOVE. The mixture level overshoot logic for a filling situation is analogous to the draining situation described above, except that no PBELOW calculation is needed, and the newly formed mixture region in interior fluid node NABOVE is allowed to be subcooled if it is determined to be. Note that in the case of a mixture level filling out of the top interior fluid node of a stack, the original region depletion model described in Section 2.5.1 is employed.

2.6 References

1. Meyer, P. E., "NOTRUMP: A Nodal Transient Small Break And General Network Code", WCAP-10079-P-A (Proprietary), WCAP-10080-A (Non-Proprietary), August 1985.
2. Fittante, R. L., et. al., "NOTRUMP Final Validation Report for AP600", WCAP-14807 (Proprietary), WCAP-14808 (Non-Proprietary), Revision 5, August 1998.

3.0 Clarification of Westinghouse Loop Seal Restriction Modeling Methodology

The following section is being provided to clarify the Westinghouse Small Break LOCA (SBLOCA) methodology associated with the imposition of/removal of the artificial loop seal restriction model utilized in the NOTRUMP Evaluation Model (EM). This section documents some background information as well as the Westinghouse traditional practice of the removal of the artificial loop seal restriction under specified conditions.

3.1 Background Information on Westinghouse Loop Seal Restriction Model

1. In a SBLOCA transient, at least one loop seal would vent steam (and possibly more depending on loop-to-loop interactions).
2. For 3-loop or 4-loop plants, the Westinghouse intact loop model [

]^{a,c} With lumped loops, it is not possible to model the loop-to-loop interactions in sufficient detail to accurately predict the behavior in such cases.
3. Without sufficient steam flow to ensure that all loops will vent steam for an extended period of time, venting of steam was chosen to occur in the broken loop only via the imposition of a loop seal restriction as described in item 4.
4. The loop seal restriction in the NOTRUMP SBLOCA EM is an artificiality imposed on calculations to restrict steam flow through the [

]^{a,c} to ensure that venting of steam flow through the loop seal of the broken loop would occur first. The reasons for the imposition of this restriction and the justification for its conservative effect on calculations are described in more detail in WCAP-10054-P-A (Reference 1) and WCAP-11145-P-A (Reference 2).
5. For 3 and 4 loop plants with an explicit N-loop noding scheme, as well as for 2 loop plants (where the standard model represents explicit loop noding), the technical reasons for restricting the steam flow in any loop are not applicable. Although artificial, the restriction has routinely been applied for these cases, when steam flow is not sufficient to vent through all loops for an extended period of time, to maintain consistency with the licensing documentation.
6. In application, the artificial loop seal restriction may only be removed for breaks for which steam flow is sufficient to vent through all loops for an extended period of time [

]^{a,c} steam venting occurs in the broken loop.

3.1.1 WCAP-10054-P-A (NRC Approval 1985)

WCAP-10054-P-A (Reference 1) describes the conditions for which loop seal

WESTINGHOUSE ELECTRIC COMPANY LLC

unpredictability and loop-to-loop interactions may result in non-conservative results. To address these conditions, Westinghouse identified a model that would ensure conservative behavior for these conditions. The conditions for when the model must be applied are described by a threshold break size below which the loop seal restriction is **required**. The following are pertinent excerpts from this topical report related to the loop seal restriction:

Page 5-101:

“A method to ensure the conservative behavior for appendix K analysis is discussed and break spectrum calculations using the evaluation model with appendix K modification are presented. When the loop seal steam venting was limited to the broken loop, limiting core uncover and cladding heatup results were calculated with results well below the limits of 10CFR50 part 46 and appendix K.”

Page 5-45:

“...This modification [loop-seal restriction] is used in the evaluation model to ensure conservative behavior for break sizes below the threshold break size, Reiterating, break sizes larger than the threshold break size will realistically vent steam through more than one loop seal and in doing so will result in minimal core uncover. The modification to assure conservative behavior is also applied to those breaks to ensure a continuum of response in terms of peak cladding temperature when only the broken loop is artificially forced to vent steam.”

While there is some reason associated with maintaining a “continuum of response”, especially in the presentation of the generic model application in WCAP-10054-P-A, this would rarely be the case in practice. Typically, the smallest break size at which loop seal restriction removal is justified is the []^{a,c} break. This also typically coincides with the smallest break size at which []^{a,c} are invoked. As a result, transient behavior is often “discontinuous” between the []^{a,c} break cases, independent of loop seal restriction modeling considerations.

The SER for WCAP-10054-P-A does not specifically address the loop seal restriction. However, TABLE VI-1 (p. 37 of the SER) identifies the analysis assumptions for the SBLOCA audit calculations. Included in this table is reference to a “Westinghouse conservative assumption” in item 15, which states, “Loop seals in the intact loops are not permitted to clear prior to clearing of the loop seal in the broken loop.” This condition is met even for larger breaks where the loop seal restriction is removed, because the restriction is removed only []^{a,c} occurs.

3.1.2 WCAP-11145-P-A (NRC Approval 1986)

WCAP-11145-P-A (Reference 2) provides further clarification on the Westinghouse loop seal restriction modeling. The following are pertinent excerpts from this topical report related to the loop seal restriction:

Pages 2-11 and 2-12:

“...The loop seal clearing behavior may be delineated by defining threshold and critical break sizes. The threshold break size is the break size at which the transient loop seal perturbations are large enough to always result in more than one loop seal venting steam for a period of time. Break sizes below the threshold break size tend to vent steam through only one loop. For break sizes above the threshold break size, but below the critical break size, there are multiple loop seal clearings which will be oscillatory in nature and may involve loop-to-loop interactions. At the critical break size and above, the loop seal perturbations are large enough to always result in all loop seals venting steam for a period of time...Consequently, for breaks below the critical break size, the NOTRUMP SBLOCA EM only allows the broken loop seal to clear and to vent significant amounts of steam...Restricting the intact loop seal from clearing for breaks above the critical break size is unnecessarily conservative. Consequently, for breaks above the critical break size, the [

]a,c...”

Cases for which the loop seal restriction has been removed are also presented in the WCAP. The SER for WCAP-11145-P-A does not specifically address the loop seal restriction.

3.2 Westinghouse Methodology

During the development and early applications of the NOTRUMP Evaluation Model, Westinghouse worked closely with the WOG and the NRC to ensure that the new model would adequately and appropriately address the requirements of the TMI action plan. While not documented, this topic was presented to the NRC in April 1985. Close participants in the process were aware of the refinement of key assumptions leading to the application of NOTRUMP in addressing the requirements of NUREG-0737, II.K.3.31 under the umbrella of the WOG. It was in this environment that Westinghouse’s clarification of the intended removal of the loop seal restriction, under clearly defined conditions, was placed in the public record with the publication of WCAP-11145-P-A (Reference 2). Since that time, it has been the Westinghouse business practice to allow the analysts to remove the loop seal restriction when the appropriate technical conditions are satisfied.

Based on the technical justifications and identifications of intended applications of the

WESTINGHOUSE ELECTRIC COMPANY LLC

loop seal restriction in the NRC-approved topical reports, WCAP-10054-P-A and WCAP-11145-P-A, which describe the NOTRUMP EM and its application, Westinghouse believes that its long-standing business practice of removal of the artificial loop seal restriction is appropriate under the following conditions:

1. removal of the loop seal restriction occurs only [
] ^{a,c}, and
2. with the loop seal restriction removed, there is sufficient steam flow to result in all loop seals venting steam for a period of time, consistent with the conditions identified in WCAP-11145-P-A [
] ^{a,c}

3.3 References

1. WCAP-10054-P-A (Proprietary), WCAP-10081-A (Non-Proprietary), "Westinghouse Small Break ECCS Evaluation Model Using the NOTRUMP Code," N. Lee, et al., August 1985.
2. WCAP-11145-P-A (Proprietary), WCAP 11372-A (Non-Proprietary), "Westinghouse Small Break LOCA ECCS Evaluation Model Generic Study with the NOTRUMP Code," S. D. Rupprecht, et al., October 1986.

4.0 Enhanced Model Validation

4.1 Separate Effects Validation

4.1.1 Validation of Implicit Bubble Rise Model

The purpose of this section is to validate the implementation of the implicit bubble rise model formulation in the NOTRUMP Evaluation Model (EM). This validation will also demonstrate the improvement of using implicit treatment of bubble rise over the explicit bubble rise treatment used in the previous NOTRUMP EM for plant calculations. This demonstration is accomplished by simulating a constant-pressure boiling-pot problem which features the bubble rise process and comparing the results of code calculations where the only difference is the explicit versus implicit treatment of bubble rise. The derivations of the equations associated with both explicit and implicit bubble rise models are contained in Section 2.1 of this report.

4.1.1.1 Bubble Rise Model Test Case Description

The NOTRUMP noding scheme for the validation of the bubble rise model consists of a simple, two-node (interior fluid nodes) stack partially filled (into the upper fluid node) with saturated water/steam mixture connected to a large third interior fluid node, which essentially serves as a boundary node (Figure 4.1.1-1). Energy is added to the bottom node of the stack via a single, critical heat link. The addition of heat causes the two-phase mixture level to initially swell into the upper node due to void formation. The calculation then proceeds as a low-pressure boil-off of water occurs. The two-phase mixture level eventually falls into the lower fluid node and the calculation terminates when all the fluid mass of the two-phase mixture in the stack is depleted.

The NOTRUMP model (Figure 4.1.1-1) consists of two stacked interior fluid nodes and a third node (modeled as an interior fluid node) which serves as the boundary fluid node above them. The interior fluid nodes are modeled as a cylinder with a total height of 10.0 ft and a cross-sectional area of 0.7854 ft². The bottom node (node 1) has a height of 1.0 ft and the top node (node 2) has a height of 9.0 ft. An initial mixture level of 1.5 ft is utilized, so that the mixture level is in node 2. Two non-critical flow links are utilized to connect the three interior fluid nodes. The lower fluid node has heat added to it via a critical heat link that is connected to a boundary metal node. The model utilizes the NOTRUMP EM Yeh drift flux correlation.

The bubble rise model validation test cases are designed to demonstrate the impact of switching from the previous Evaluation Model (EM) explicit formulation to the more stable implicit formulation. As these particular test cases are simple thought problems developed for the purpose of demonstrating implicit versus explicit features of bubble rise, there is no intention here to validate results with experimental test data. All that is

being assessed here is the relative performance of the explicit and implicit treatments in providing results judged to be more reasonable or stable.

The following enhanced model features are activated in all of the test cases presented here:

1. Implicit droplet fall model (described in Section 2.2).
2. Implicit fluid node gravitational head model (described in Section 2.3).
3. Semi-implicit metal node model (described in Section 2.4).
4. Improved region depletion model (described in Section 2.5).

The following cases are performed:

1. Base Case - Includes all the above features and the explicit bubble rise model and 0.25 maximum time step size.
2. Fully implicit - Same as 1 with implicit bubble rise model.
3. Same as 1 with 0.1 maximum time step size.
4. Same as 2 with 0.1 maximum time step size.

In all of these simulations, heat is added to the mixture region at a constant rate following a 100 second ramp up starting at 10 seconds. The following sections compare the test results with the expected results for the cases described above.

4.1.1.2 Comparison of Test Results with Expected Results

To validate that the implicit treatment of the bubble rise model is implemented correctly, the results of the implicit versus explicit treatments are compared to each other (using plot comparisons of key quantities). The expected result is that the implicit and explicit solutions will converge as the time step size is reduced. It is expected that by switching to the implicit formulation, as the mixture level decreases, the behavior of bubble rise will be stable as will fluid node mixture region properties. This will allow for a more continuous transition of the fluid node mixture level across nodal boundaries by maintaining consistent properties.

4.1.1.2.1 Case 1 - Explicit Bubble Rise Model With 0.25 Maximum Time Step Size

The base or explicit bubble rise case consists of explicit bubble rise treatment coupled with the other enhanced models. The explicit treatment of the bubble rise model is expected to result in oscillatory behavior of the calculated bubble rise mass flow rate as the mixture level decreases and approaches the node boundary. The reason for this is the calculated bubble rise rate for a time step can be larger than the available inventory, thereby resulting in oscillatory flow behavior. The results of this case are compared to the fully implicit case in the next section (4.1.1.2.2). Therefore, they are not discussed here separately.

4.1.1.2.2 Case 2 - Fully Implicit Model With 0.25 Maximum Time Step Size

The implicit bubble rise case is the same as the base case except that the bubble rise is treated implicitly in order to focus on the difference between explicit and implicit bubble rise treatment and the improvement associated with implicit treatment. The simulation with the fully implicit model is expected to produce smooth results (e.g., bubble rise rate, mixture region void fraction, specific enthalpy, and specific volume).

The results of the calculations for Case 1 and Case 2 are compared in Figures 4.1.1-2 - 4.1.1-8. The results show some noticeable and expected differences in quantities of significant interest for this test case, such as the mixture level shown in Figure 4.1.1-2. From this figure, it can be seen that the explicit bubble rise treatment is not as smooth as the implicit bubble rise treatment, especially as the mixture level nears a node boundary crossing (1 ft. elevation). In fact, the explicit bubble rise treatment exhibits a discontinuity as it crosses the node boundary. This discontinuity in the mixture level is unrealistic and therefore, the implicit bubble rise treatment clearly provides a more reasonable simulation of the physical situation.

While quantities such as mixture level are different between the two bubble rise treatments as expected, other quantities which were also expected to be different and could influence mixture level, such as the bubble rise mass flow rate itself, were not. This can be seen in Figures 4.1.1-3 and 4.1.1-4, where the bubble rise mass flow rates for explicit and implicit treatments are virtually identical. Also, Figures 4.1.1-5 - 4.1.1-8 indicate that well before the node boundary crossing, the node 2 mixture region void fraction, specific enthalpy and specific volume calculated with the explicit bubble rise treatment diverge significantly from the implicit model results. These results were not expected.

In an effort to understand these unexpected results, the explicit and implicit bubble rise formulations were reviewed. As explained in Section 2.1.2, the explicit bubble rise treatment in NOTRUMP applies a restriction on the bubble rise mass flow rate in an attempt to prevent the depletion of the current vapor mass in the node's mixture region in a given time step. The intent of this restriction is to prevent the material Courant limit from being violated by limiting the explicit bubble rise mass flow rate (instead of the more traditional approach of limiting the time step size) as the mixture region is depleted. However, this restriction is not sufficiently restrictive, due to its use of too large a vapor mass in the limit expression. Instead of using either a predicted average value that applies over the time step or a predicted end-of-time step value, the limit expression uses the vapor mass that exists in the mixture region at the beginning of the time step. The use of the beginning of step value is too large in a depleting mixture region situation; consequently, the restriction does not enforce the material Courant limit. The material Courant limit violation manifests itself in an abnormal solution of the mixture region total energy, and thereafter in the mixture region calculated thermodynamic properties.

The timing of the restriction implementation in this case occurs at approximately 330 seconds, as can be seen in Figure 4.1.1-9. The effect of the material Courant limit violation can be seen in the abnormal changes in the mixture region properties of void fraction, specific volume, and specific enthalpy (Figures 4.1.1-10 through 4.1.1-12). The impact of the elimination of the explicit bubble rise restriction is investigated in Section 4.1.1.3 to demonstrate that the expected results of an explicit bubble rise model implementation can indeed be obtained.

4.1.1.2.3 Case 3 - Explicit Bubble Rise Model with 0.1 Time Step Size

This case is utilized for a comparison to the fully implicit bubble rise model simulation performed in Section 4.1.1.2.4. The purpose of this case is to demonstrate that as the maximum time step size is reduced for the explicit formulation, the results between the implicit and explicit bubble rise simulations will converge. Here, Case 1 is repeated with smaller time step size. To make the comparison between the explicit and implicit case more meaningful, a fixed time step of 0.1 is used (by setting the maximum time step size equal to the minimum time step size) in this case. The results of this case are compared to the fully implicit case (with fixed time step size of 0.1) in the next section (4.1.1.2.4).

4.1.1.2.4 Case 4 - Fully Implicit Model with 0.1 Time Step Size

As stated in Section 4.1.1.2.3, this case is performed to provide a one-to-one comparison of the results between implicit and explicit bubble rise formulations by using the same (constant) time step size in both cases.

The results of the calculations for Cases 3 and 4 are compared in Figure 4.1.1-13. This figure shows that the mixture level for the case with the explicit bubble rise model converges or approaches the case with the implicit model as expected. As indicated earlier, additional cases are performed (see Section 4.1.1.3) with the bubble rise restriction circumvented, to demonstrate the effect of the imposed restriction on the calculated results for the explicit case.

4.1.1.3 Explicit Formulation Sensitivity Studies

Two additional cases were performed based on the discussion in Section 4.1.1.2.2, which indicated that comparison of the results between the case with the explicit bubble rise model and the implicit bubble rise model showed no difference in bubble rise mass flow rate, contrary to what was expected. Yet, other quantities that were not expected to be significantly different due to the difference in bubble rise treatment were in fact significantly different. As explained in Section 4.1.1.2.2, the restriction imposed on the explicit bubble rise mass flow rate contributed to this behavior. The two additional cases were made with the explicit bubble rise model to circumvent this restriction which allowed better focus on explicit versus implicit bubble rise treatment. In order to circumvent this restriction with code input (and not have to modify the code), it was necessary to employ

a constant time step size for these simulations.

Only two cases will be performed both of these being for the explicit bubble rise formulation which were affected by the restriction. The cases performed are:

1. Explicit bubble rise with 0.25 time step size w/ restriction disabled.
2. Explicit bubble rise with 0.1 time step size w/ restriction disabled.

4.1.1.3.1 Explicit Bubble Rise Model with Constant $\Delta t=0.25$ With The Restriction Disabled

It is expected that with the restriction removed, the explicit bubble rise formulation will exhibit the traditional oscillatory behavior which would accompany the region depletion.

As can be seen in Figures 4.1.1-14 and 4.1.1-15, the expected results were obtained with the mixture level and bubble rise mass flow rate undergoing oscillations as the mixture level decreases. This instability eventually leads to an aborted calculation when the mixture level crosses the boundary between node 1 and 2 at the 1 foot elevation. Comparing these plots to Figures 4.1.1-2 and 4.1.1-3, it can be seen that the stable mixture level and the constant bubble rise mass flow rate calculated by the implicit model formulation demonstrates the advantages of using implicit bubble rise treatment whose properties are stable through this portion of the transient.

The following section will look at the reduced time-step size case to determine if the fidelity between the implicit and explicit bubble rise formulation will converge.

4.1.1.3.2 Explicit Bubble Rise Model with Constant $\Delta t=0.1$ With The Restriction Disabled

Once again, it is expected that with the restriction removed and the time step reduced, the time at which the explicit bubble rise formulation will exhibit oscillatory behavior which accompanies the mixture level drop will be delayed.

As can be seen in Figures 4.1.1-16 and 4.1.1-17, the results are as expected with the unlimited bubble rise rate resulting in flow oscillations similar to those observed in Section 4.1.1.3.1, albeit delayed due to the time step size reduction. Comparing these plots to Figures 4.1.1-14 and 4.1.1-15, it can be seen that the time at which the flow oscillations occur is significantly delayed (from ~600 seconds to ~850 seconds), thereby supporting the implicit model results.

At this point, the implicit bubble rise model can be considered to be appropriately implemented and validated.

4.1.1.4 Bubble Rise Model Simulation Conclusion

The conclusions which can be reached based on the results of the simulations performed in the previous sections are as follows:

1. The implementation of the implicit bubble rise model over the explicit bubble rise model improves region properties as the mixture level decreases (approaches a node boundary). This results in improved continuity when mixture levels cross fluid node boundaries. In addition, the implicit bubble rise model behaves as expected; therefore, it is appropriate for use.
2. The implicit bubble rise treatment is validated via favorable comparison with explicit bubble rise treatment at smaller time steps and provides a more stable and smooth calculation compared to the explicit treatment, especially at larger time steps. Therefore, the implicit bubble rise model will become the default model for the new NOTRUMP EM for plant calculations.
3. From the above documentation, explicit methods for bubble rise should not be utilized where implicit methods are available.

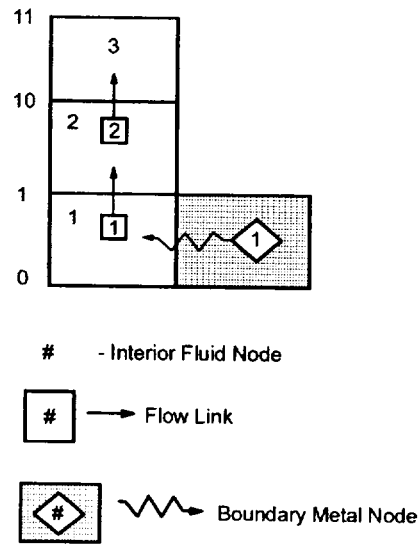


Figure 4.1.1-1 NOTRUMP Bubble Rise Model Noding Diagram

Boiling Pot Test Case Stack Mixture Level

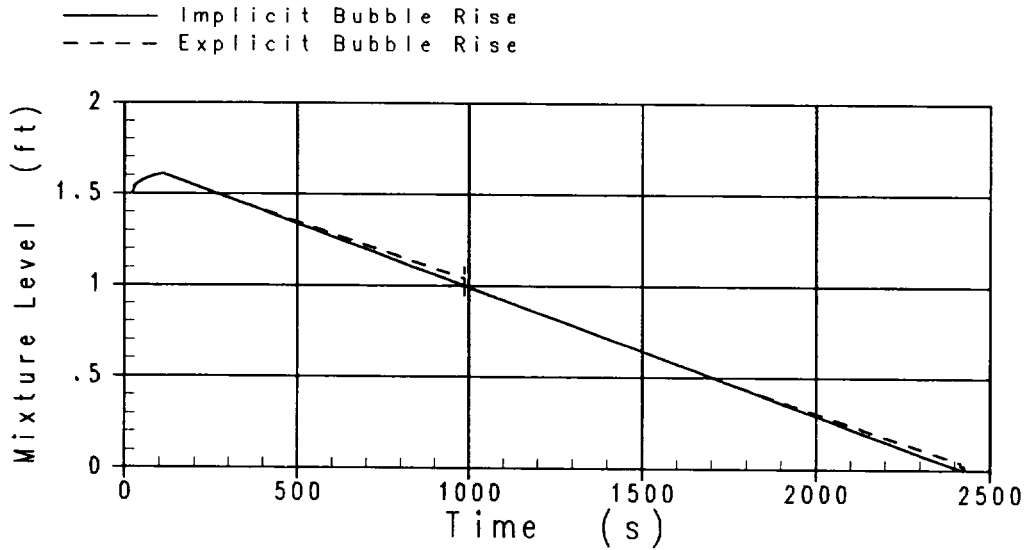


Figure 4.1.1-2 Stack Mixture Level Comparison

Boiling Pot Test Case Bubble Rise Massflow

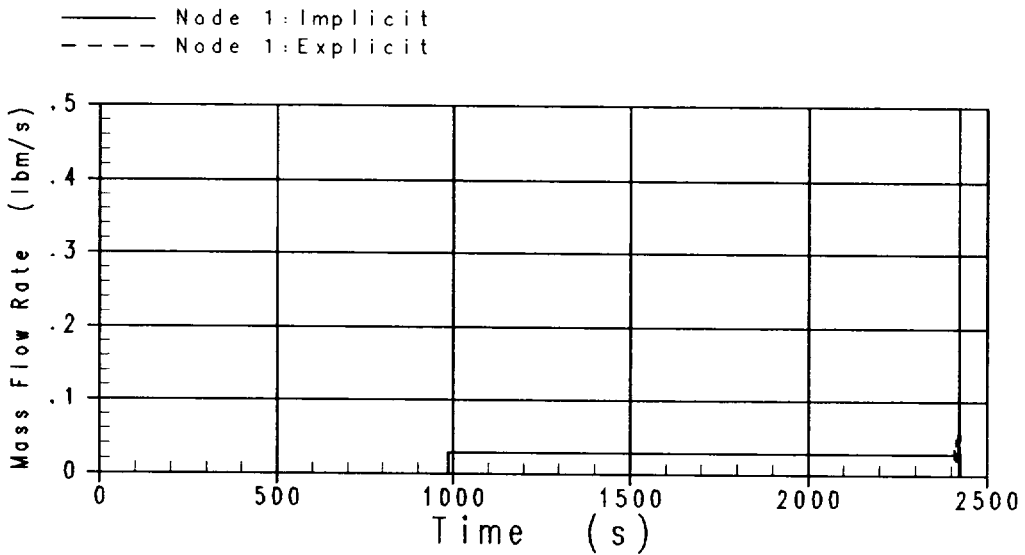


Figure 4.1.1-3 Bubble Rise Massflow Comparison- Node 1

Boiling Pot Test Case Void Fraction

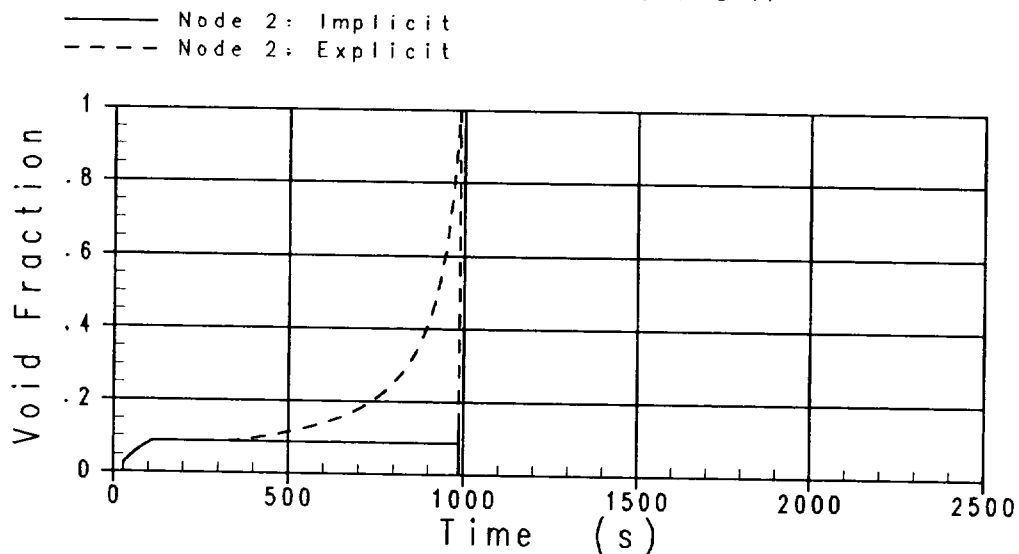


Figure 4.1.1-6 Void Fraction Comparison - Node 2

Boiling Pot Test Case Mixture Specific Enthalpy

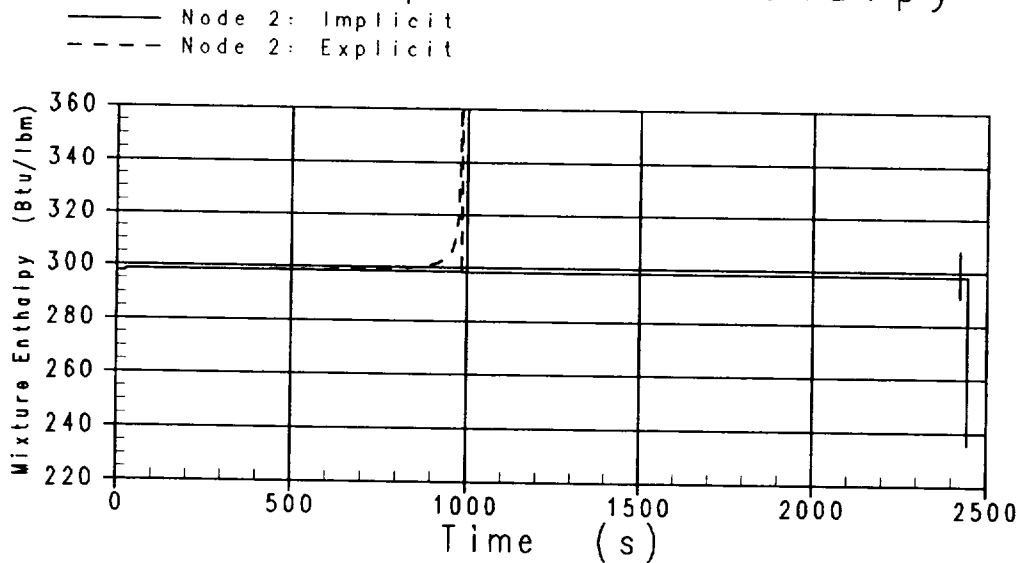


Figure 4.1.1-7 Mixture Specific Enthalpy Comparison - Node 2

Boiling Pot Test Case Mixture Specific Volume

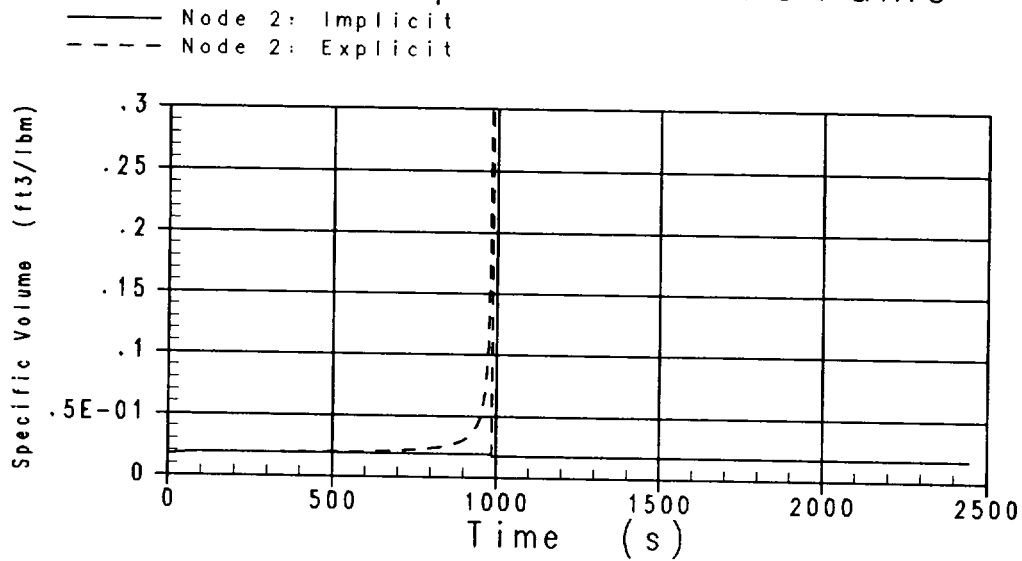


Figure 4.1.1-8 Mixture Specific Volume Comparison - Node 2

Boiling Pot Test Case Bubble Rise Massflow Limit

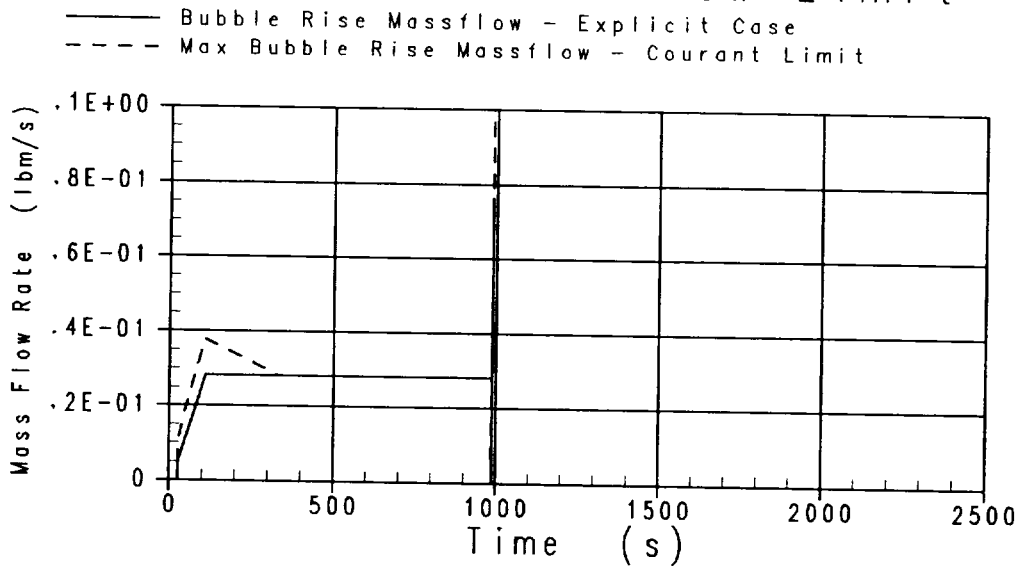


Figure 4.1.1-9 Bubble Rise Mass Flow Comparison with Restriction

BOILING POT TEST CASE
Explicit Bubble Rise Model

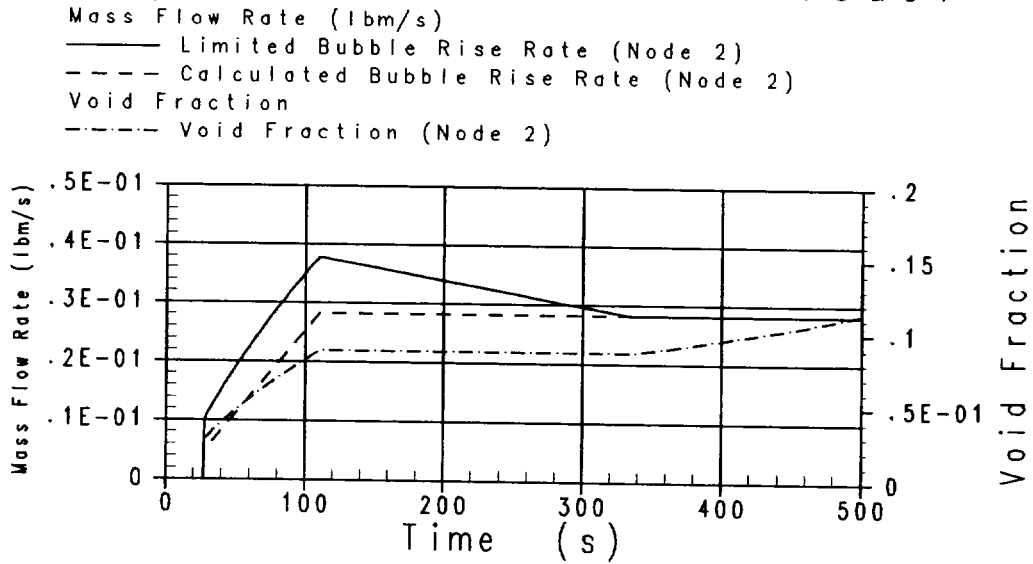


Figure 4.1.1-10 Bubble Rise Massflow and Void Fraction Comparison with Restriction

BOILING POT TEST CASE
Explicit Bubble Rise Model

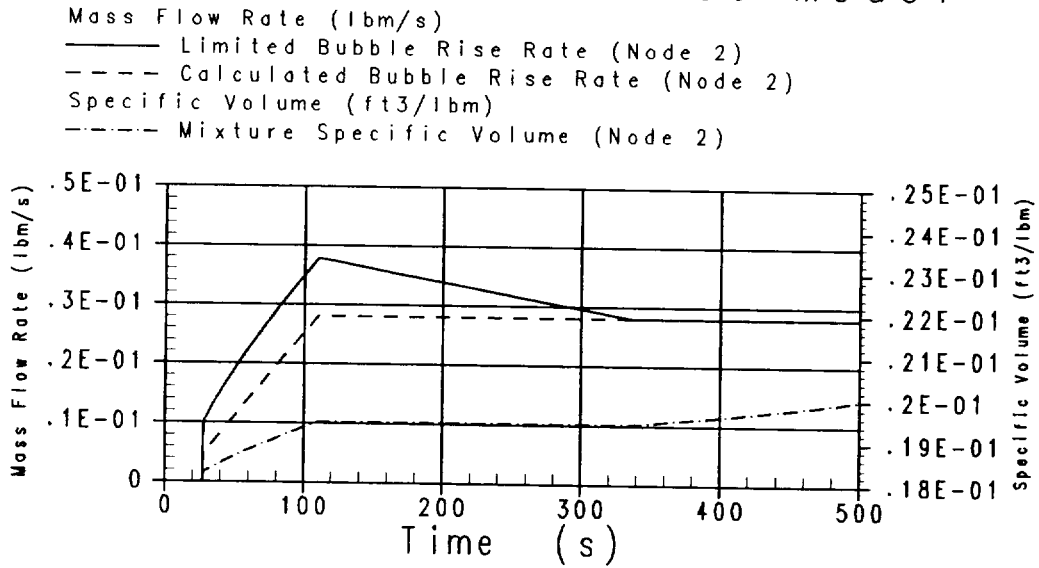


Figure 4.1.1-11 Bubble Rise Massflow and Mix. Sp. Volume Comparison with Restriction

BOILING POT TEST CASE
Explicit Bubble Rise Model

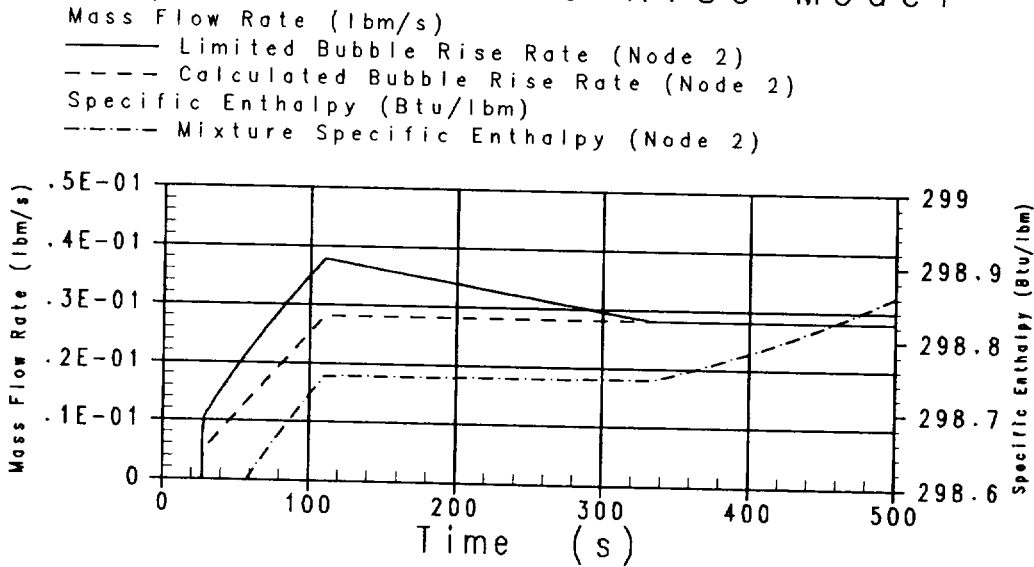


Figure 4.1.1-12 Bubble Rise Massflow and Mix. Sp. Enthalpy Comparison with Restriction

Boiling Pot Test Case
Fixed Time Step = 0.1 sec.
Stack Mixture Level

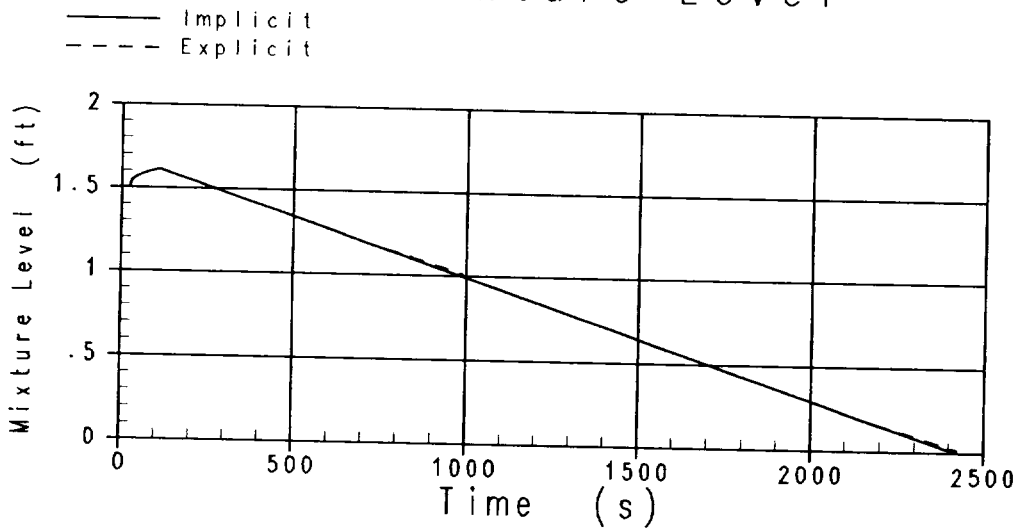


Figure 4.1.1-13 Stack Mixture Level Comparison with Time Step = 0.1 seconds

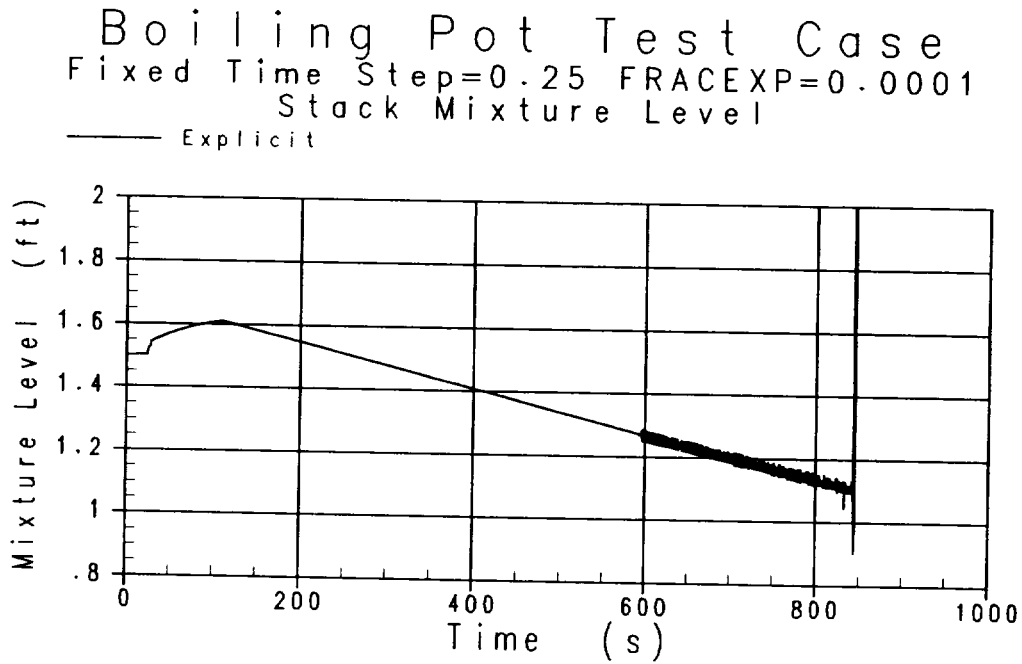


Figure 4.1.1-14 Stack Mixture Level Comparison with Bubble Rise Restriction Circumvented

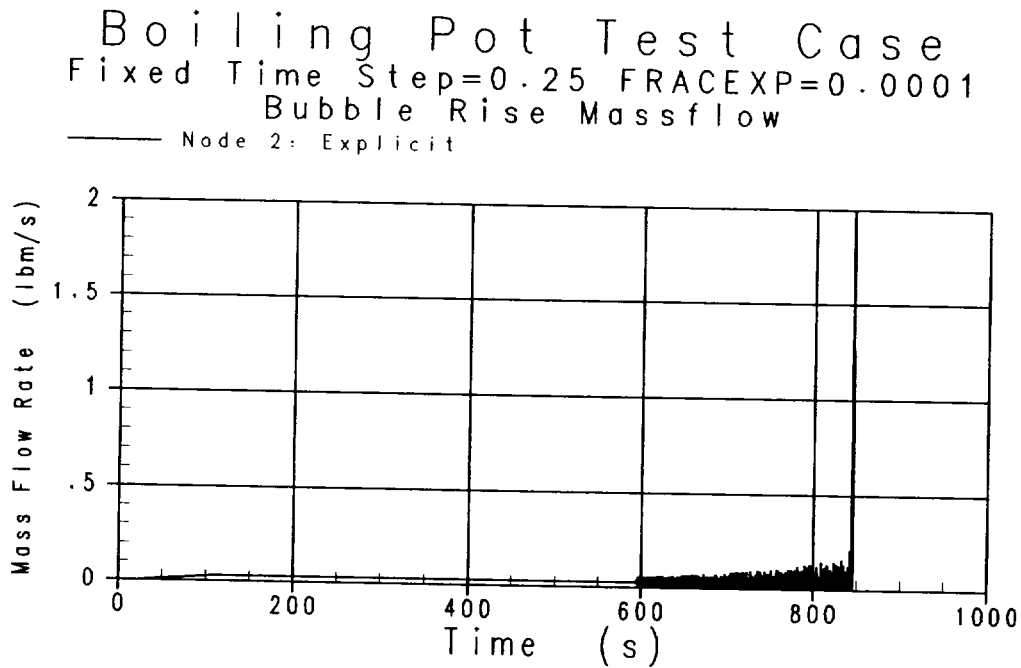


Figure 4.1.1-15 Bubble Rise Mass Flow with Bubble Rise Restriction Circumvented

Boiling Pot Test Case
Fixed Time Step=0.1 FRACEXP=0.0001
Stack Mixture Level
— Node 2: Explicit

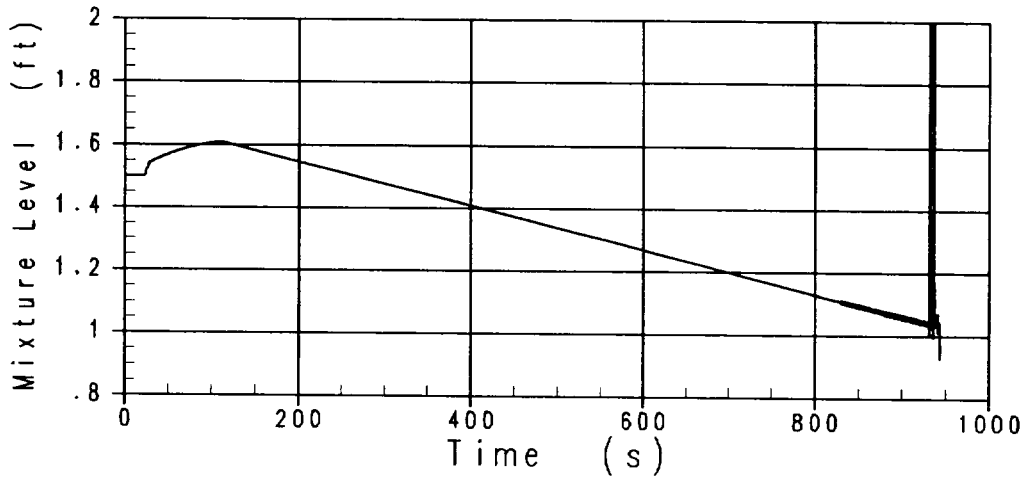


Figure 4.1.1-16 Stack Mixture Level Comparison with Bubble Rise Restriction Circumvented

Boiling Pot Test Case
Fixed Time Step=0.1 FRACEXP=0.0001
Bubble Rise Massflow
— Node 2: Explicit

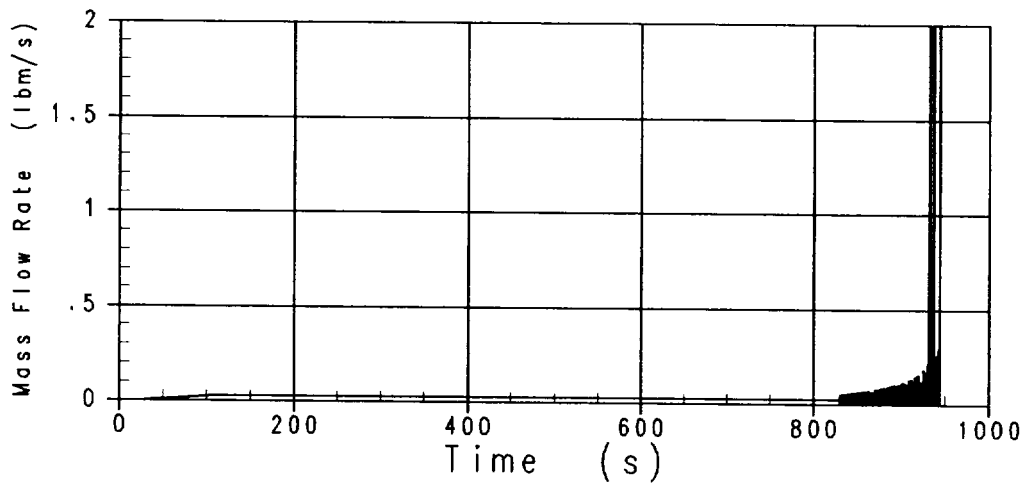


Figure 4.1.1-17 Bubble Rise Mass Flow with Bubble Rise Restriction Circumvented

4.1.2 Validation of Implicit Droplet Fall Model

The purpose of this section is to validate the implementation of the implicit droplet fall model formulation in the NOTRUMP Evaluation Model (EM). This validation will also demonstrate the improvement of using implicit treatment of droplet fall over the explicit droplet fall treatment used in the previous NOTRUMP EM for plant calculations. This demonstration is accomplished by simulating a constant-pressure cooling-pot problem which features the droplet fall process and comparing the results of code calculations where the only difference is the explicit versus implicit treatment of droplet fall. The derivations of the equations associated with both explicit and implicit droplet fall models are contained in Section 2.2 of this report. The following sections describe the simulations performed, a description of the methodology utilized, and the results of the simulations.

4.1.2.1 Droplet Fall Model Test Case Description

In order to validate the droplet fall model, it was necessary to create a simple model which could be utilized for this purpose. A simple two-node model was created, as can be seen in Figure 4.1.2-1, to show the basic droplet fall model behavior between the explicit and implicit model formulations. Energy is removed from the upper region of fluid node 1 via a single critical heat link. The heat being removed is intended to cause vapor condensation to occur in the lower node vapor space, thus activating the droplet fall model as conditions drop below saturation. This process causes the mixture level to subsequently increase until the node eventually fills. It is expected to be at these conditions (i.e., near region full) where the explicit and implicit droplet fall model implementations will show differences in response.

The noding diagram for this model can be seen in Figure 4.1.2-1. The model consists of two fluid nodes. The lower node is defined as an interior fluid node containing an active mixture level. The upper fluid node is a boundary fluid node which is utilized to control system pressure as well as to provide conditions by which the lower node vapor space is fed. This was done to single-effect the droplet fall model response. The bottom node is simply modeled as a 10 foot high cylinder with a cross-sectional area of 0.7854 ft² and an initial mixture level of 0.4 ft. A single non-critical flow link is utilized to connect the lower interior fluid node to the upper boundary fluid node. This is so that as the lower node vapor space is condensed, the boundary node can provide make-up to maintain pressure and vapor space region conditions. The lower fluid node has heat being removed via a single critical heat link connected to a boundary metal node. The model utilizes the NOTRUMP EM Yeh drift flux correlation, general droplet fall model, and the standard core node flooding parameters.

The droplet fall model validation test cases are designed to demonstrate the impact of switching from the previous NOTRUMP EM explicit formulation to the more stable implicit formulation. As these particular test cases are simple "thought" problems

developed for the purpose of demonstrating implicit versus explicit features of droplet fall, there is no intention here to validate results with experimental test data. All that is being assessed here is the relative performance of the explicit and implicit treatments in providing results judged to be more reasonable or stable.

The following enhanced model features are activated in all of the test cases presented here:

1. Implicit bubble rise model (described in Section 2.1).
2. Implicit fluid node gravitational head model (described in Section 2.3).
3. Semi-Implicit metal node model (described in Section 2.4).
4. Improved region depletion model (described in Section 2.5).

The following cases are performed:

1. Fully implicit - includes the implicit droplet fall model in addition to all of the above features, with 0.25 maximum time step size.
2. Same as 1 except with explicit droplet fall model.
3. Same as 1 with 0.01 maximum time step size.
4. Same as 3 except with explicit droplet fall model.

In all of these simulations, heat is removed from the vapor space at a constant rate following a 10 second ramp up starting at 100 seconds. The following section compares the test results with the expected results for the cases described above.

4.1.2.2 Comparison of Test Results with Expected Results

To validate that the implicit treatment of the droplet fall model is implemented correctly, the results of the implicit versus explicit treatments are compared to each other (using plot comparisons of key quantities). The expected result is that the implicit and explicit solutions will converge as the time step size is reduced. It is expected that by switching to the implicit formulation, as the mixture level increases, the behavior of droplet fall will be stable as will fluid node vapor space properties. This will allow for a more continuous transition of the fluid node mixture level across nodal boundaries by maintaining consistent properties.

4.1.2.2.1 Case 1 - Fully Implicit Model With 0.25 Maximum Time Step Size

The fully implicit treatment of the droplet fall model is expected to result in a nearly constant calculation of droplet fall rates for the given conditions. As can be seen in Figures 4.1.2-2 - 4.1.2-6, that's exactly what was obtained for this test simulation. In Figures 4.1.2-4 - 4.1.2-6, the vapor space conditions respond as expected to the heat removal process, causing a drop in the region enthalpy and void fractions. As the void fraction decreases, nodal droplet fall is activated (Figure 4.1.2-6) and equilibrium

conditions are achieved. As can be observed, the calculated droplet fall rate remains constant until the node completely fills to the 10 foot elevation at approximately 560 seconds. This is the expected response.

4.1.2.2.2 Case 2 - Explicit Droplet Fall Model With 0.25 Maximum Time Step Size

The explicit treatment of the droplet fall model is expected to result in oscillatory behavior of the calculated droplet fall rate when the region becomes small (i.e., node filling). The reason for this is that the calculated droplet fall rate for the time step can be larger than the available inventory, thereby resulting in oscillatory flow behavior. The results included in this section are presented in the form of comparison plots to the implicit model results. As can be seen from Figures 4.1.2-7 - 4.1.2-12, the expected results are not what was obtained. Instead of the expected oscillatory behavior in the droplet fall model flow rate, variations in the vapor region nodal properties were obtained.

In an effort to understand these unexpected results, the explicit and implicit droplet fall formulations were reviewed. As explained in Section 2.2.2, the explicit droplet fall treatment in NOTRUMP applies a restriction on the droplet fall mass flow rate in an attempt to prevent the depletion of the current liquid mass in the node's vapor region in a given time step. The intent of this restriction is to prevent the material Courant limit from being violated by limiting the explicit droplet fall mass flow rate (instead of the more traditional approach of limiting the time step size) as the vapor region is depleted. However, this restriction is not sufficiently restrictive, due to its use of too large a liquid mass in the limit expression. Instead of using either a predicted average value that applies over the time step or a predicted end-of-time step value, the limit expression uses the liquid mass that exists in the vapor region at the beginning of the time step. The use of the beginning of step value is too large in a depleting vapor region situation; consequently, the restriction does not enforce the material Courant limit. The material Courant limit violation manifests itself in an abnormal solution of the vapor region total energy, and thereafter in the vapor region calculated thermodynamic properties.

The timing of the restriction implementation in this case occurs at ~500 seconds as can be seen in Figure 4.1.2-9. The effect of the material Courant limit violation can be seen in the abnormal changes in the vapor region properties of void fraction, and specific enthalpy (Figures 4.1.2-10 - 4.1.2-11). The impact of the elimination of the explicit droplet fall restriction will be investigated in Section 4.1.2.3 to demonstrate that the expected results of an explicit droplet fall model implementation can indeed be obtained.

4.1.2.2.3 Case 3 - Fully Implicit Model With 0.01 Maximum Time Step Size

This case is utilized for a comparison to the explicit droplet fall simulation performed in Section 4.1.2.2.4. It is expected that this case will perform virtually identically to that in Section 4.1.2.2.1 above.

Figures 4.1.2-13 - 4.1.2-15 present the comparison plots between the base implicit and reduced time step results. As can be seen, the results are indeed virtually identical as expected. Therefore, no additional discussion will be provided.

4.1.2.2.4 Case 4 - Explicit Droplet Fall Model With 0.01 Maximum Time Step Size

The purpose of this case is to demonstrate that as the maximum time step size is reduced for the explicit formulation, the results between the implicit and explicit droplet fall simulations will converge. This means that the time at which instability, or in this case reaching the restriction, will be reached will be delayed relative to the 0.25 time-step size case.

By comparing Figures 4.1.2-9 and 4.1.2-16, it can be seen that the time at which the restriction is reached is delayed from approximately 500 seconds to 557 seconds as expected. Figure 4.1.2-17 demonstrates that the results between the two formulations (implicit vs. explicit) are not as one would expect (per the discussion in Section 4.1.2.2.2) due to the restriction application. The impact of removing the explicit droplet fall restriction will be examined in Section 4.1.2.3 to further clarify the argument.

4.1.2.3 Explicit Formulation Sensitivity Studies

This section details the results of the two-node model droplet fall validation cases with the restriction disabled. In order to circumvent the restriction on the droplet fall mass flow rate with code input (and not have to modify the code), it was necessary to employ a constant time step size. Only two cases will be performed both of these being for the explicit droplet fall formulation which were affected by the restriction. The cases performed are:

1. Explicit droplet fall with 0.25 time step size with the restriction disabled.
2. Explicit droplet fall with 0.01 time step size with the restriction disabled.

4.1.2.3.1 Case 1 - Explicit Droplet Fall Model With 0.25 Time Step With The Restriction Disabled

It is expected that with the restriction removed, the explicit droplet fall formulation will exhibit the traditional oscillatory behavior which would accompany the region depletion.

As can be seen in Figures 4.1.2-18 - 4.1.2-21, the expected results were obtained with the mixture level, droplet fall flow rate and region void fractions undergoing oscillations as the vapor region is depleted. This compares to the stable near constant behavior of the implicit model formulation seen in the same figures. The following section will look at the reduced time-step size case to determine if the fidelity between the implicit and explicit droplet fall formulation will converge.

4.1.2.3.2 Case 2 - Explicit Droplet Fall Model With 0.01 Time Step With The Restriction Disabled

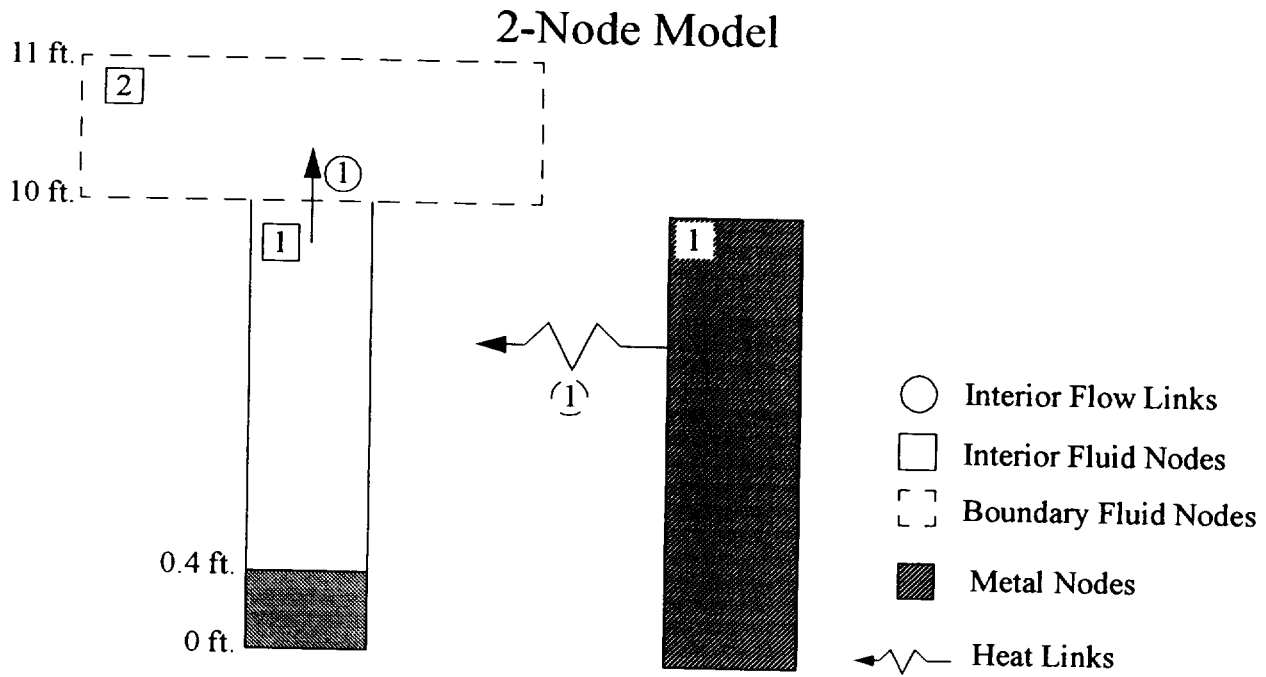
Once again, it is expected that with the restriction removed and the time step reduced, the time at which the explicit droplet fall formulation will exhibit oscillatory behavior which accompanies region depletion will be delayed.

As can be seen in Figures 4.1.2-22 - 4.1.2-25, the results are as expected with the unlimited droplet fall rate resulting in flow oscillations similar to those observed in Section 4.1.2.3.1, albeit delayed due to the time step size reduction. At this point, the implicit droplet fall model has been implemented appropriately and can be considered adequately validated.

4.1.2.4 Droplet Fall Model Simulation Conclusions

Based on the results of the simulations performed in the previous sections, the following conclusions can be reached:

1. The implementation of the implicit droplet fall model improves region properties as the region is depleted over the explicit droplet fall model. This will result in improved continuity when mixture levels cross fluid node boundaries. In addition, the implicit droplet fall model behaves as expected; therefore, it is appropriate for use.
2. The implicit droplet fall treatment is validated via favorable comparisons with explicit droplet fall treatment at small time steps and provides a more stable and smooth calculation compared to the explicit treatment, especially at larger time steps. Therefore, the implicit droplet fall model should be used as the new default NOTRUMP EM for plant calculations.
3. From the above documentation, explicit methods for droplet fall should not be utilized where implicit methods are available.



Cooling Pot Case (Droplet Fall Verification Model)

Figure 4.1.2-1 Two-Node Droplet Fall Model Noding Diagram

Droplet Fall Model Validation, $D_{tmax}=0.25$ Node 1 Pressure

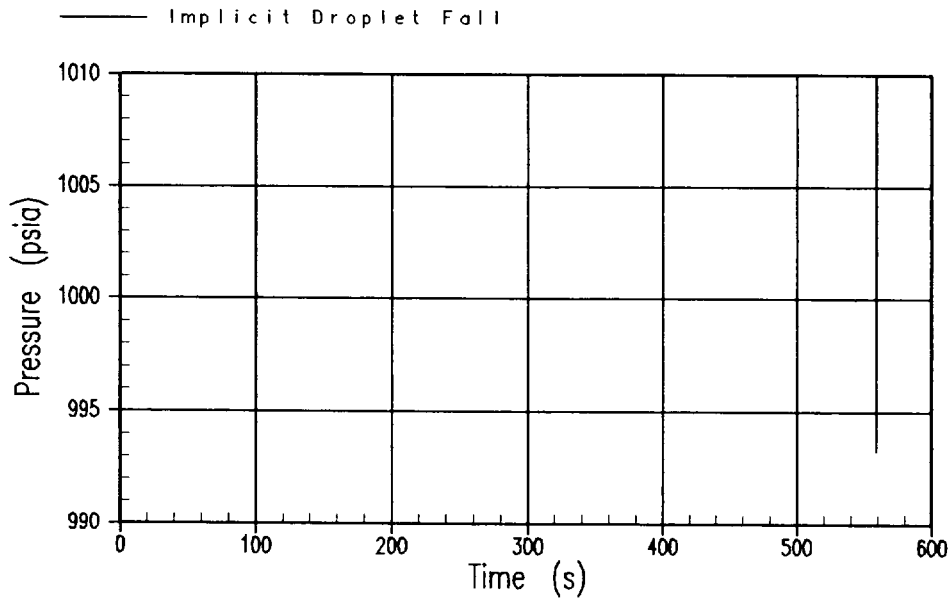


Figure 4.1.2-2 Implicit Model, Node Pressure

Droplet Fall Model Validation, $D_{tmax}=0.25$ Node 1 Mixture Level

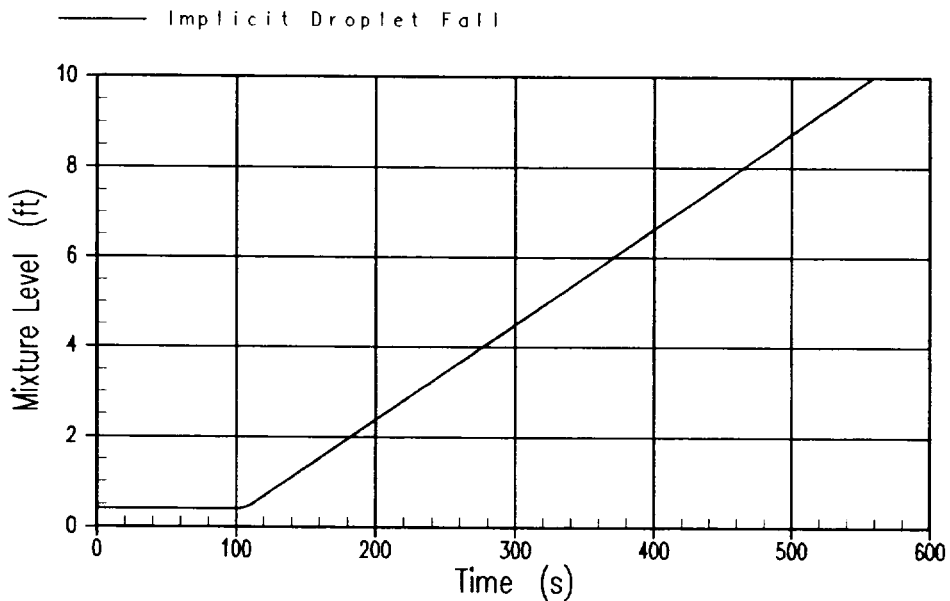


Figure 4.1.2-3 Implicit Model, Mixture Level

Droplet Fall Model Validation, $D_{tmax}=0.25$ Node 1 Vapor Region Void Fraction

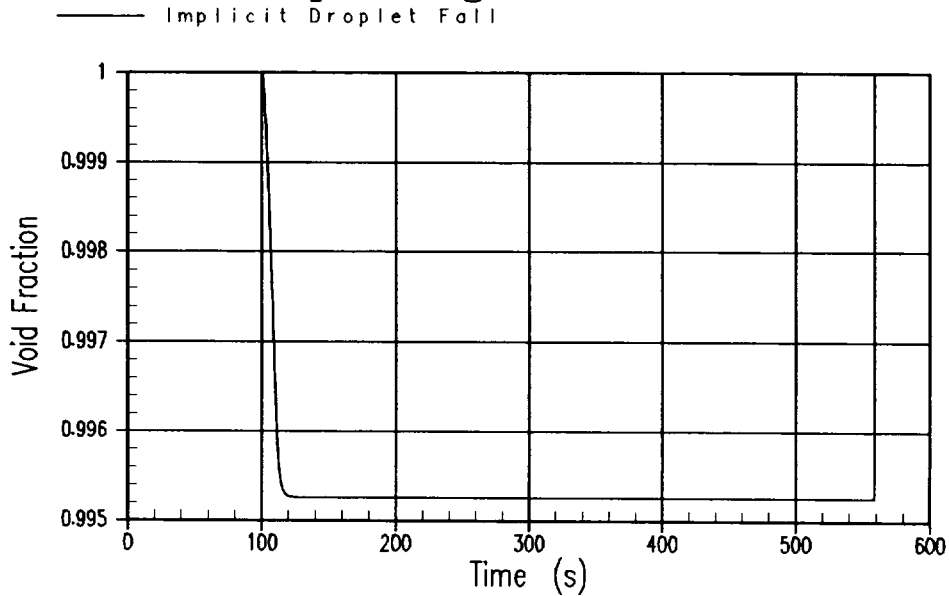


Figure 4.1.2-4 Implicit Model, Vapor Void Fraction

Droplet Fall Model Validation, $D_{tmax}=0.25$ Node 1 Vapor Region Enthalpy

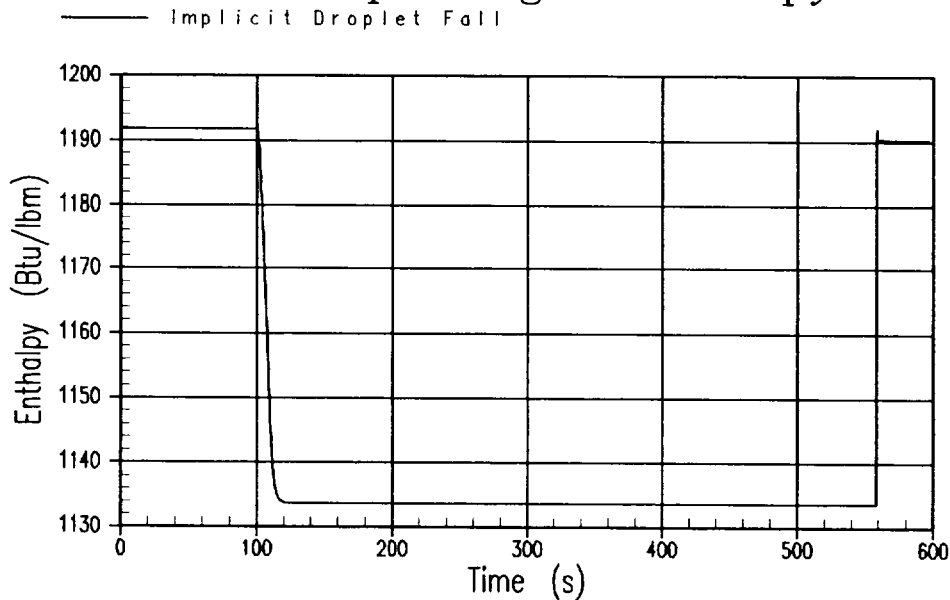


Figure 4.1.2-5 Implicit Model, Vapor Region Enthalpy

Droplet Fall Model Validation, $D_{tmax}=0.25$ Node 1 Droplet Fall Mass Flow

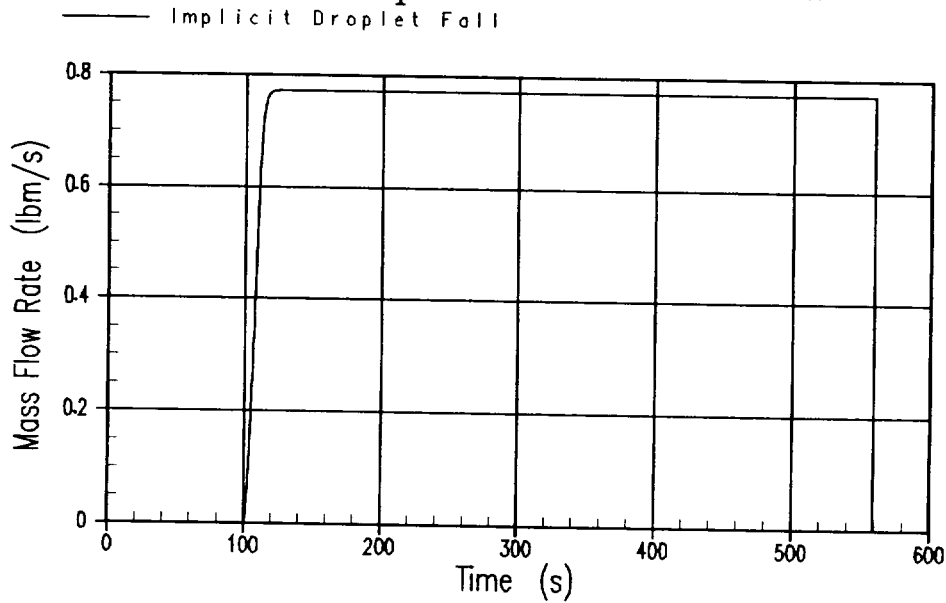


Figure 4.1.2-6 Implicit Model, Droplet Fall Rate

Droplet Fall Model Validation, $D_{tmax}=0.25$ Node 1 Pressure

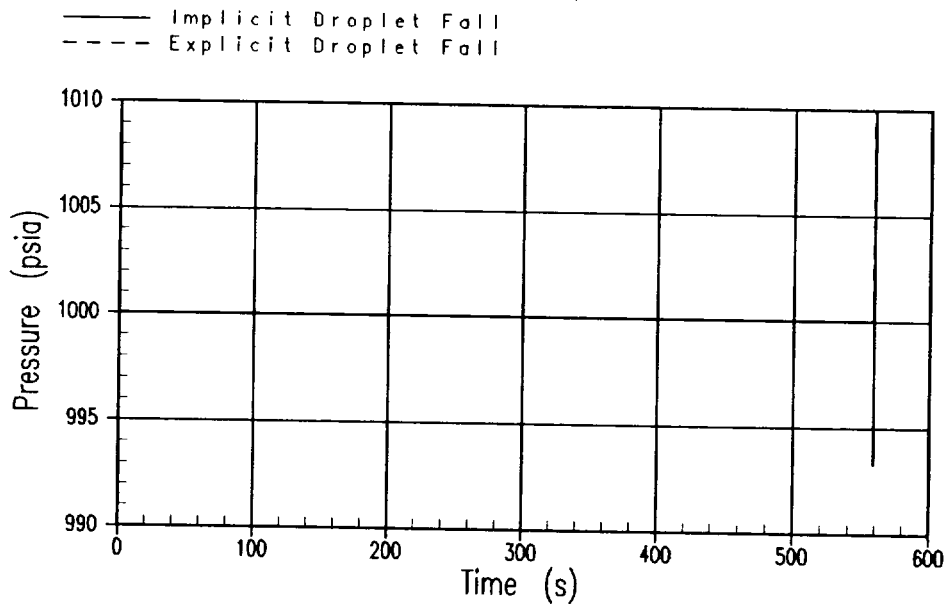


Figure 4.1.2-7 Comparison of Implicit vs. Explicit, $DTMAX=0.25$, Node Pressure

Droplet Fall Model Validation, $Dt_{max}=0.25$ Node 1 Mixture Level

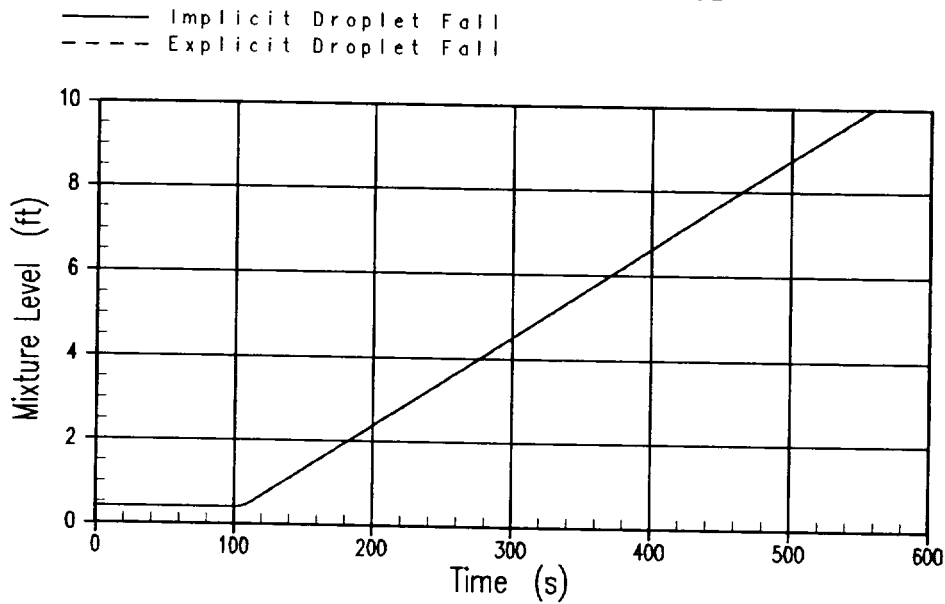


Figure 4.1.2-8 Comparison of Implicit vs. Explicit, $DTMAX=0.25$, Mixture Level

Droplet Fall Model Validation, $Dt_{max}=0.25$ Node 1 Droplet Fall Mass Flow Rate

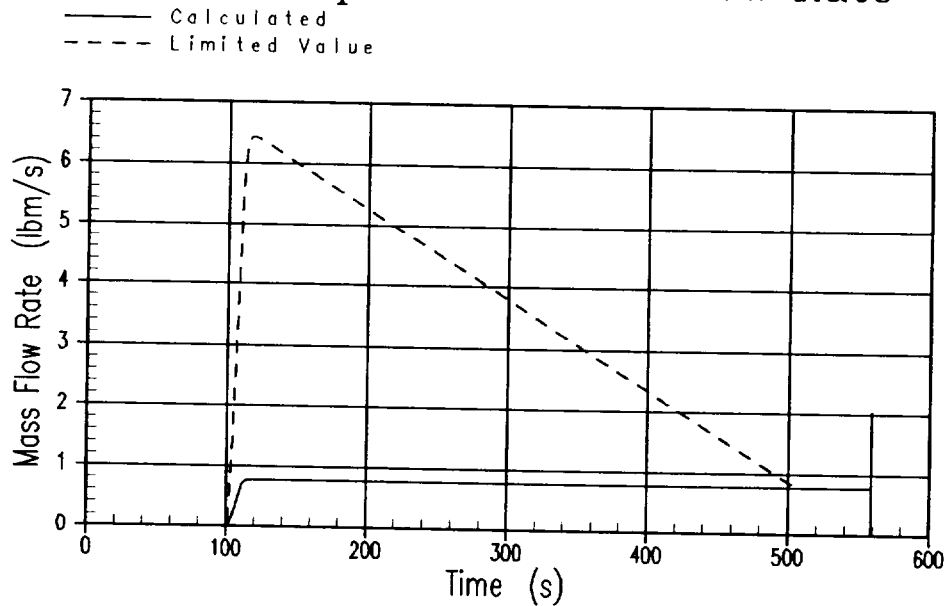


Figure 4.1.2-9 Explicit Droplet Fall Model, $DTMAX=0.25$, with Restriction

Droplet Fall Model Validation, $Dt_{max}=0.25$ Node 1 Vapor Region Void Fraction

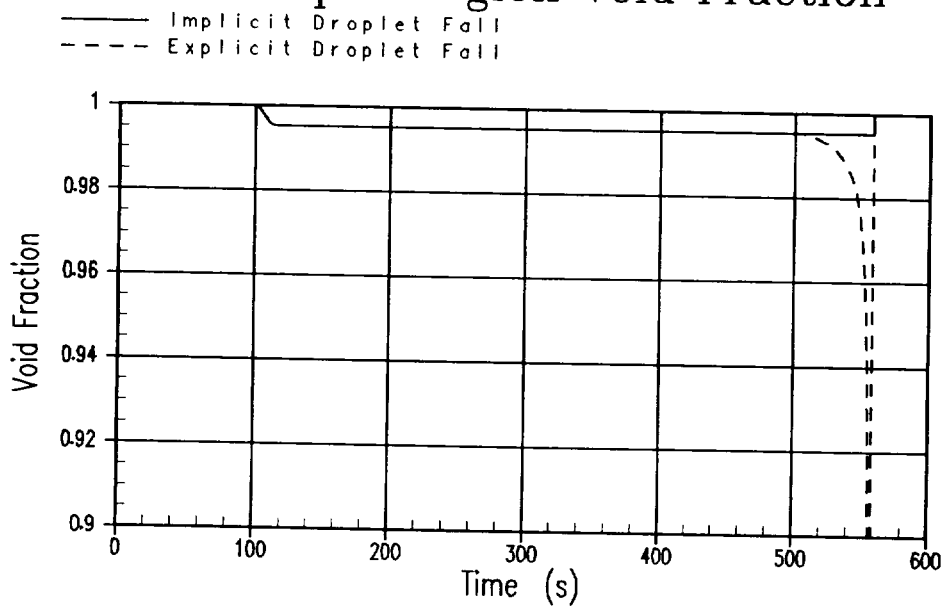


Figure 4.1.2-10 Comparison of Implicit vs. Explicit, $DTMAX=0.25$, Vapor Void Fraction

Droplet Fall Model Validation, $Dt_{max}=0.25$ Node 1 Vapor Region Enthalpy

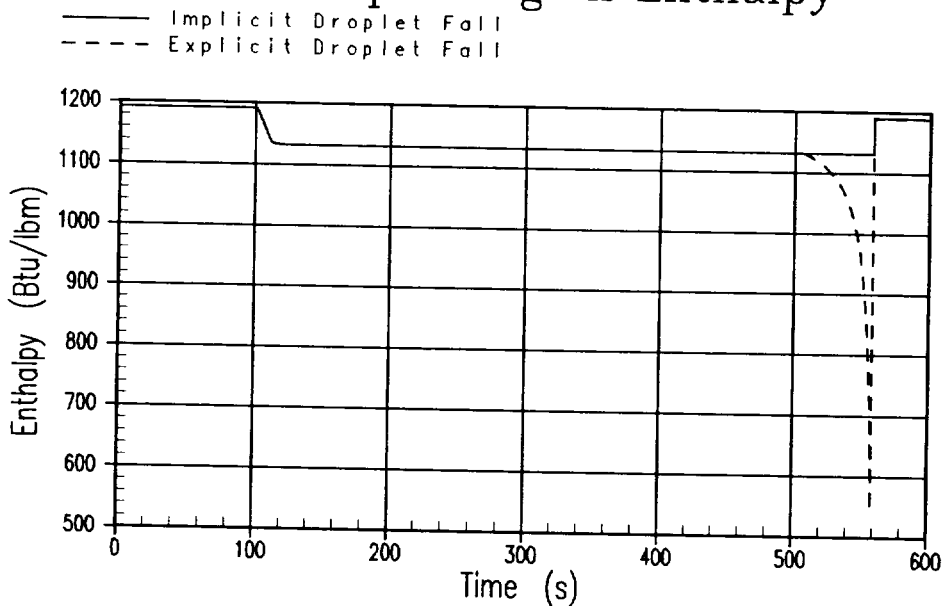


Figure 4.1.2-11 Comparison of Implicit vs. Explicit, $DTMAX=0.25$, Vapor Enthalpy

Droplet Fall Model Validation, $D_{tmax}=0.25$ Node 1 Droplet Fall Mass Flow

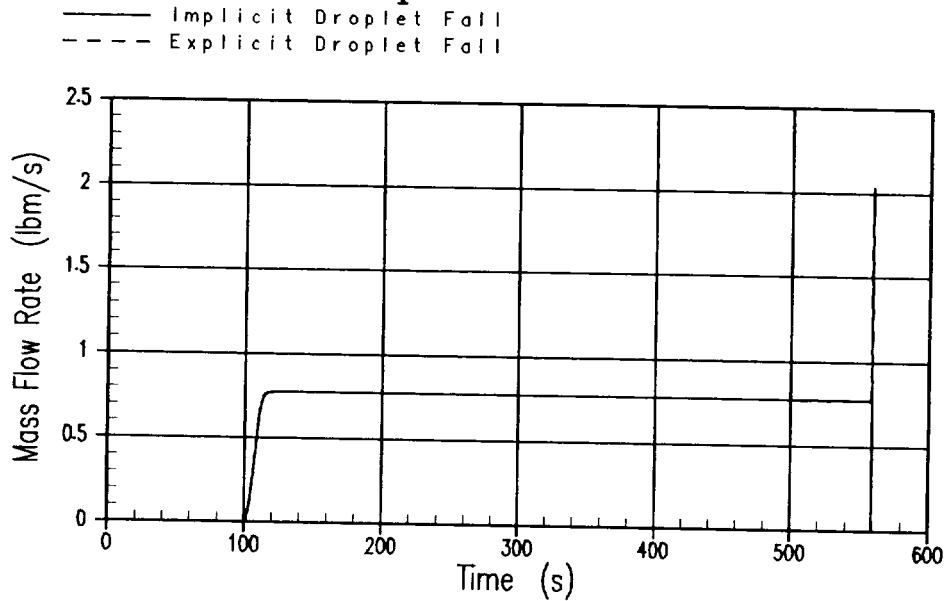


Figure 4.1.2-12 Comparison of Implicit vs. Explicit, $DTMAX=0.25$, Droplet Fall Rate

Droplet Fall Model Validation Node 1 Mixture Level

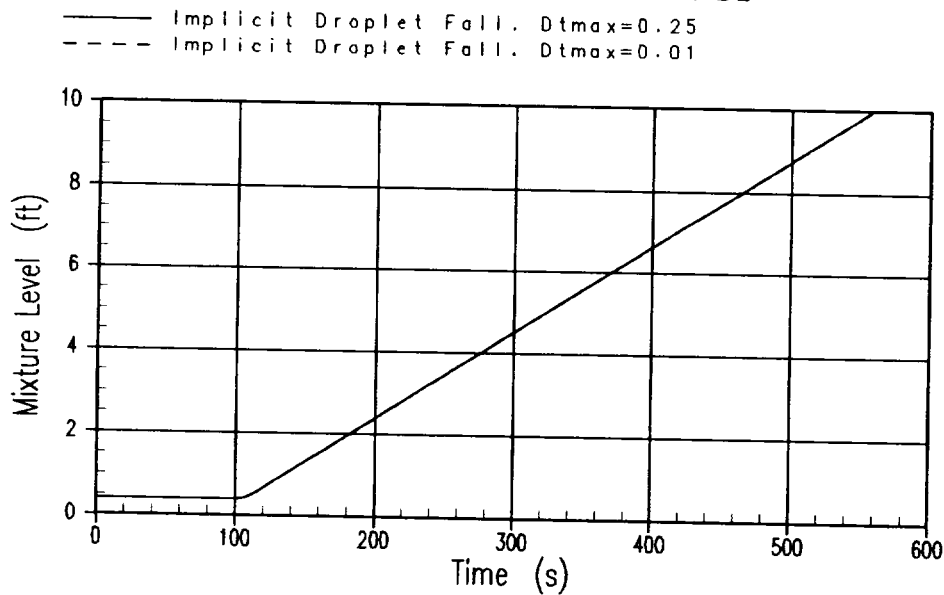


Figure 4.1.2-13 Implicit Model, DT Study, Mixture Level

Droplet Fall Model Validation Node 1 Vapor Region Enthalpy

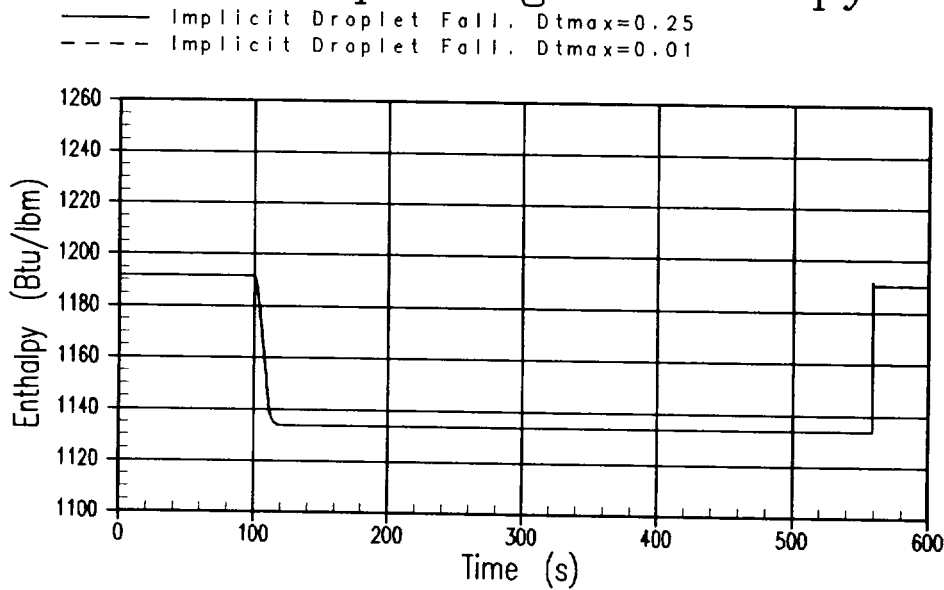


Figure 4.1.2-14 Implicit Model, DT Study, Vapor Enthalpy

Droplet Fall Model Validation Node 1 Droplet Fall Mass Flow

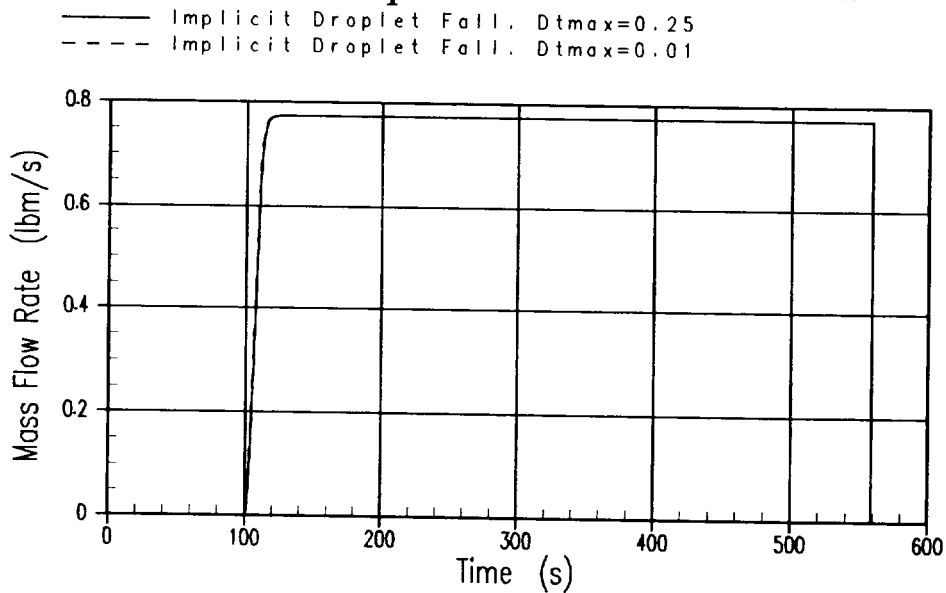


Figure 4.1.2-15 Implicit Model, DT Study, Droplet Fall Rate

Droplet Fall Model Validation Dt=0.01 Node 1 Droplet Fall Mass Flow Rate

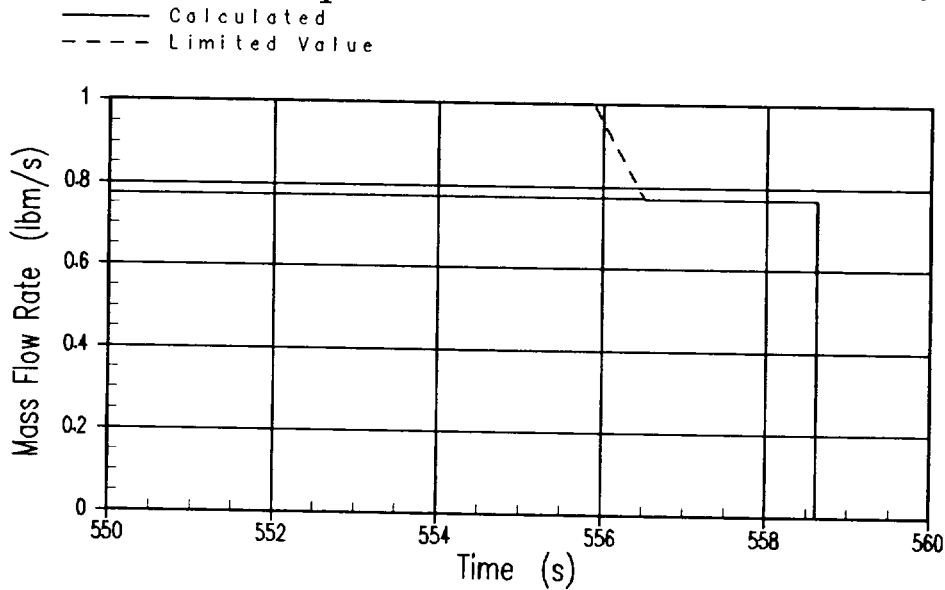


Figure 4.1.2-16 Explicit Droplet Fall Model, DT Study, with Restriction

Droplet Fall Model Validation Dt=0.01 Node 1 Vapor Region Void Fraction

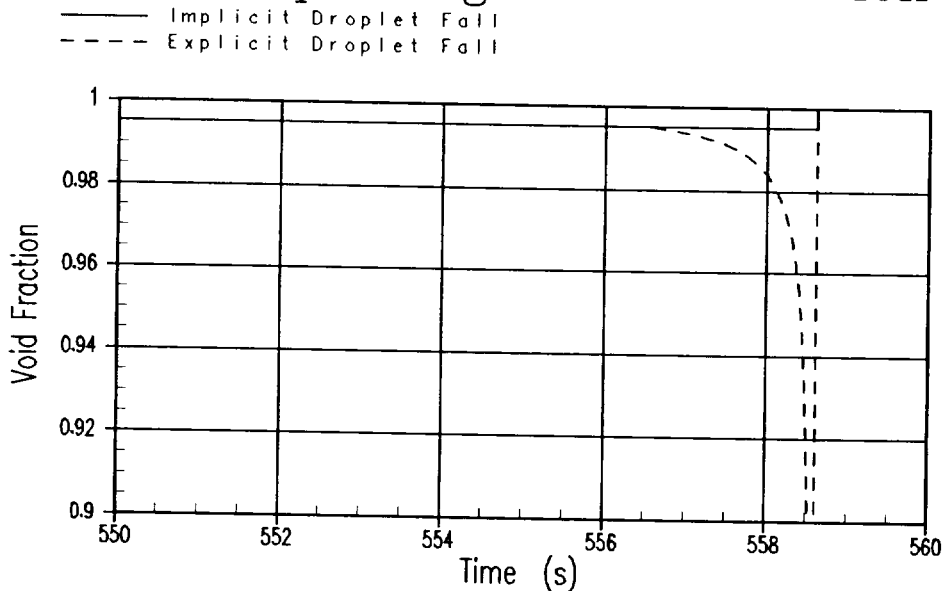


Figure 4.1.2-17 Comparison of Implicit vs. Explicit, DTMAX=0.01, Vapor Void Fraction

Droplet Fall Model Validation, $D_{tmax}=0.25$ Node 1 Mixture Level

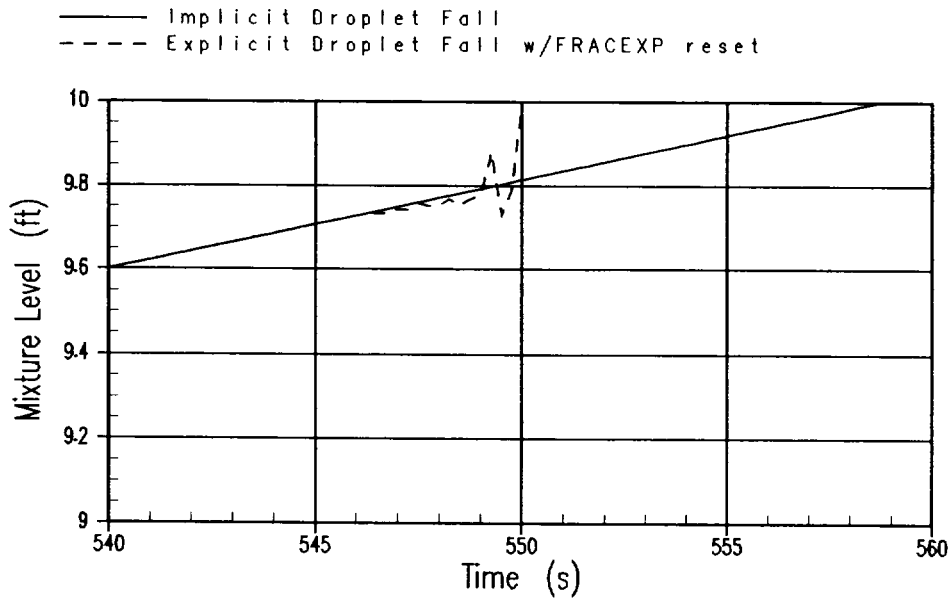


Figure 4.1.2-18 Explicit Droplet Fall Model, Restriction Disabled, $DTMAX=0.25$, Mixture Level

Droplet Fall Model Validation, $D_{tmax}=0.25$ Node 1 Droplet Fall Mass Flow Rate

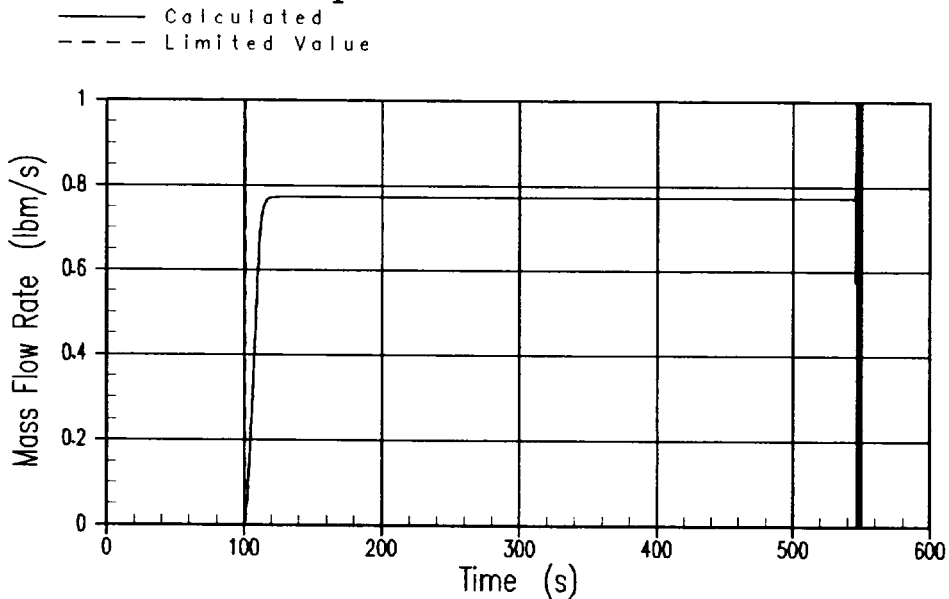


Figure 4.1.2-19 Explicit Droplet Fall Model, Restriction Disabled, $DTMAX=0.25$

Droplet Fall Model Validation, $Dt_{max}=0.25$ Node 1 Droplet Fall Mass Flow

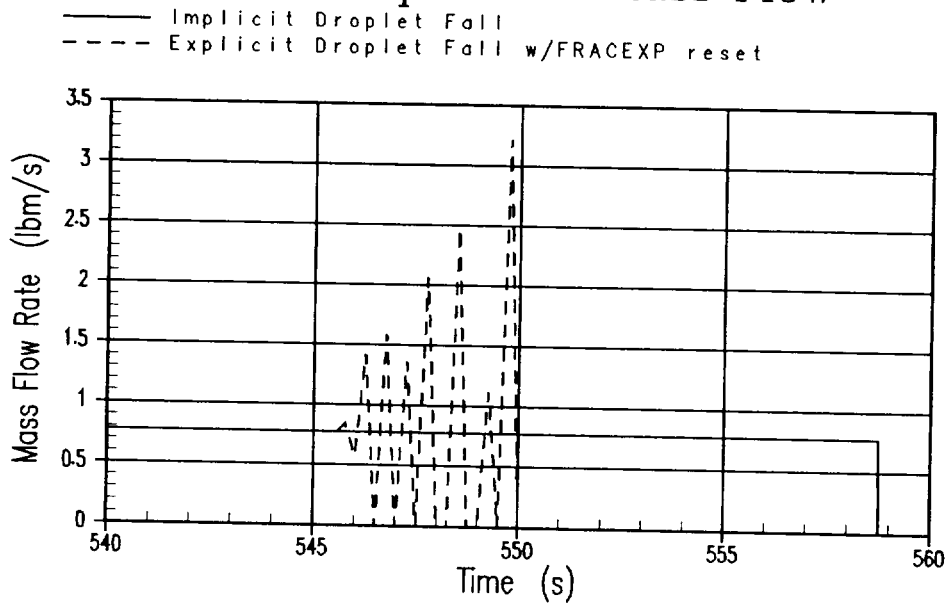


Figure 4.1.2-20 Explicit Droplet Fall Model, Restriction Disabled, $DTMAX=0.25$, Droplet Fall Rate

Droplet Fall Model Validation, $Dt_{max}=0.25$ Node 1 Vapor Region Void Fraction

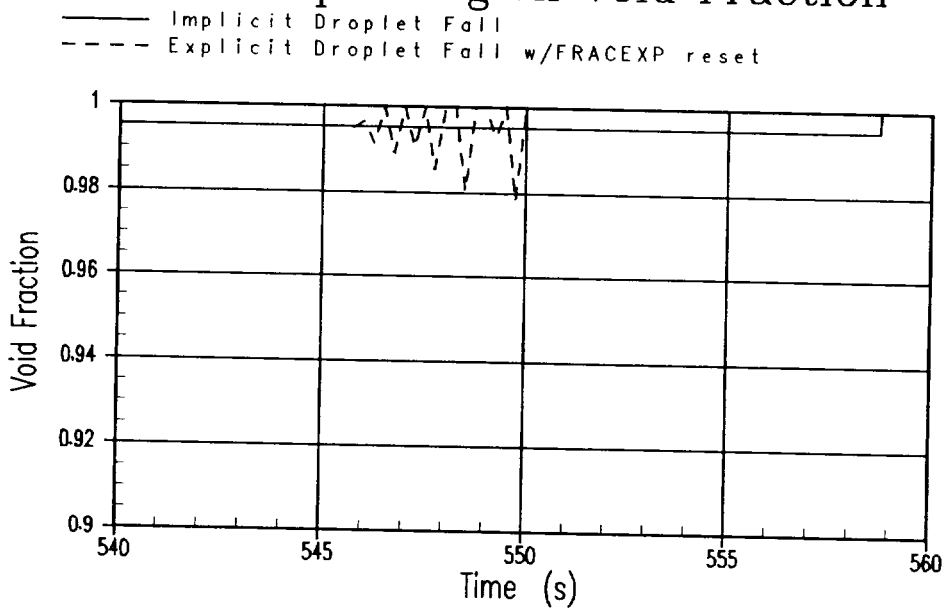


Figure 4.1.2-21 Explicit Droplet Fall Model, Restriction Disabled, $DTMAX=0.25$, Vapor Void Fraction

Droplet Fall Model Validation, Dt=0.01 Node 1 Mixture Level

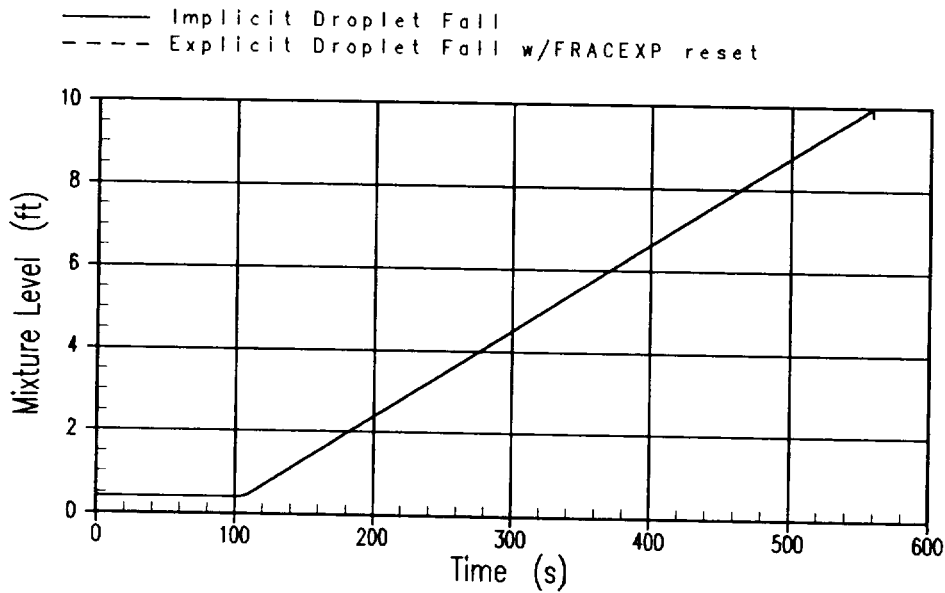


Figure 4.1.2-22 Explicit Droplet Fall Model, Restriction Disabled, DTMAX=0.01, Mixture Level

Droplet Fall Model Validation Dt=0.01 Node 1 Droplet Fall Mass Flow Rate

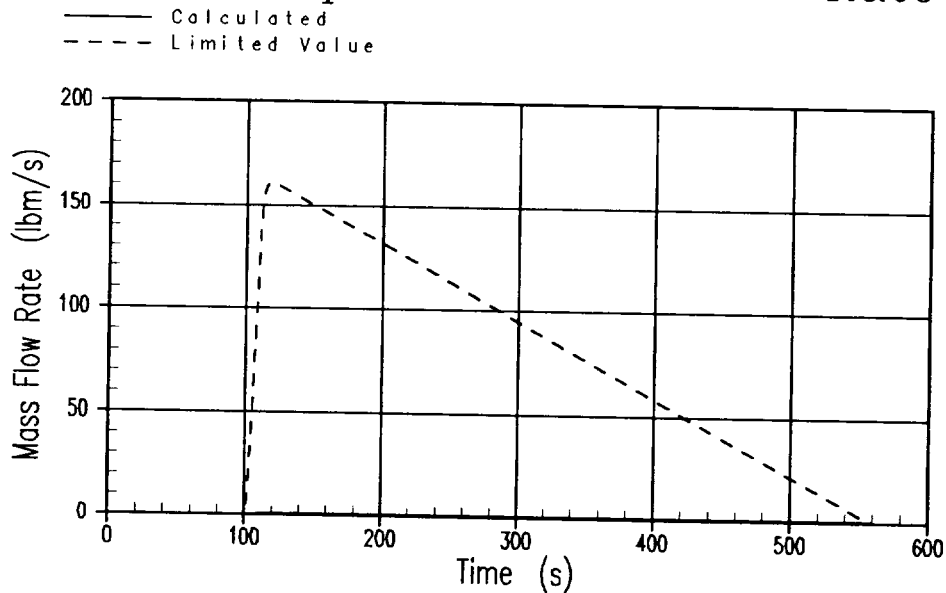


Figure 4.1.2-23 Explicit Droplet Fall Model, Restriction Disabled, DTMAX=0.01

Droplet Fall Model Validation, Dt=0.01 Node 1 Droplet Fall Mass Flow Rate

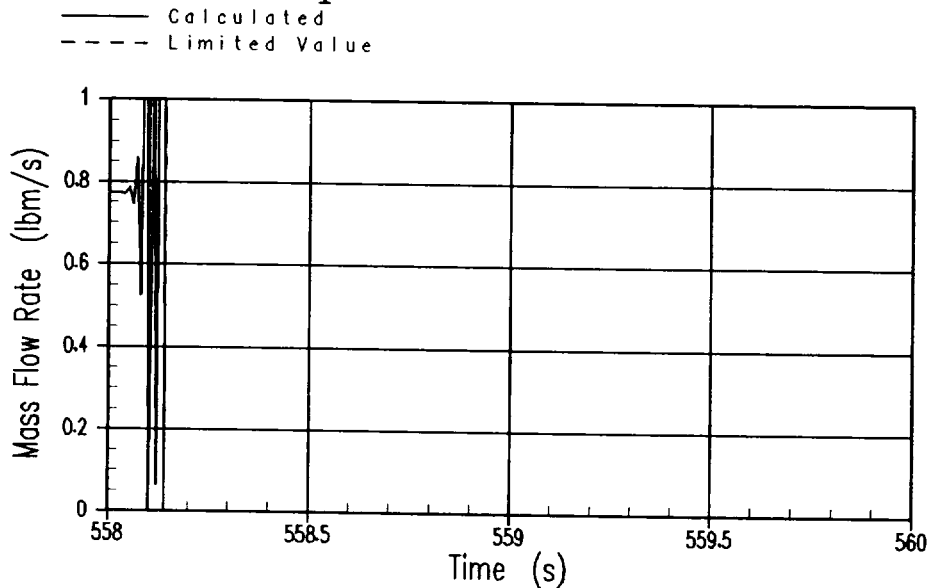


Figure 4.1.2-24 Explicit Droplet Fall Model, Restriction Disabled, DTMAX=0.01, Droplet Fall Rate

Droplet Fall Model Validation, Dt=0.01 Node 1 Droplet Fall Mass Flow

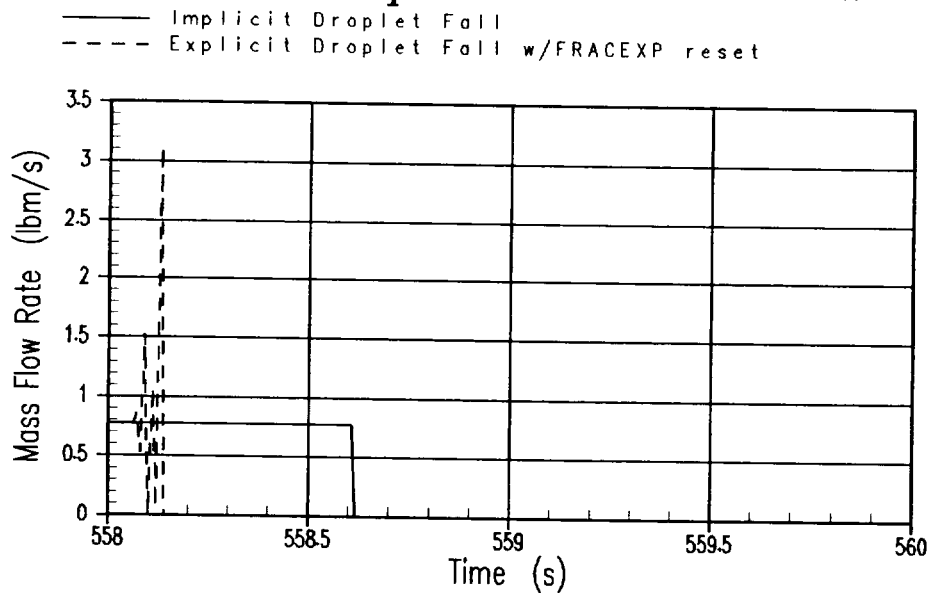


Figure 4.1.2-25 Explicit Droplet Fall Model, Restriction Disabled, DTMAX=0.01, Droplet Fall Rate

4.1.3 Validation of Implicit Fluid Node Gravitational Head Model

The purpose of this section is to validate the implementation of the implicit fluid node gravitational head model formulation in the NOTRUMP Evaluation Model (EM). In the previous NOTRUMP EM, the fluid node gravitational head model is treated explicitly. The use of the implicit treatment of the model is expected to be a benefit for code stability. The derivations of the implicit fluid node gravitational head model are discussed in Section 2.3 of this report. The following subsections describe the test cases and the comparison of test results versus expected results for the validation of the implicit fluid node gravitational head model.

4.1.3.1 Description of Test Cases

In the NOTRUMP EM, the fluid node gravitational head model applies at the upstream and downstream ends of mass flow-based non-critical flow links that are modeled as either point-contact or continuous-contact flow links. The latter includes both regular continuous-contact flow links, and horizontally stratified flow link (HSFL) pair continuous-contact flow links. To validate the implicit formulation of the fluid node gravitational head model for the aforementioned situations, a simple thought problem was developed. This same thought problem is used for three independent test subcases that are all included in the same NOTRUMP run for convenience. The noding diagrams for these three independent test subcases are shown in Figures 4.1.3-1 through 4.1.3-3.

The first of the three independent test subcases in Figure 4.1.3-1 consists of interior fluid nodes 1 and 2, each of which is 10.0 ft. high, 10.0 ft.³ in volume, and modeled with two-region capability. These interior fluid nodes are connected to each other by horizontal non-critical flow link 1 at a centerline elevation of 5.0 ft. Non-critical flow link 1 has a diameter of 2.0 ft., a length of 1.0 ft., a constant friction (fL/D) value of 1.0, and is modeled as a continuous-contact flow link. Interior fluid nodes 1 and 2 are each connected at the top to constant-pressure boundary fluid node 20, by point contact non-critical flow links 20 and 21, respectively, to maintain system pressure. Non-critical flow links 20 and 21 have an area of 1.0 ft.², a length of 1.0 ft., and a constant friction (fL/D) value of 0.01. Interior fluid node 1 is connected at the bottom to boundary fluid node 50, by critical flow link 50, for removal of mixture region material.

The problem is initialized to a non-equilibrium condition with a high (9.5 ft.) mixture level in interior fluid node 1, and a low (0.5 ft.) mixture level in interior fluid node 2. The initial pressure in all fluid nodes is 1000.0 psia. Single-phase fluids are employed for simplicity. The mixture regions are initialized subcooled with a specific enthalpy of 50.0 Btu/lbm, and the vapor regions are initialized superheated with a specific enthalpy of 1300.0 Btu/lbm. The initial mass flowrate in all flow links is zero. The simulation is run for 10.0 seconds. After the mixture levels in both interior fluid nodes have had a chance to equilibrate (or approach a near equilibrium state), critical flow link 50 is activated for

removal of mixture region material, beginning at a transient time of 5.0 seconds (the critical flow link mass flow rate is ramped from 0.0 to 100.0 lbm/sec from 5.0 to 10.0 seconds transient time). The purpose of this simulation is to drive at least one end of non-critical flow link 1 through all of the applicable regimes (mixture level above the top of the flow link, mixture level within the diameter of the flow link, and mixture level below the bottom of the flow link).

The second of the three independent test subcases in Figure 4.1.3-2 utilizes a point-contact horizontal non-critical flow link, and is identical to the first test subcase, except in the following ways:

1. The interior fluid nodes are numbered 3 and 4.
2. The horizontal non-critical flow link that connects interior fluid nodes 3 and 4 is numbered 2, and is modeled as a point-contact flow link.
3. The point contact non-critical flow links that connect interior fluid nodes 3 and 4 at the top to boundary fluid node 20 are numbered 22 and 23, respectively.
4. The critical flow link that connects interior fluid node 3 at the bottom to boundary fluid node 50 is numbered 51.

The third of the three independent test subcases in Figure 4.1.3-3 utilizes a horizontally stratified flow link (HSFL) pair, and is identical to the first or second test subcase, except in the following ways:

1. The interior fluid nodes are numbered 5 and 6.
2. The horizontal flow path that connects interior fluid nodes 5 and 6 is modeled as a HSFL pair, numbered 3 (liquid flow link) and 4 (vapor flow link).
3. The point contact non-critical flow links that connect interior fluid nodes 5 and 6 at the top to boundary fluid node 20 are numbered 24 and 25, respectively.
4. The critical flow link that connects interior fluid node 5 at the bottom to boundary fluid node 50 is numbered 52.

For the validation of the implicit fluid node gravitational head model, the following test cases are performed, each of which includes all three of the aforementioned subcases:

1. Base Case, with the implicit treatment of the fluid node gravitational head model, and the NOTRUMP EM maximum (0.25 seconds) and minimum (0.001 seconds) time step sizes.
2. Same as Case 1, but with the explicit treatment of the fluid node gravitational head model.

The results of Case 1 will be compared to the results of Case 2 in Section 4.1.3.2. To illustrate convergence of the implicit and explicit formulations of the fluid node gravitational head model, Cases 1 and 2 are rerun with a constant time step size of

0.001 seconds, in order to obtain a step-for-step equivalent comparison, as follows (with Cases 3 and 4):

3. Same as Case 1, but with a constant time step size of 0.001 seconds.
4. Same as Case 2, but with a constant time step size of 0.001 seconds.

The results of Case 3 will be compared to the results of Case 4 in Section 4.1.3.2.

All of the aforementioned test cases employ the other applicable enhanced model features that are being implemented in the new NOTRUMP EM, which are:

1. Implicit bubble rise model (described in Section 2.1).
2. Implicit droplet fall model (described in Section 2.2).

Note that the improved region depletion model (i.e., mixture level overshoot model) does not apply here, since there are no fluid node stacks, and the semi-implicit metal node model does not apply here, since there are no metal nodes.

4.1.3.2 Comparison of Test Results with Expected Results

To validate that the implicit treatment of the fluid node gravitational head model is implemented correctly, the results of the implicit versus explicit treatments are compared to each other (using plot comparisons of key quantities). The expected result is that the implicit and explicit solutions will converge as the time step size is reduced. It is also expected that the natural oscillating mixture level behavior in the cases will be more damped with the implicit fluid node gravitational head treatment as the time step size is increased. This is the case due to the numerical damping that occurs with implicit methods, which permits the use of larger time step sizes while remaining stable. Note that the quantities that most directly relate to the fluid node gravitational head are the non-critical flow link total pressure drop and the non-critical flow link total mass flowrate. The non-critical flow link total pressure drop contains all of the pressure drop terms which appear on the right-hand side of the non-critical flow link momentum conservation equation (Equation 2-33 of Reference 1), including the upstream and downstream fluid node gravitational head terms which are being treated either implicitly or explicitly. The non-critical flow link total mass flowrate is the NOTRUMP non-critical flow link central variable being solved for in the linearized mass flow-based momentum conservation equation.

Plot comparisons of key quantities from Case 1 versus those from Case 2 are contained in Figures 4.1.3-4 through 4.1.3-28. Figures 4.1.3-5 through 4.1.3-12 apply to the first of the three independent test subcases included in the runs, Figures 4.1.3-13 through 4.1.3-20 apply to the second subcase, and Figures 4.1.3-21 through 4.1.3-28 apply to the third subcase. From Figure 4.1.3-4, it is observed that a larger time step size

is calculated for the cases with the implicit formulation of fluid node gravitational head. This larger time step size yields more differences in the results of the implicit versus explicit runs. Specifically, the natural oscillating mixture level behavior (Figures 4.1.3-5 and 4.1.3-6 for the first subcase, Figures 4.1.3-13 and 4.1.3-14 for the second subcase, and Figures 4.1.3-21 and 4.1.3-22 for the third subcase) is more damped with the implicit formulation than it is with the explicit formulation, as expected. All of the cases behave as expected, although it is noted that the third subcase with the HSFL pairs results in the most realistic modeling of this horizontal flow thought problem, whether the implicit or explicit formulations are employed (see Figures 4.1.3-7 and 4.1.3-8 for the first subcase, Figures 4.1.3-15 and 4.1.3-16 for the second subcase, and Figures 4.1.3-23 and 4.1.3-24 for the third subcase).

For example, in both the continuous-contact and point-contact subcases, the equilibrium mixture level converges to an elevation that is slightly higher than the 5.0 ft. midpoint elevation, due to heating of the mixture regions that occurs from contact with steam flow in the horizontal flow link. This heating results in an expansion of the mixture regions and subsequently a higher equilibrium mixture level than initial conditions would indicate viable. Specifically in the point-contact subcase, the mixture level in fluid node 3 drops to slightly below the flow link interface elevation (5.0 ft.), which then allows steam flow to contact the fluid node 4 mixture region. This occurs due to the code's explicit treatment of the contact of the donor region for the flow link. On the time step before this occurs, when the fluid node 3 mixture level is above the flow link elevation/contact point, the setup for the code's central solution scheme (in the donor region logic) detects that the flow link is in contact with the vapor region of fluid node 3. The solution for the time step is completed with this assumption (i.e., explicit with respect to donor region contact), which then overdepletes the vapor region. The flow link really should have been in contact with the vapor region of fluid node 3 for a portion of the time step, and then in contact with the mixture region of fluid node 3 for the remainder of the time step.

Thus, the HSFL pairs are the only cases (in a horizontal configuration) which accurately predict the equilibrium mixture level condition. This suggests that all "true" horizontal flow paths would be more accurately modeled utilizing the HSFL pair types, otherwise region overdepletion can occur and energy deposition can be inaccurate.

Plot comparisons of key quantities from Case 3 versus those from Case 4 are contained in Figures 4.1.3-29 through 4.1.3-46. Figures 4.1.3-29 through 4.1.3-34 apply to the first of the three independent test subcases included in the runs, Figures 4.1.3-35 through 4.1.3-40 apply to the second subcase, and Figures 4.1.3-41 through 4.1.3-46 apply to the third subcase. The smaller constant time step size yields results that are extremely close in the two runs, with almost no noticeable differences, as expected.

Thus, the results are as expected, in that the implicit and explicit solutions of the fluid node gravitational head model converge as the time step size is reduced, and the natural

oscillating mixture level behavior in the cases is more damped with the implicit formulation than it is with the explicit formulation at larger time step sizes.

4.1.3.3 Implicit Fluid Node Gravitational Head Model Conclusions

The implicit fluid node gravitational head model has been adequately validated in NOTRUMP Version 38.0, and its use is expected to be a benefit for code stability. The implicit fluid node gravitational head model will be included as the default model in the new NOTRUMP EM beginning with NOTRUMP Version 38.0.

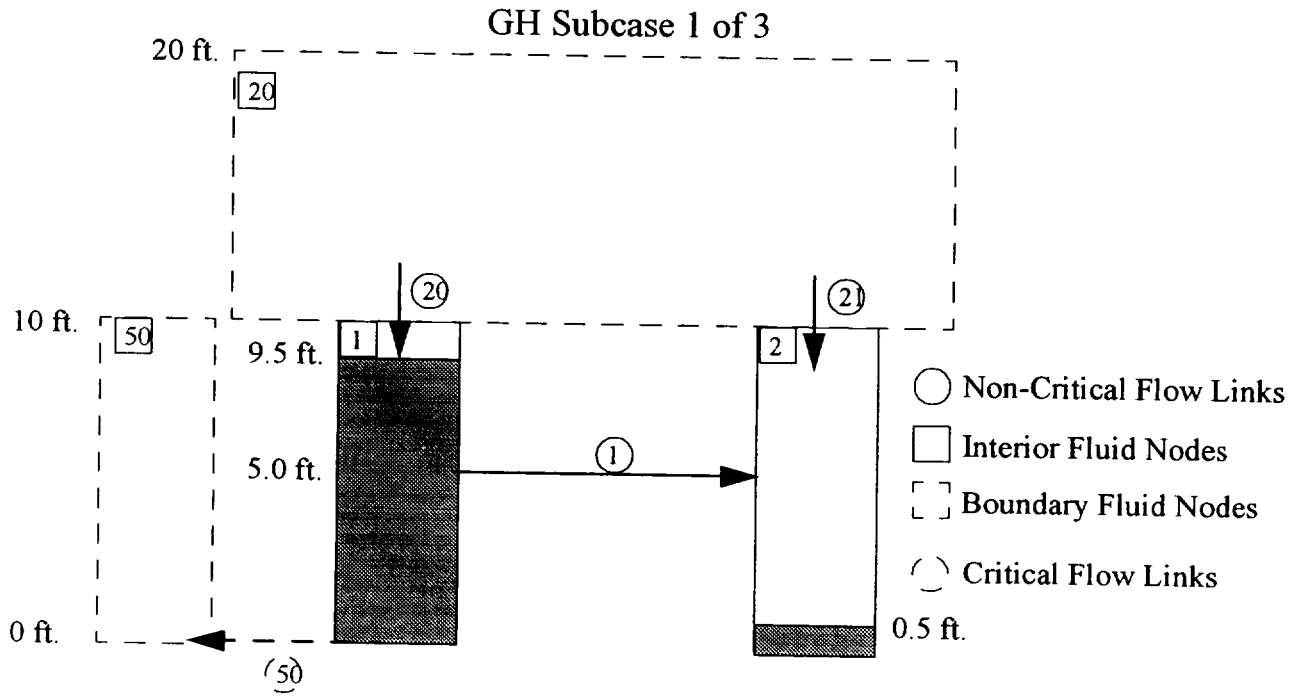


Figure 4.1.3-1 Gravitational Head Test Case Noding Diagram (Subcase 1 of 3)

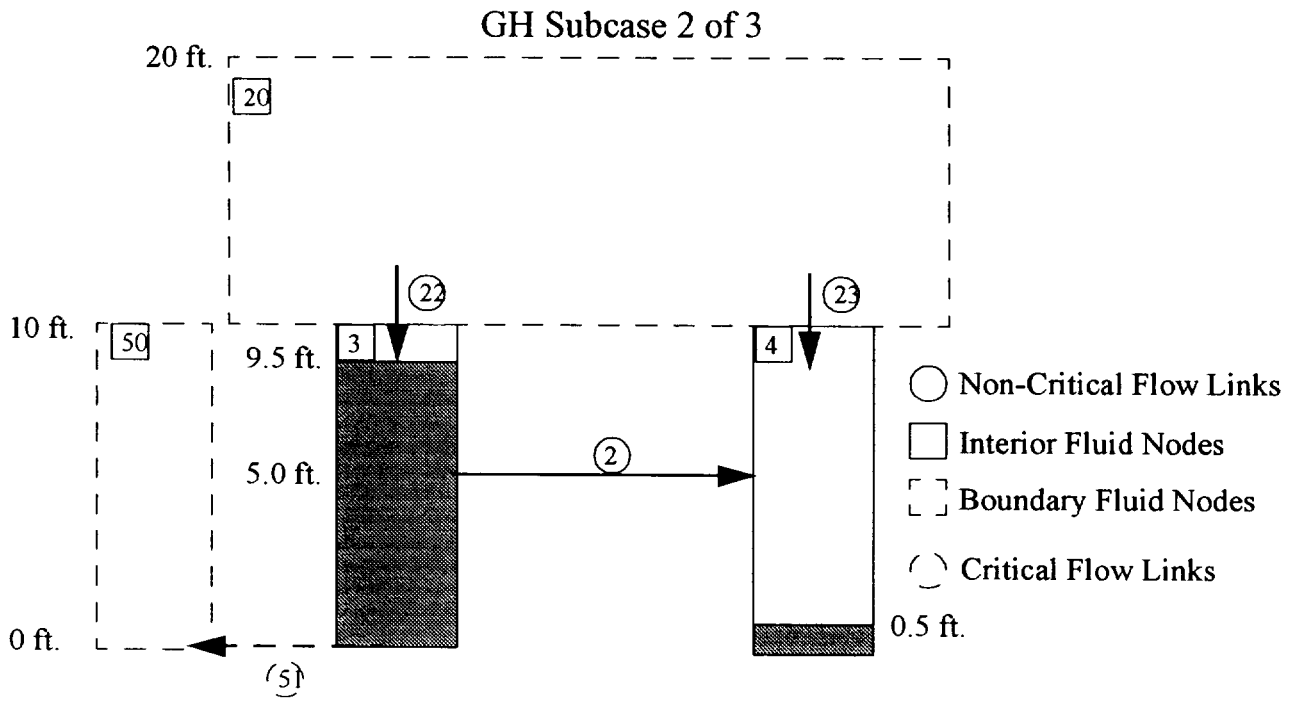


Figure 4.1.3-2 Gravitational Head Test Case Noding Diagram (Subcase 2 of 3)

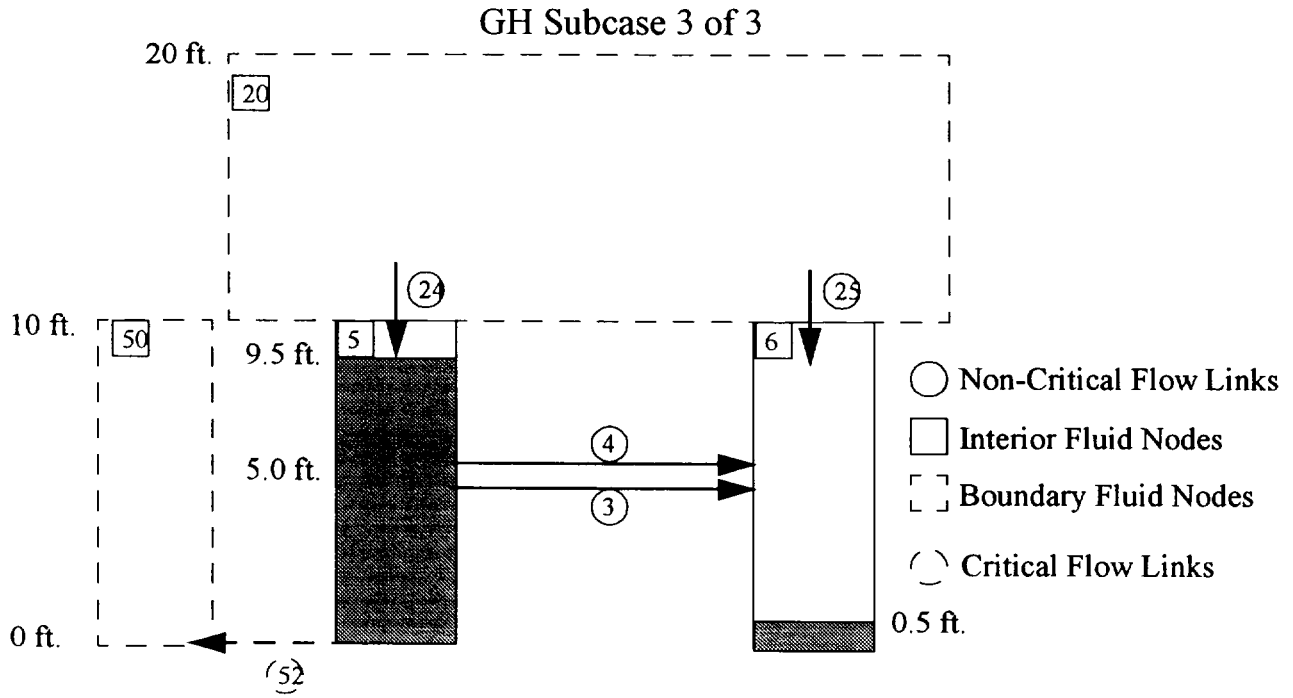


Figure 4.1.3-3 Gravitational Head Test Case Noding Diagram (Subcase 3 of 3)

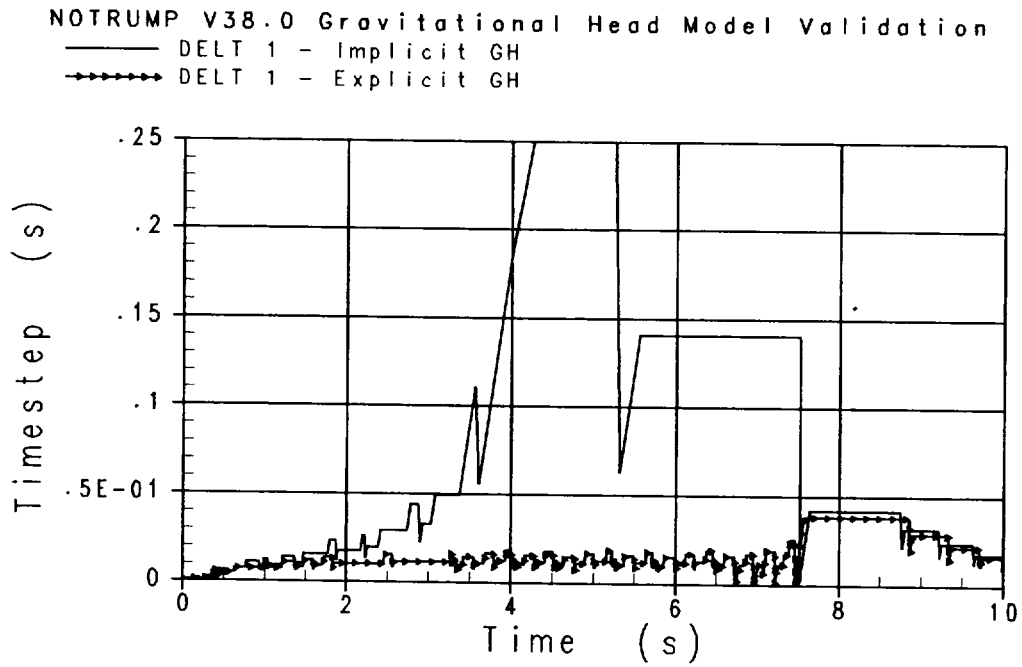


Figure 4.1.3-4 Implicit vs. Explicit GH: Time Step Size DELT

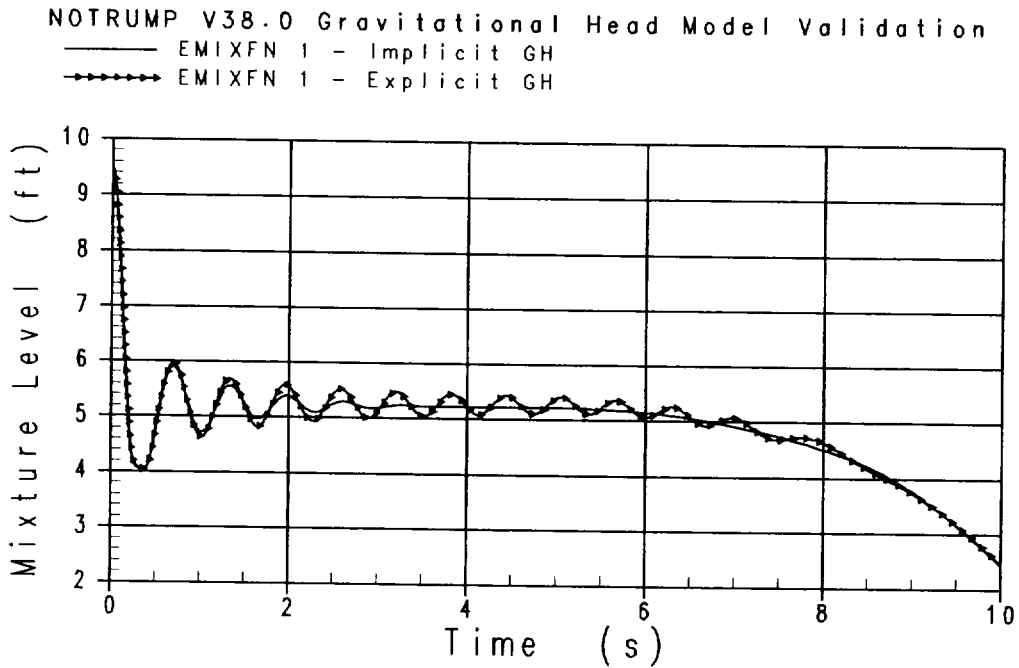


Figure 4.1.3-5 Implicit vs. Explicit GH: Fluid Node 1 Mixture Level EMIXFN 1 (Subcase 1)

WESTINGHOUSE ELECTRIC COMPANY LLC

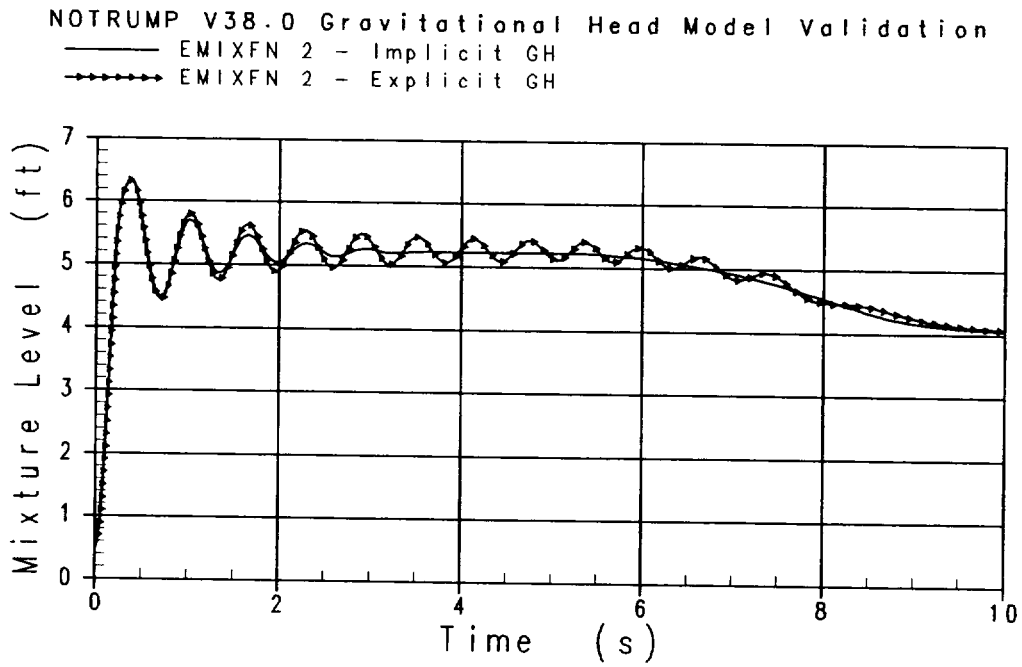


Figure 4.1.3-6 Implicit vs. Explicit GH: Fluid Node 2 Mixture Level EMIXFN 2 (Subcase 1)

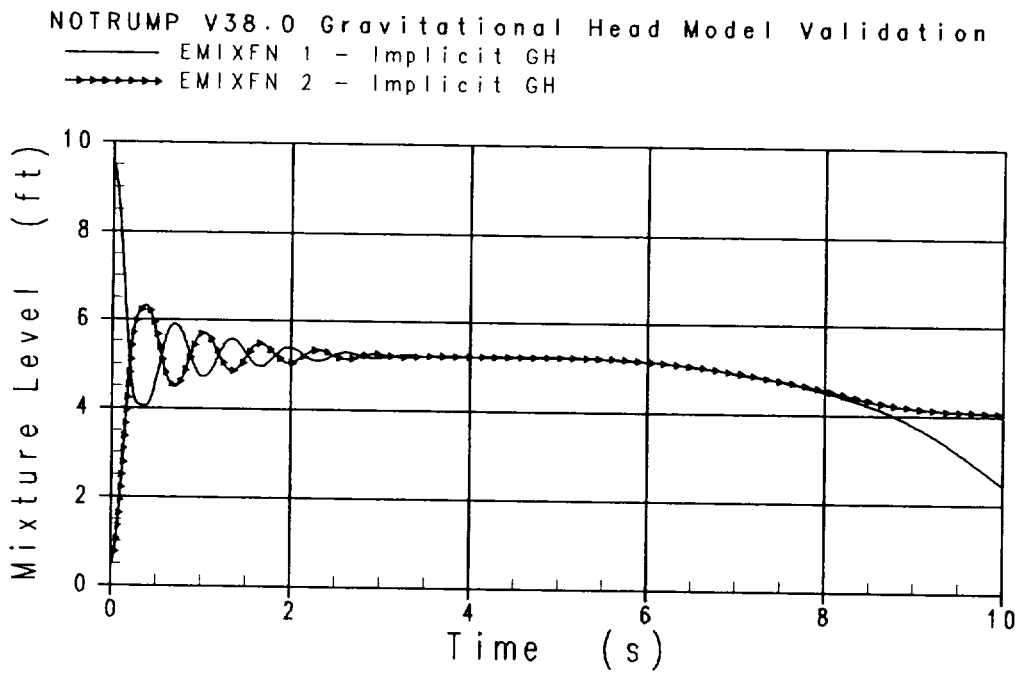


Figure 4.1.3-7 Implicit GH: EMIXFN 1 vs. EMIXFN 2 (Subcase 1)

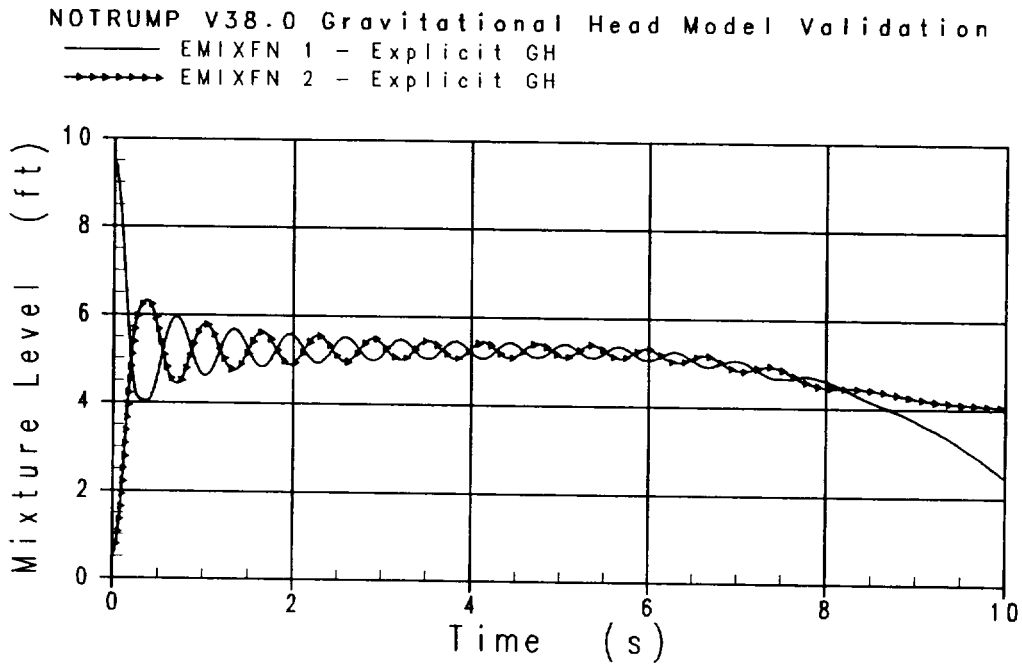


Figure 4.1.3-8 Explicit GH: EMIXFN 1 vs. EMIXFN 2 (Subcase 1)

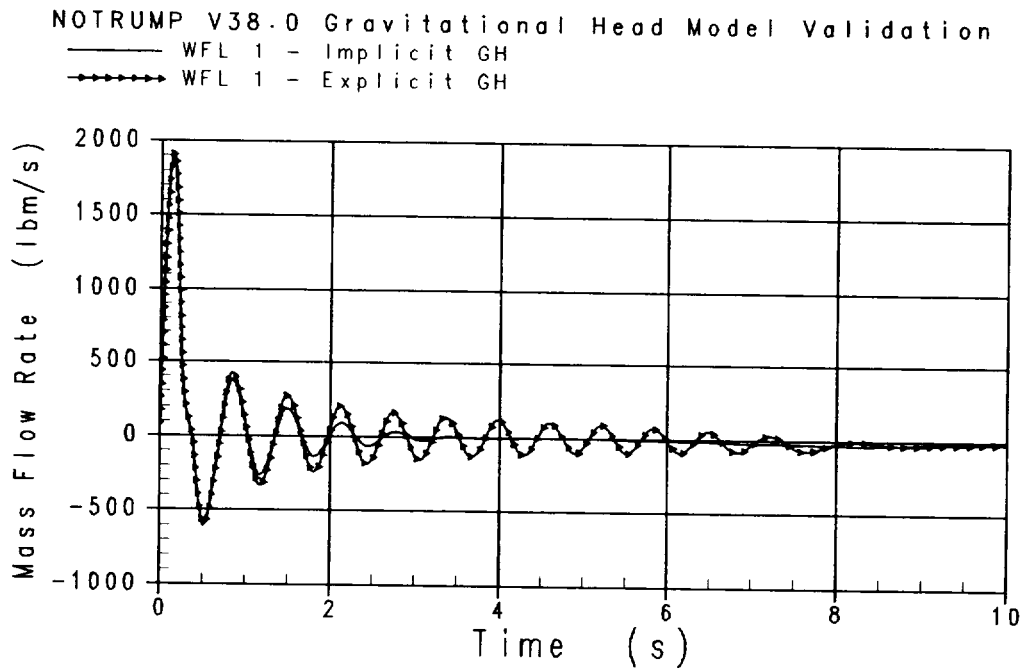


Figure 4.1.3-9 Implicit vs. Explicit GH: Flow Link 1 Total Mass Flow Rate WFL 1 (Subcase 1)

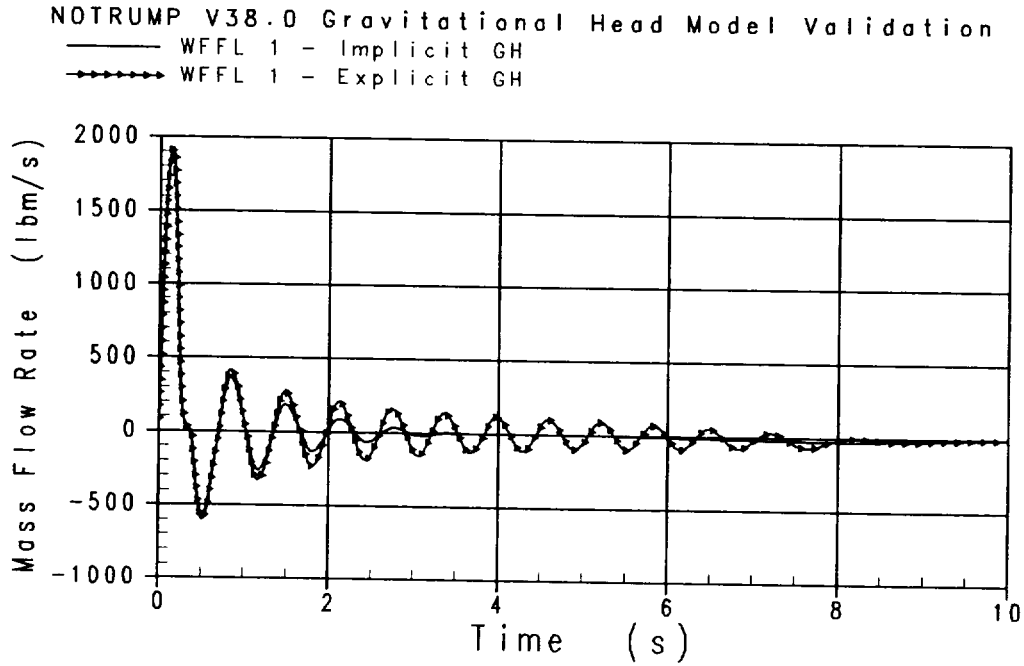


Figure 4.1.3-10 Implicit vs. Explicit GH: Flow Link 1 Liquid Mass Flow Rate WFFL 1 (Subcase 1)

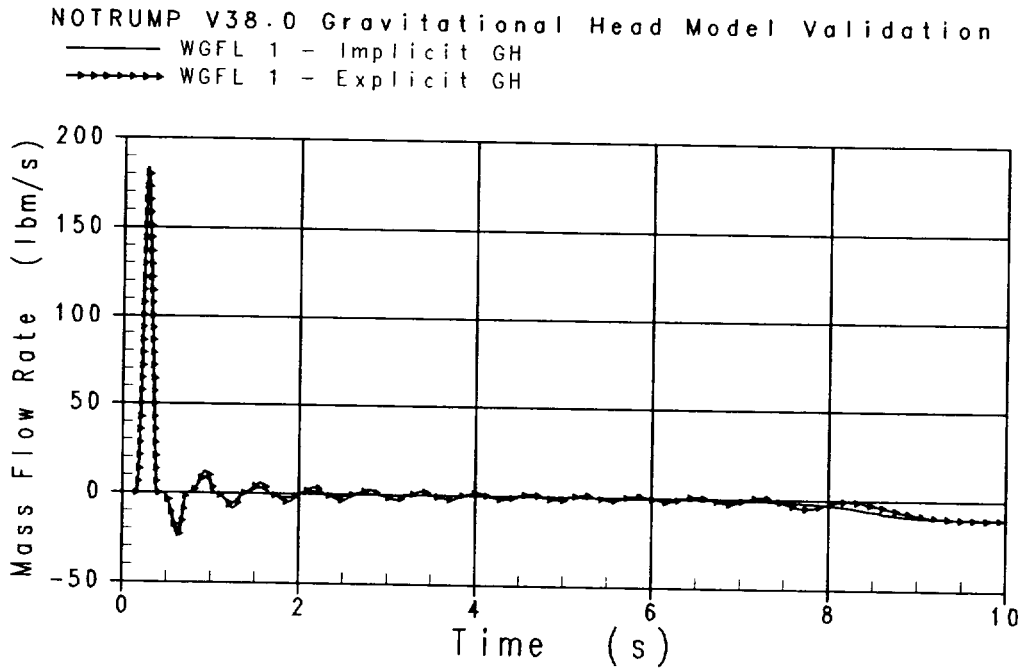


Figure 4.1.3-11 Implicit vs. Explicit GH: Flow Link 1 Vapor Mass Flow Rate WGFL 1 (Subcase 1)

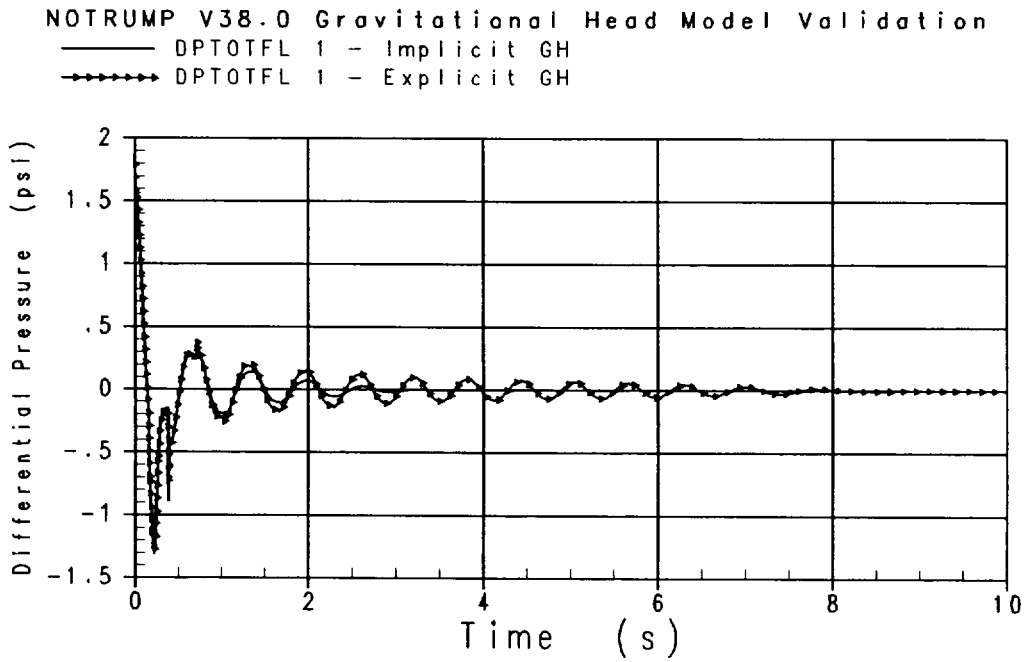


Figure 4.1.3-12 Implicit vs. Explicit GH: Flow Link 1 Total Pressure Drop DPTOTFL 1 (Subcase 1)

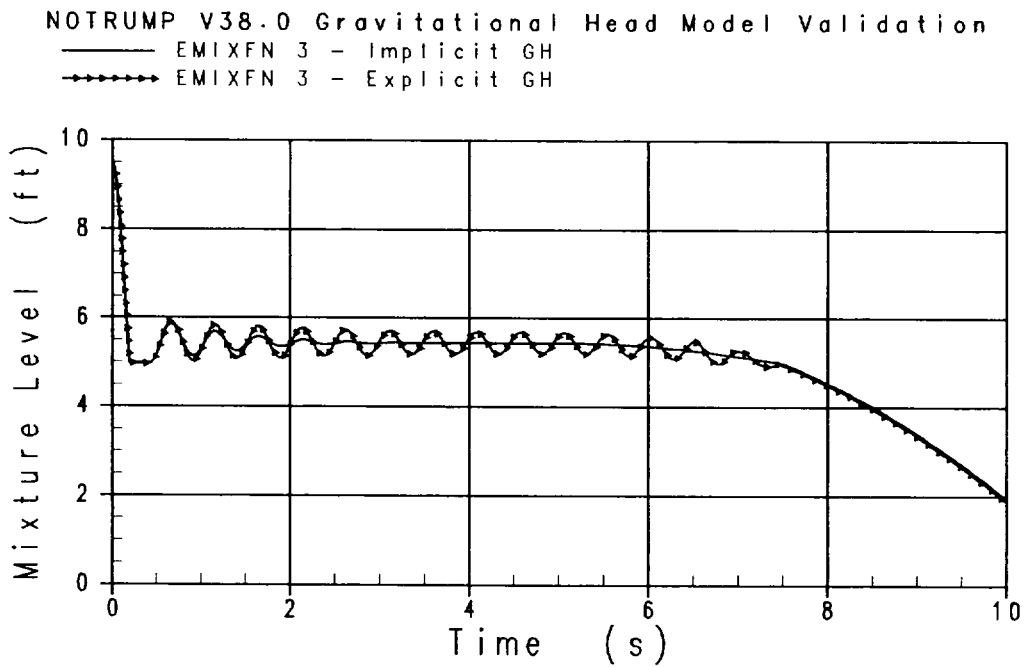


Figure 4.1.3-13 Implicit vs. Explicit GH: Fluid Node 3 Mixture Level EMIXFN 3 (Subcase 2)

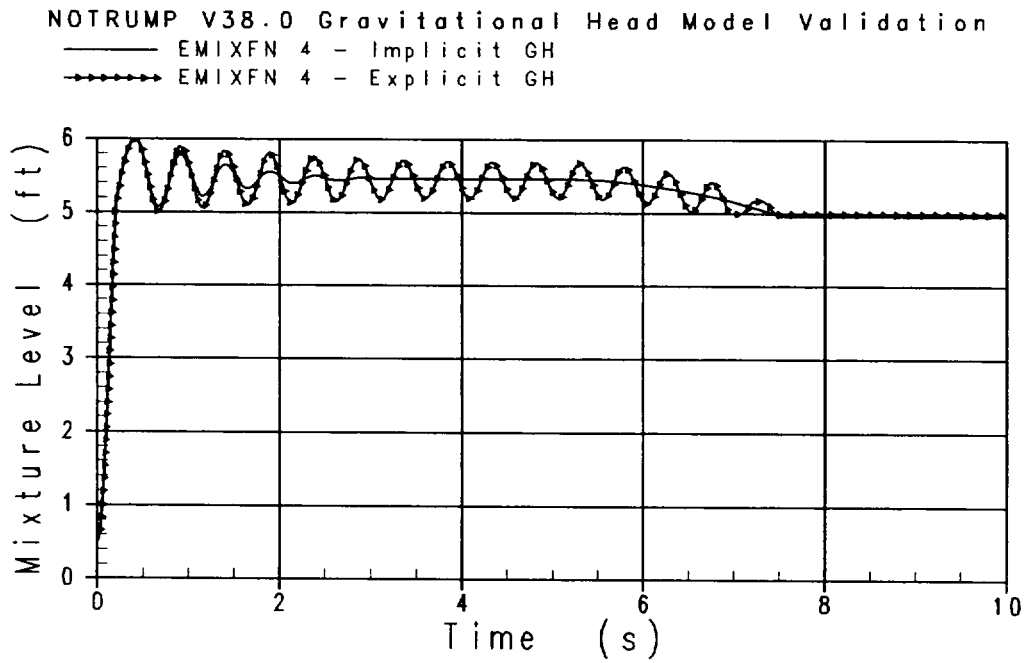


Figure 4.1.3-14 Implicit vs. Explicit GH: Fluid Node 4 Mixture Level EMIXFN 4 (Subcase 2)

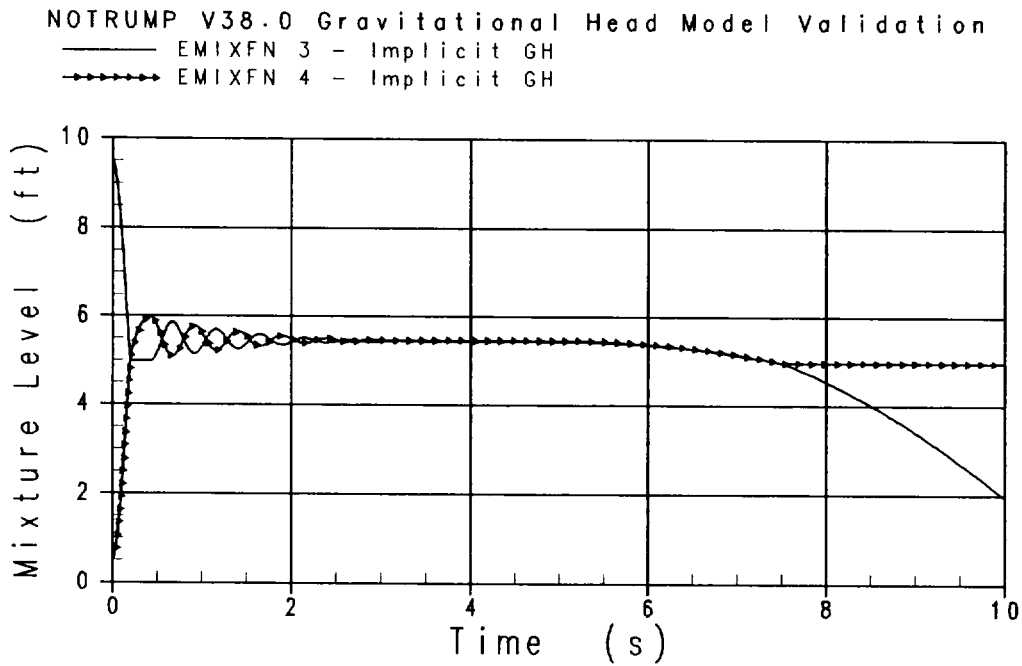


Figure 4.1.3-15 Implicit GH: EMIXFN 3 vs. EMIXFN 4 (Subcase 2)

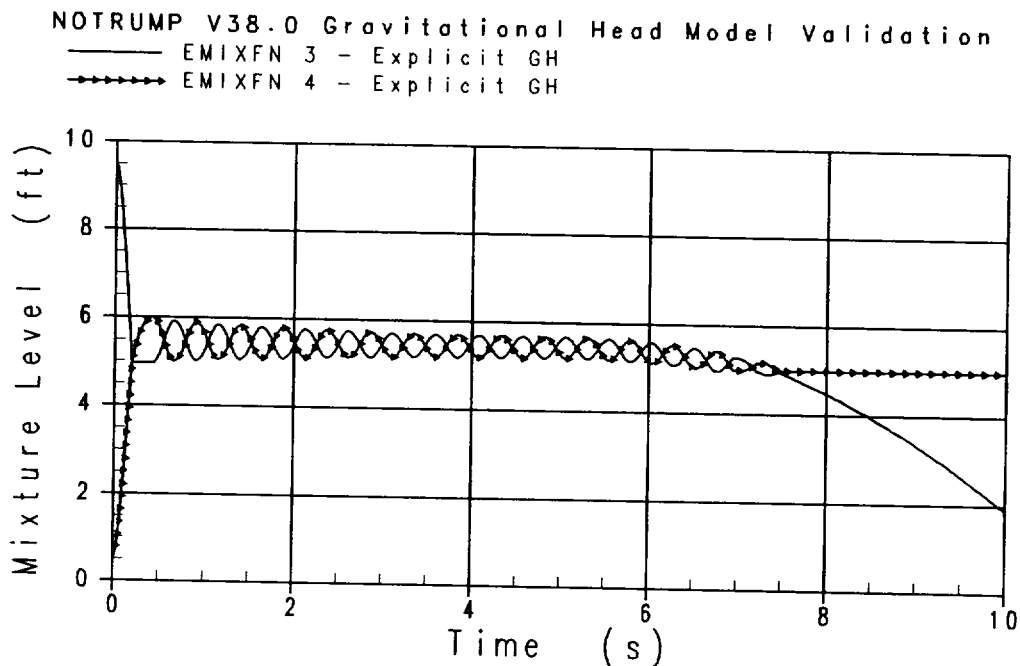


Figure 4.1.3-16 Explicit GH: EMIXFN 3 vs. EMIXFN 4 (Subcase 2)

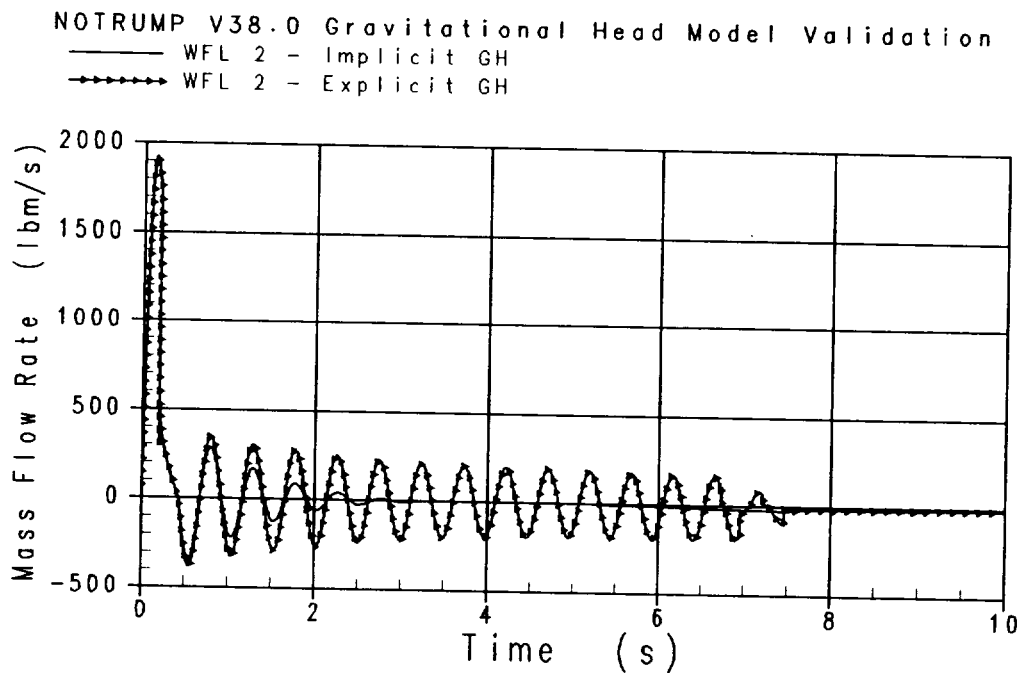


Figure 4.1.3-17 Implicit vs. Explicit GH: Flow Link 2 Total Mass Flow Rate WFL 2 (Subcase 2)

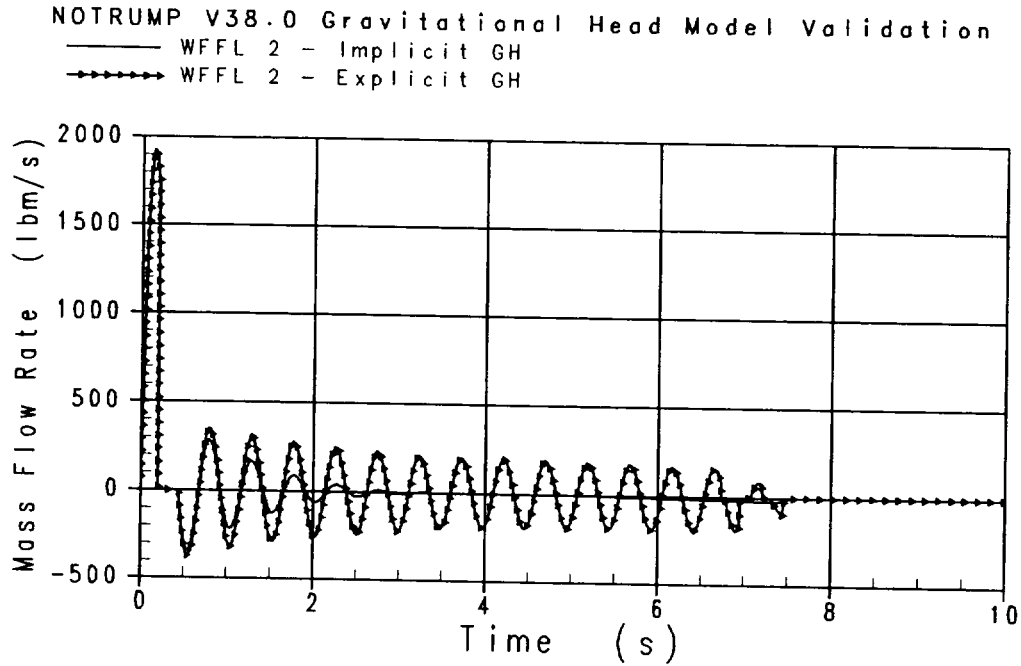


Figure 4.1.3-18 Implicit vs. Explicit GH: Flow Link 2 Liquid Mass Flow Rate WFFL 2 (Subcase 2)

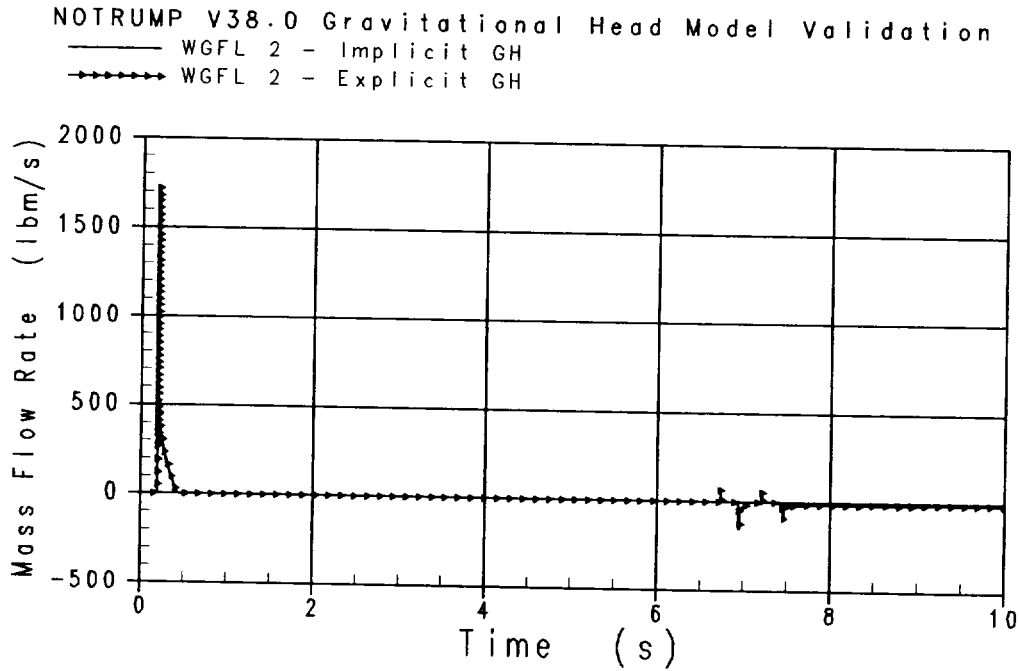


Figure 4.1.3-19 Implicit vs. Explicit GH: Flow Link 2 Vapor Mass Flow Rate WGFL 2 (Subcase 2)

WESTINGHOUSE ELECTRIC COMPANY LLC

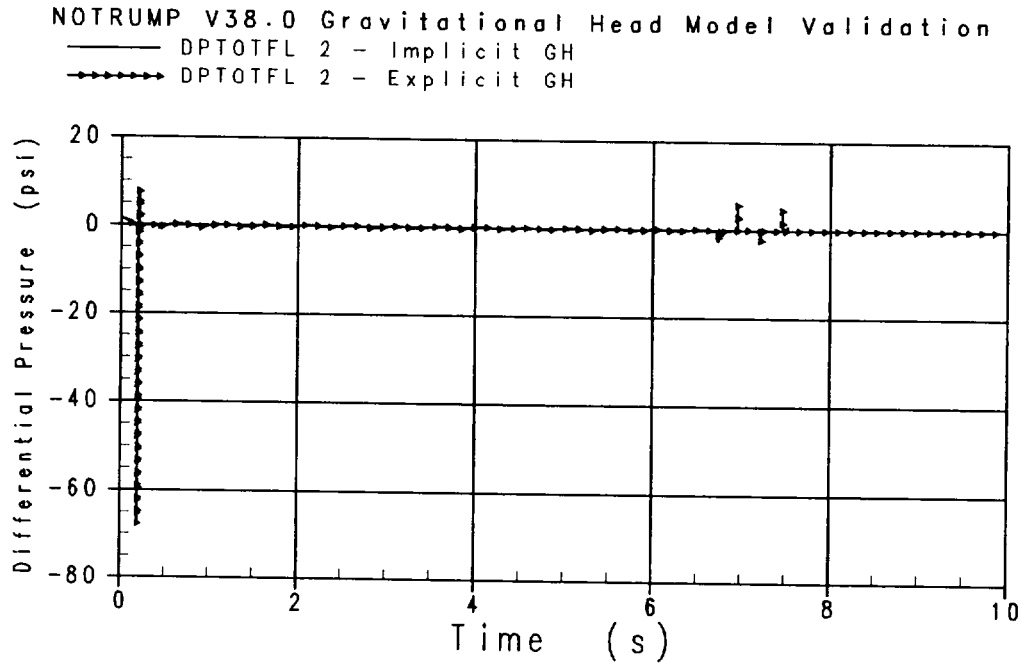


Figure 4.1.3-20 Implicit vs. Explicit GH: Flow Link 2 Total Pressure Drop DPTOTFL 2 (Subcase 2)

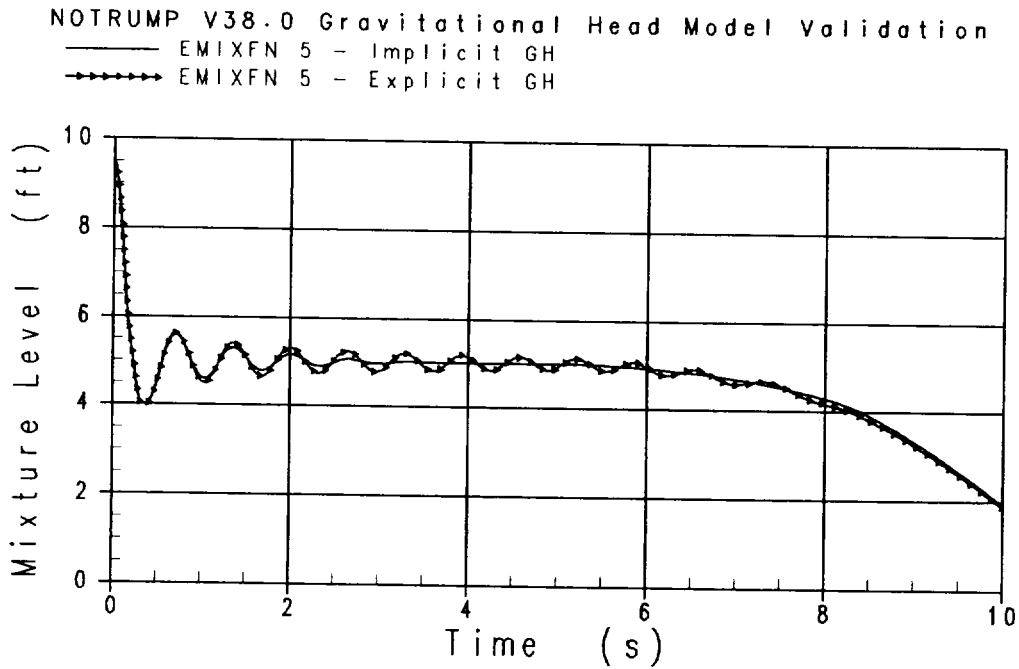


Figure 4.1.3-21 Implicit vs. Explicit GH: Fluid Node 5 Mixture Level EMIXFN 5 (Subcase 3)

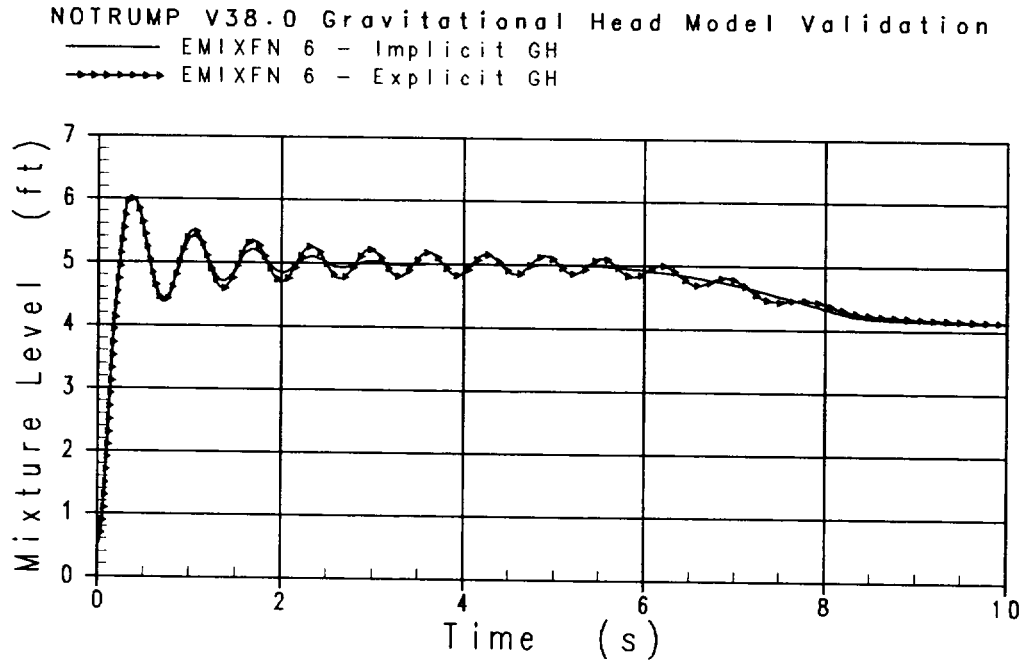


Figure 4.1.3-22 Implicit vs. Explicit GH: Fluid Node 6 Mixture Level EMIXFN 6 (Subcase 3)

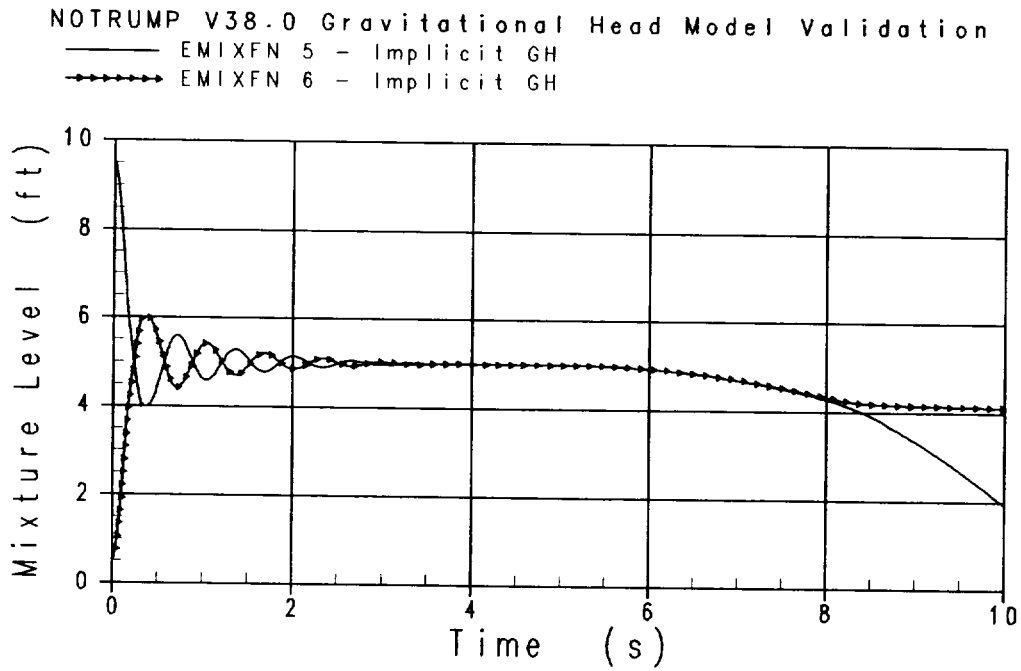


Figure 4.1.3-23 Implicit GH: EMIXFN 5 vs. EMIXFN 6 (Subcase 3)

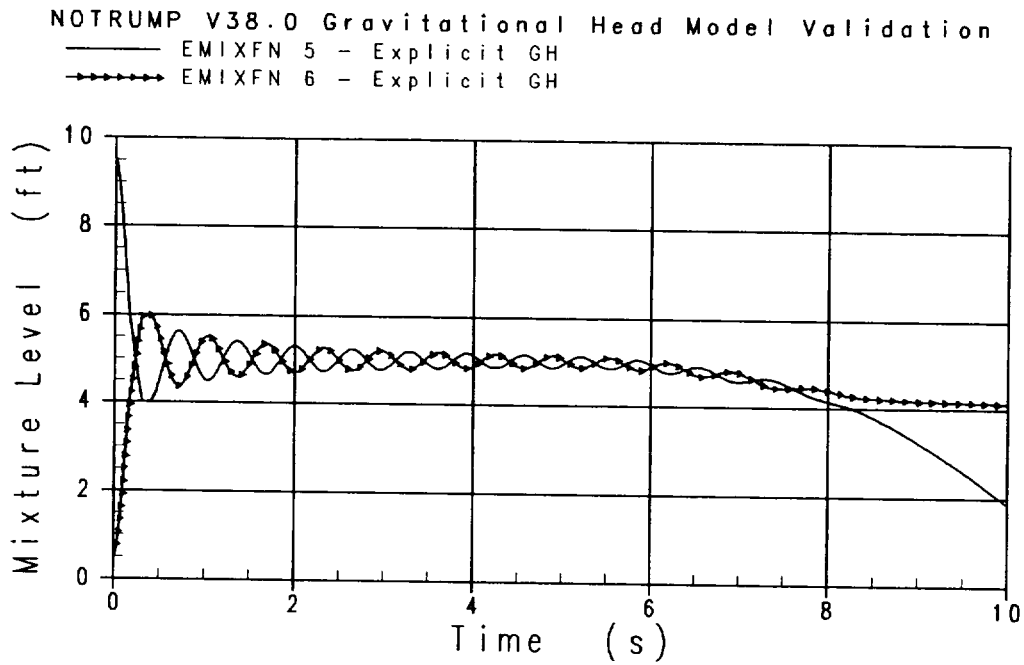


Figure 4.1.3-24 Explicit GH: EMIXFN 5 vs. EMIXFN 6 (Subcase 3)

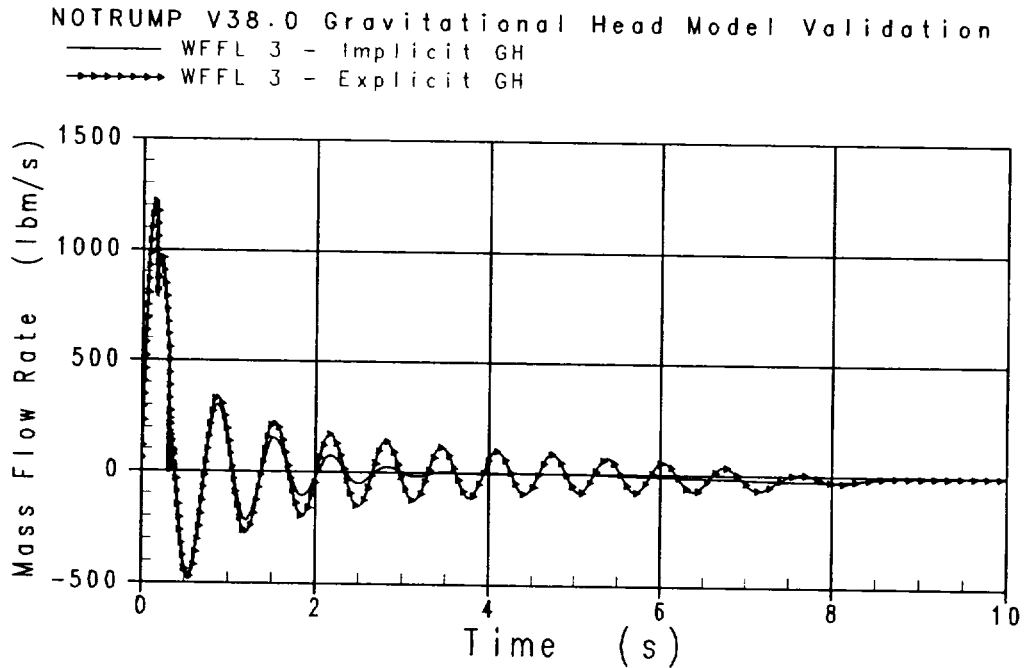


Figure 4.1.3-25 Implicit vs. Explicit GH: Flow Link 3 Liquid Mass Flow Rate WFFL 3 (Subcase 3)

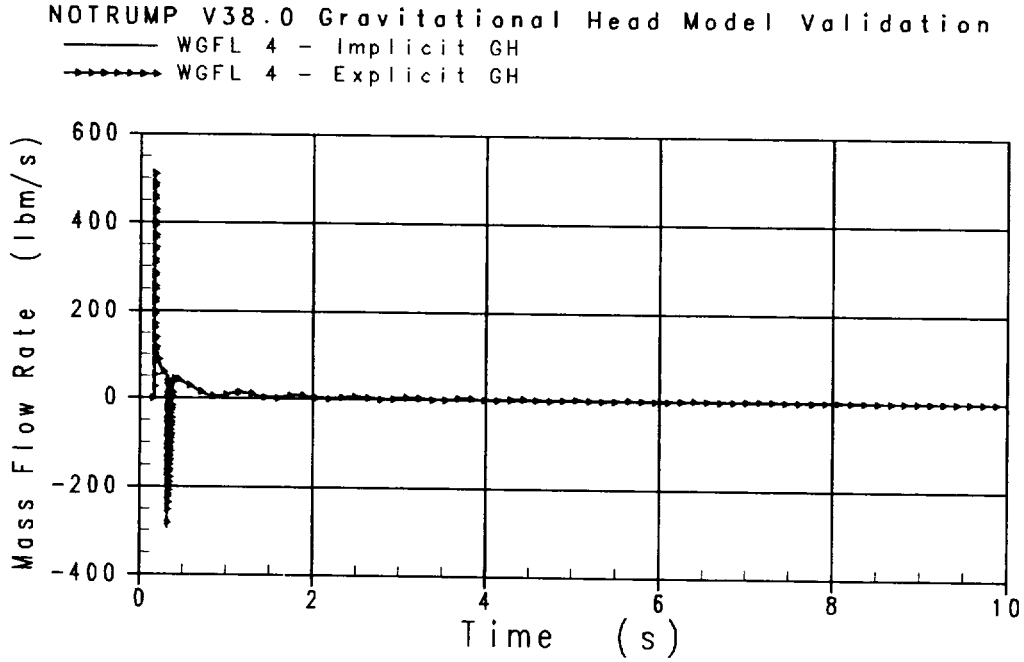


Figure 4.1.3-26 Implicit vs. Explicit GH: Flow Link 4 Vapor Mass Flow Rate WGFL 4 (Subcase 3)

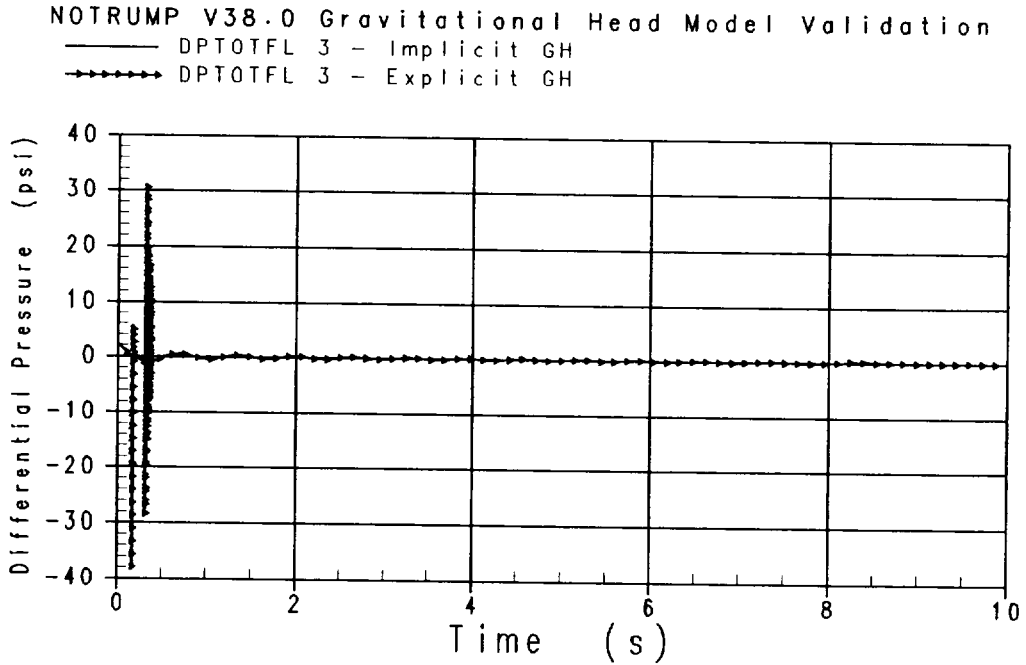


Figure 4.1.3-27 Implicit vs. Explicit GH: Flow Link 3 Total Pressure Drop DPTOTFL 3 (Subcase 3)

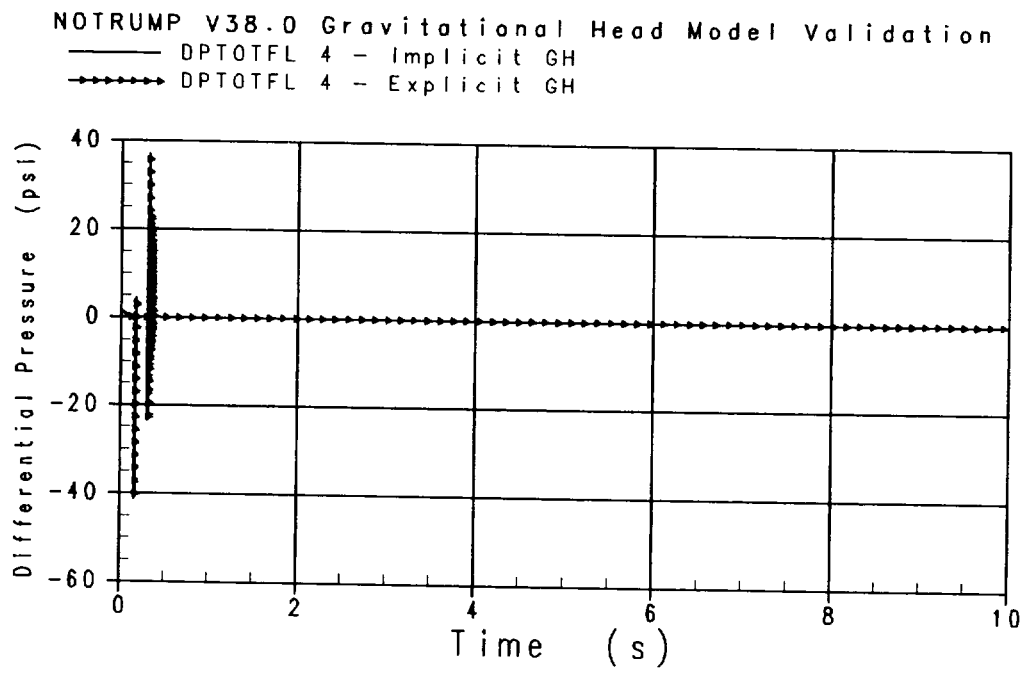


Figure 4.1.3-28 Implicit vs. Explicit GH: Flow Link 4 Total Pressure Drop DPTOTFL 4 (Subcase 3)

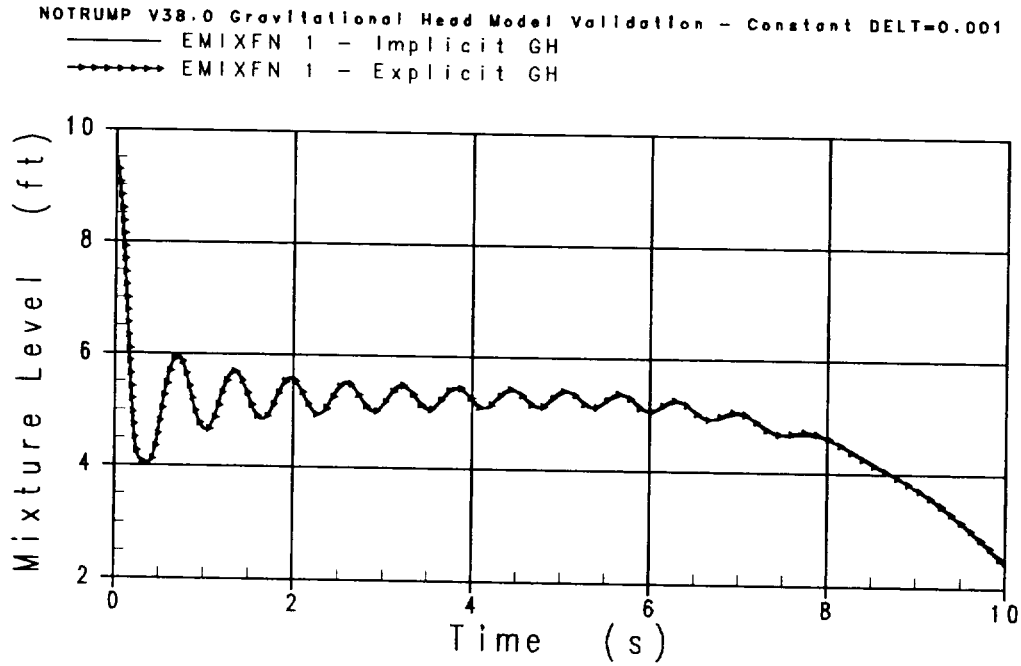


Figure 4.1.3-29 Implicit vs. Explicit GH (DELTA=0.001): Fluid Node 1 Mixture Level EMIXFN 1 (Subcase 1)

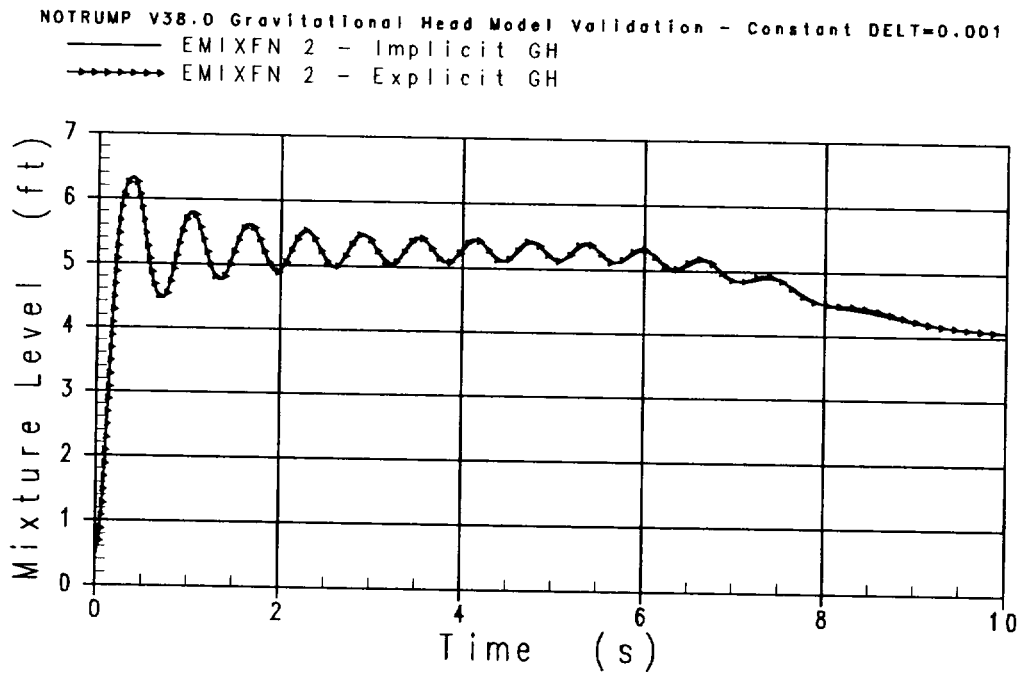


Figure 4.1.3-30 Implicit vs. Explicit GH (DELTA=0.001): Fluid Node 2 Mixture Level EMIXFN 2 (Subcase 1)

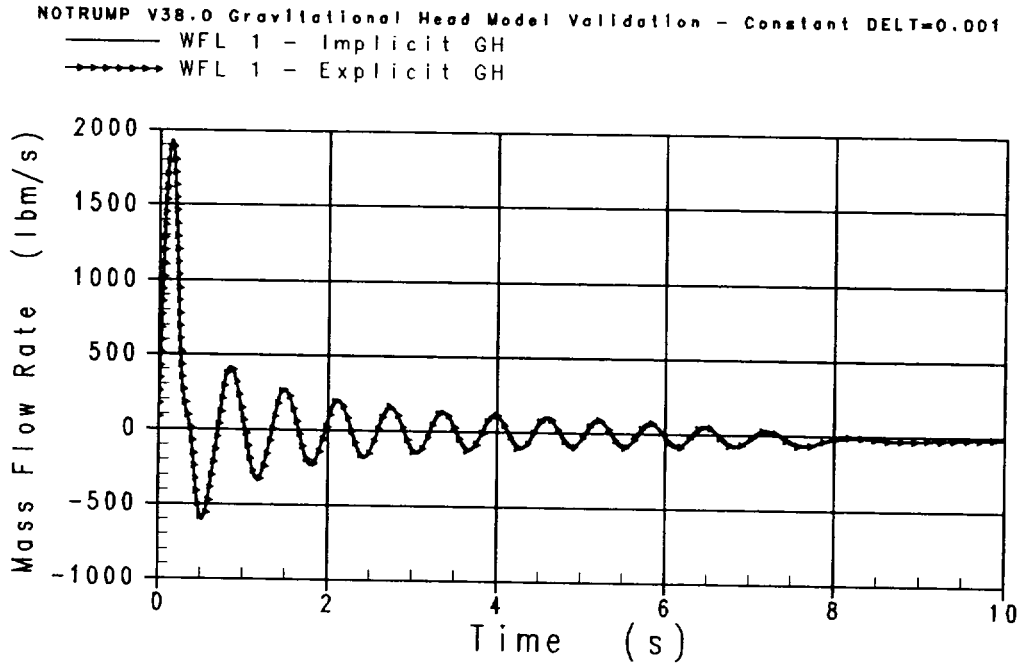


Figure 4.1.3-31 Implicit vs. Explicit GH (DELT=0.001): Flow Link 1 Total Mass Flow Rate WFL 1 (Subcase 1)

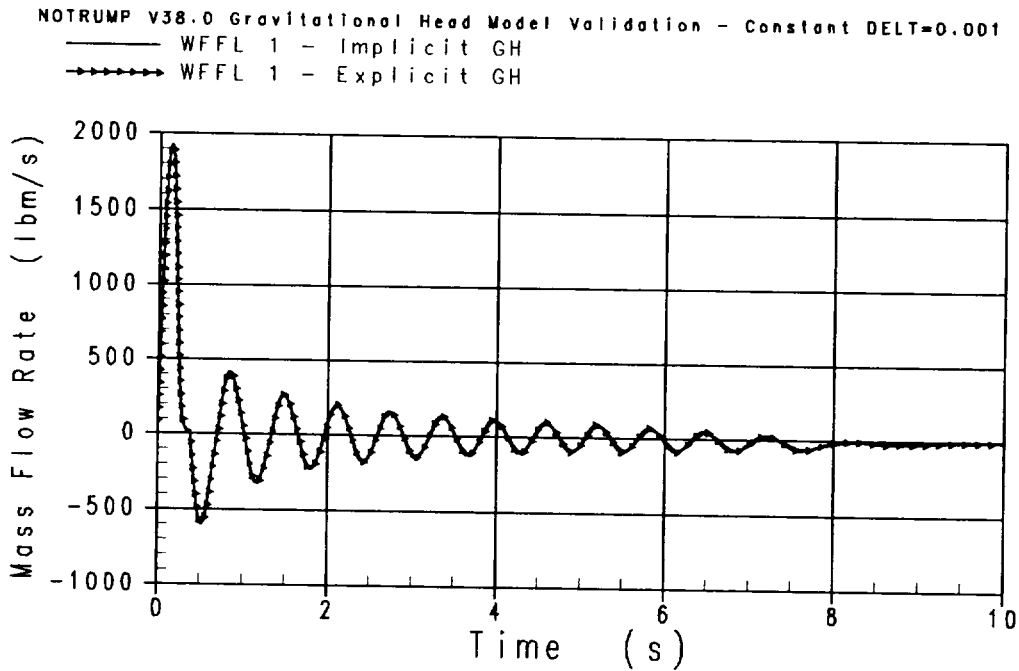


Figure 4.1.3-32 Implicit vs. Explicit GH (DELT=0.001): Flow Link 1 Liq Mass Flow Rate WFFL 1 (Subcase 1)

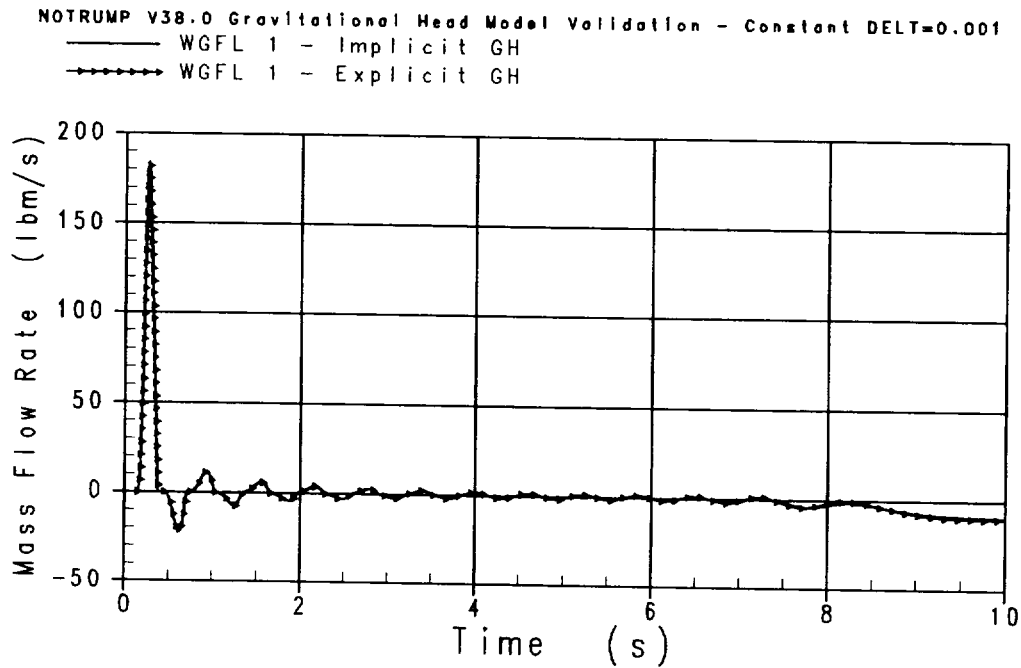


Figure 4.1.3-33 Implicit vs. Explicit GH (DELTA=0.001): Flow Link 1 Vap Mass Flow Rate WGFL 1 (Subcase 1)

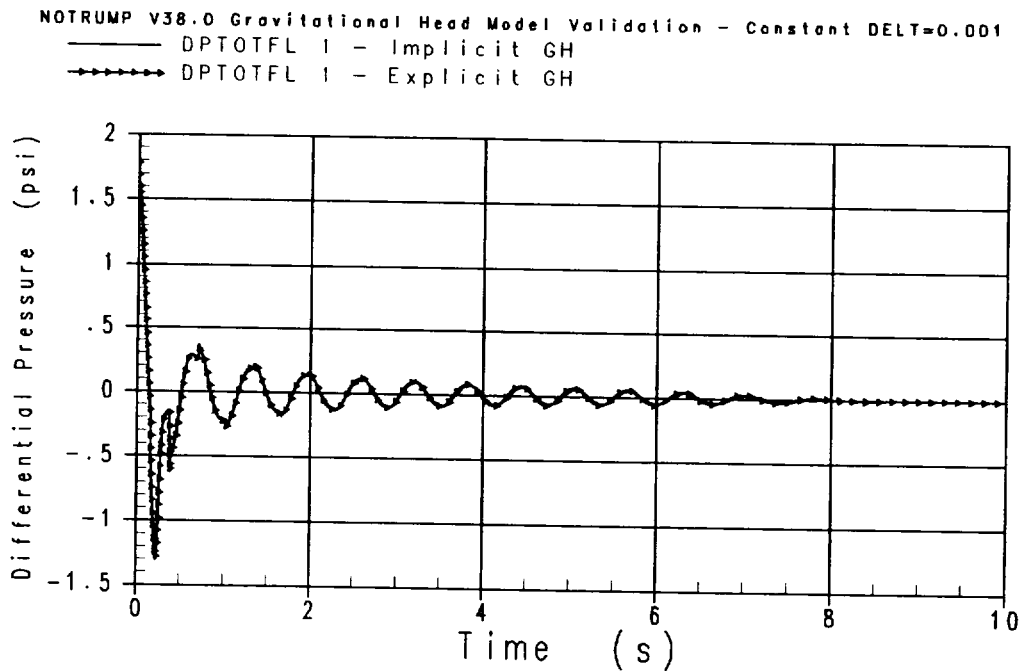


Figure 4.1.3-34 Implicit vs. Explicit GH (DELTA=0.001): Flow Link 1 Total Pressure Drop DPTOTFL 1 (Subcase 1)

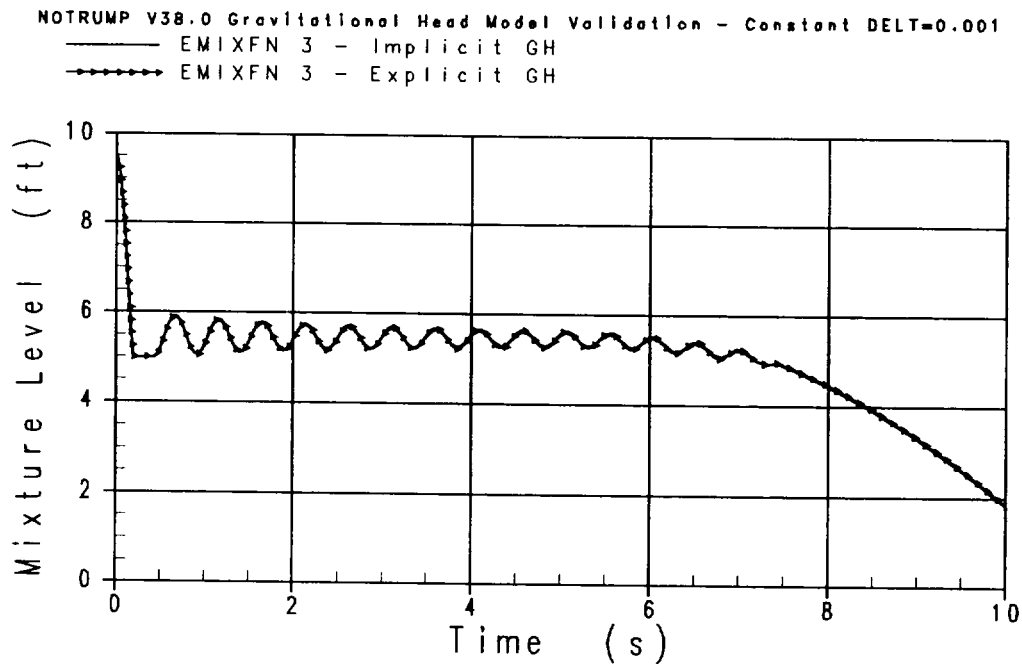


Figure 4.1.3-35 Implicit vs. Explicit GH (DELTA=0.001): Fluid Node 3 Mixture Level EMIXFN 3 (Subcase 2)

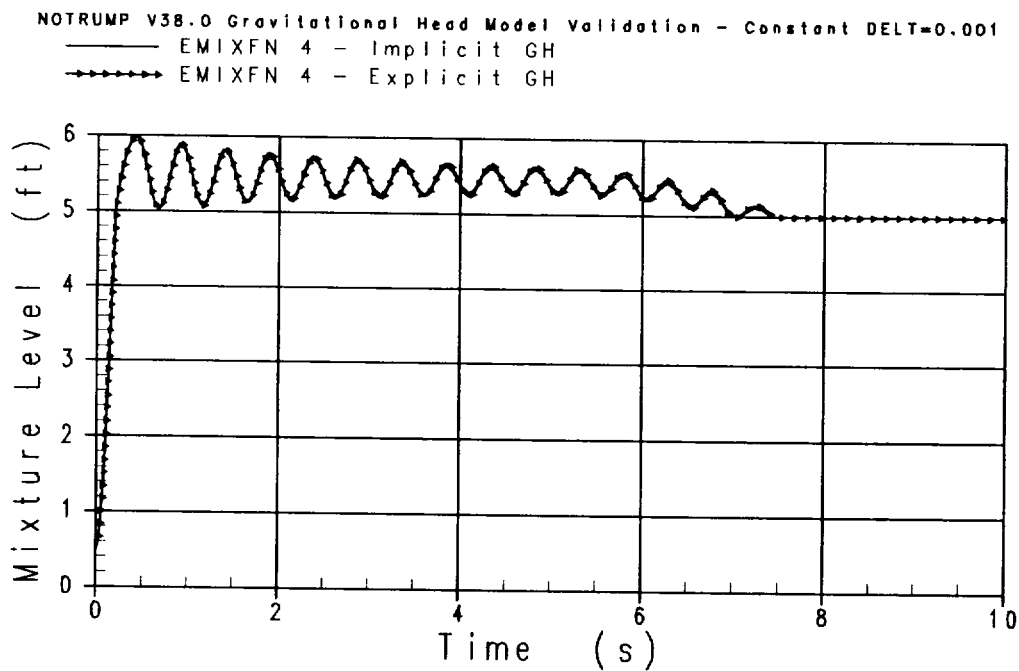


Figure 4.1.3-36 Implicit vs. Explicit GH (DELTA=0.001): Fluid Node 4 Mixture Level EMIXFN 4 (Subcase 2)

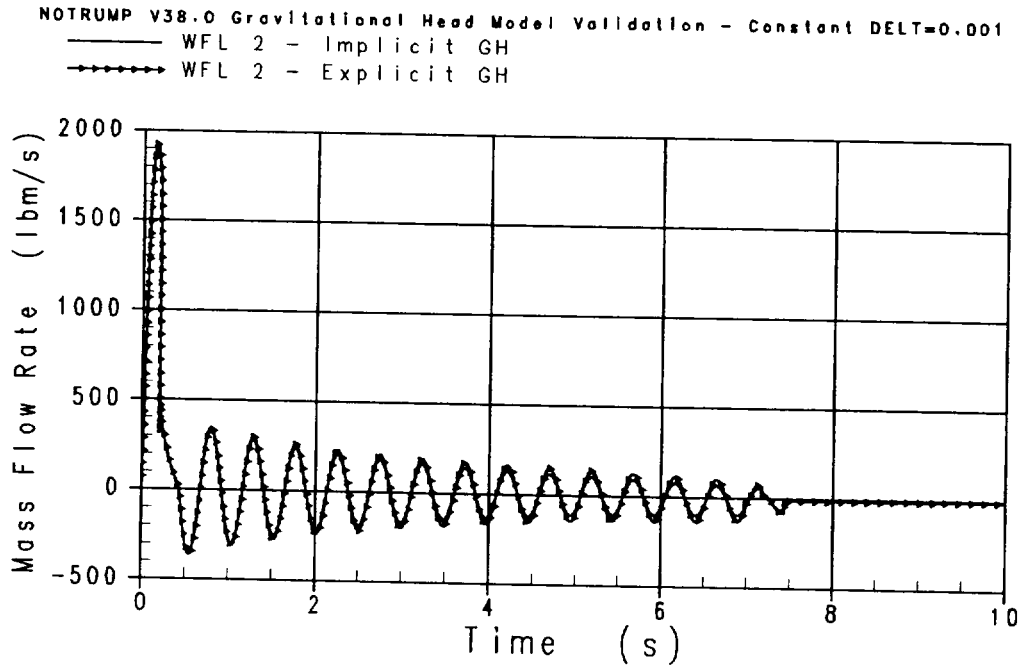


Figure 4.1.3-37 Implicit vs. Explicit GH (DELT=0.001): Flow Link 2 Total Mass Flow Rate WFL 2 (Subcase 2)

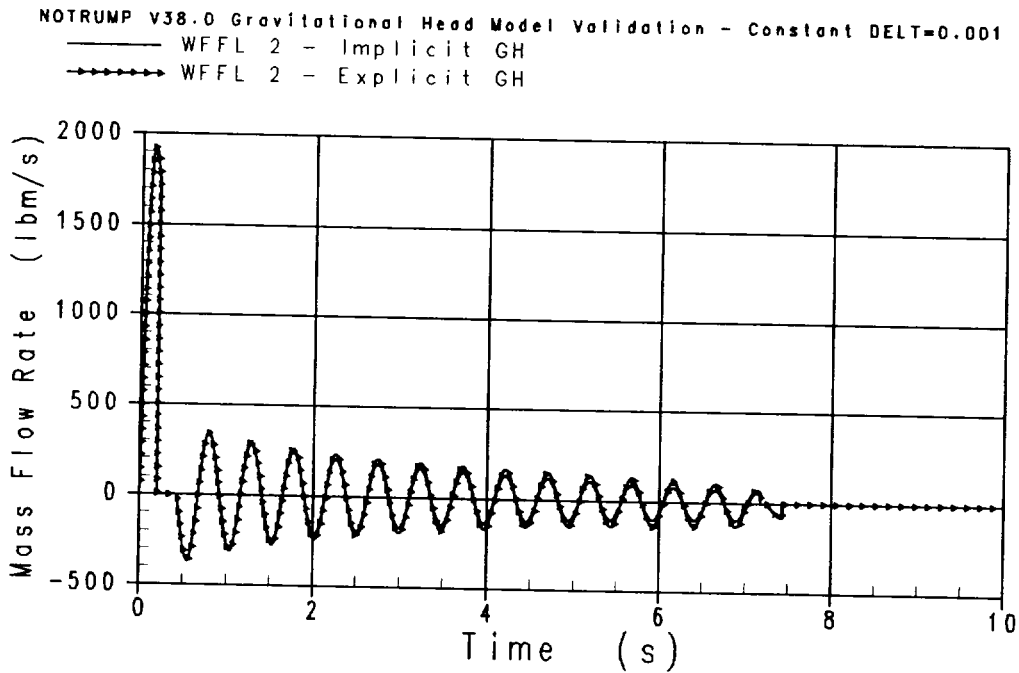


Figure 4.1.3-38 Implicit vs. Explicit GH (DELT=0.001): Flow Link 2 Liquid Mass Flow Rate WFFL 2 (Subcase 2)

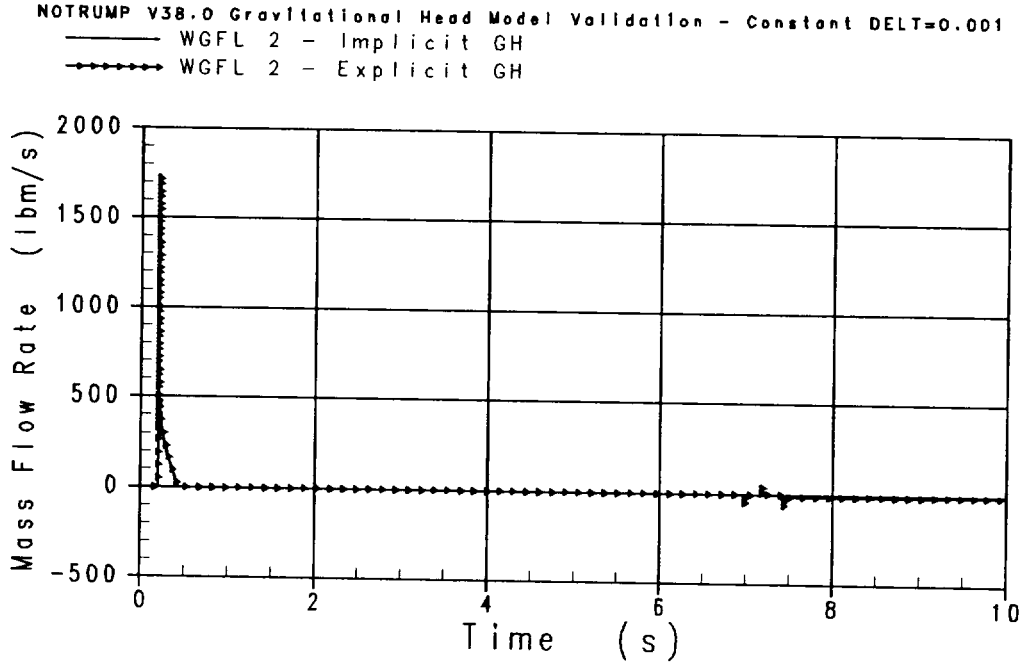


Figure 4.1.3-39 Implicit vs. Explicit GH (DELTA=0.001): Flow Link 2 Vapor Mass Flow Rate WGFL 2 (Subcase 2)

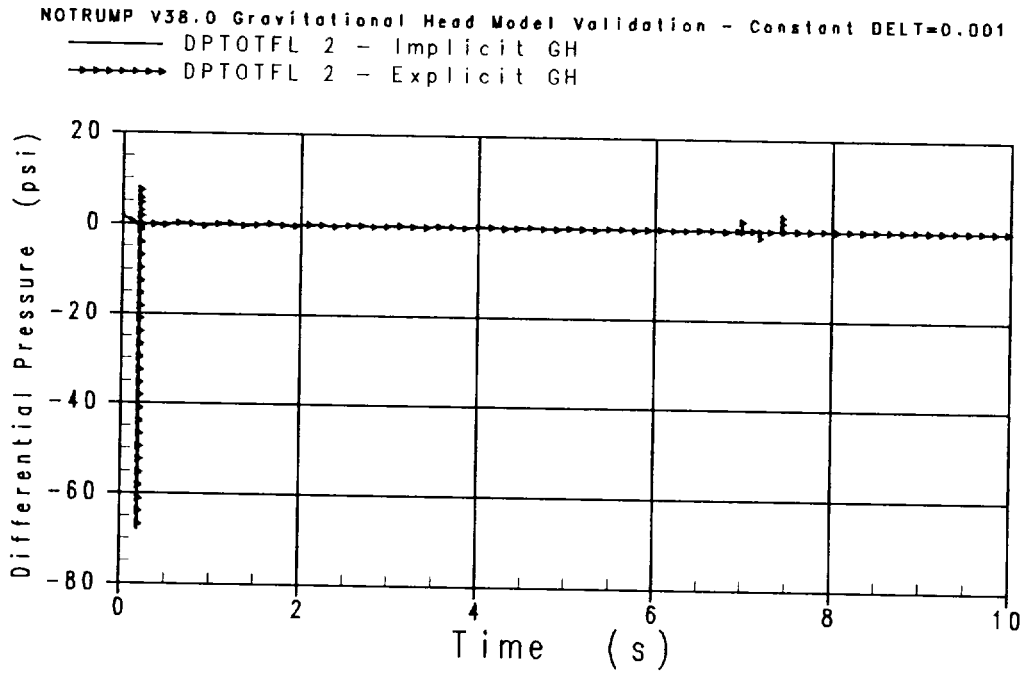


Figure 4.1.3-40 Implicit vs. Explicit GH (DELTA=0.001): Flow Link 2 Total Pressure Drop DPTOTFL 2 (Subcase 2)

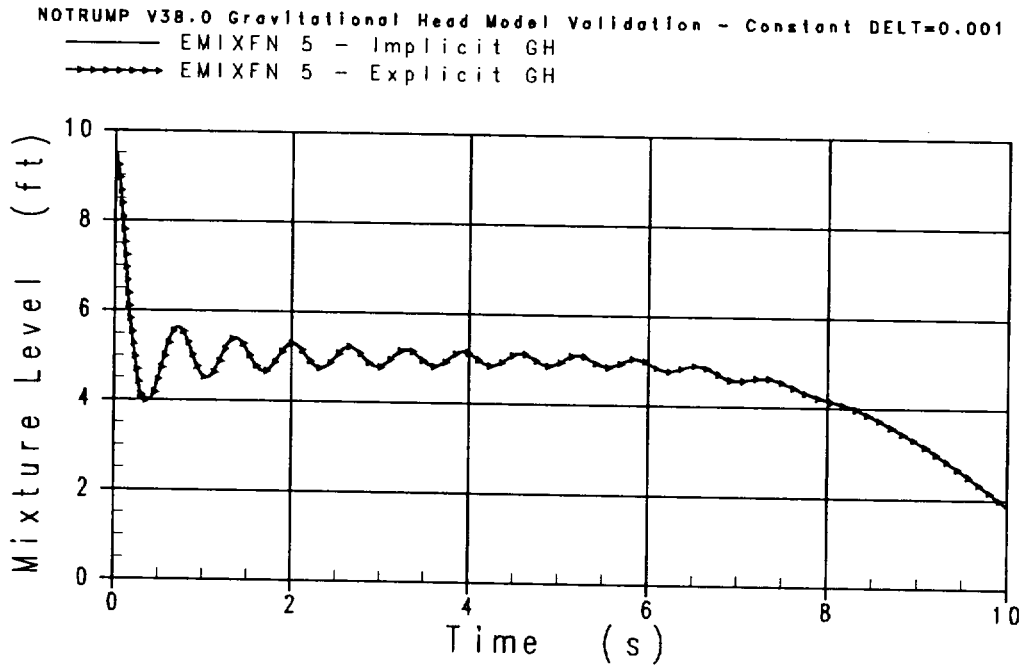


Figure 4.1.3-41 Implicit vs. Explicit GH (DELTA=0.001): Fluid Node 5 Mixture Level EMIXFN 5 (Subcase 3)

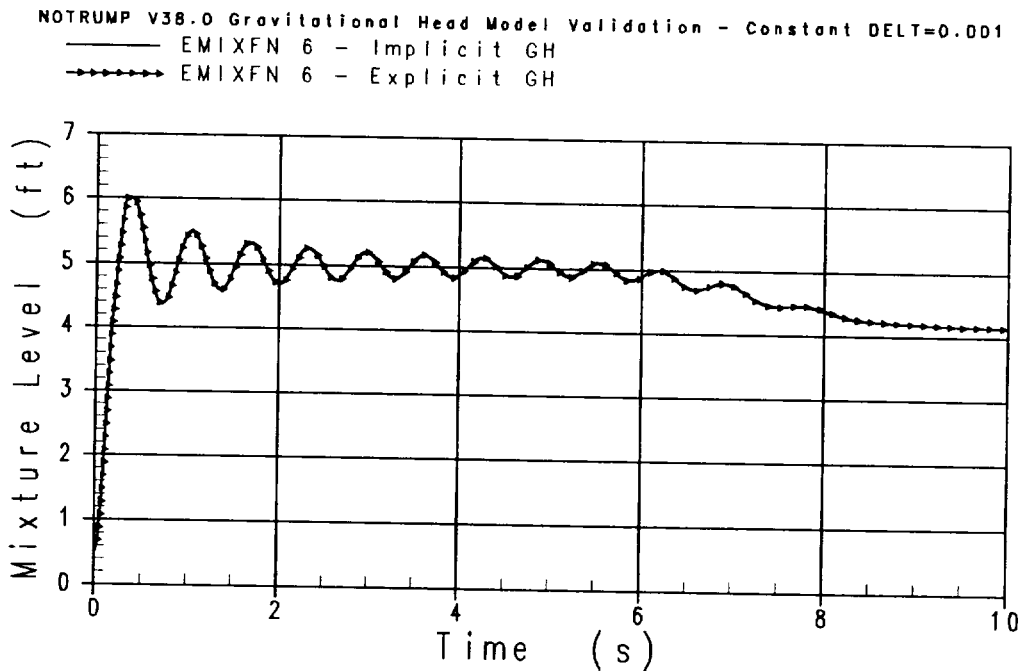


Figure 4.1.3-42 Implicit vs. Explicit GH (DELTA=0.001): Fluid Node 6 Mixture Level EMIXFN 6 (Subcase 3)

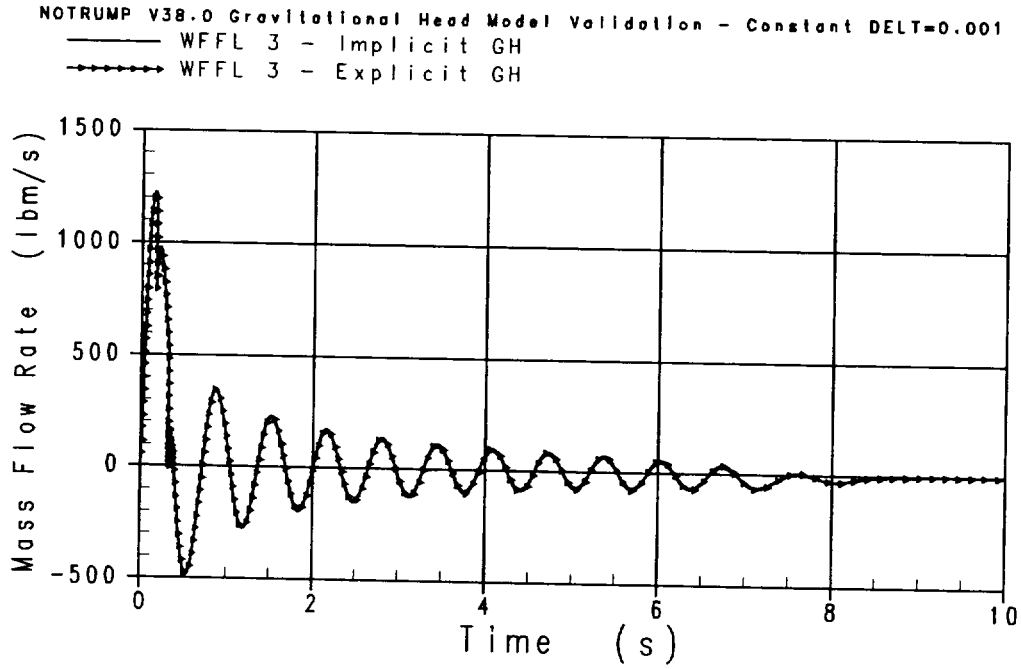


Figure 4.1.3-43 Implicit vs. Explicit GH (DELT=0.001): Flow Link 3 Liquid Mass Flow Rate WFFL 3 (Subcase 3)

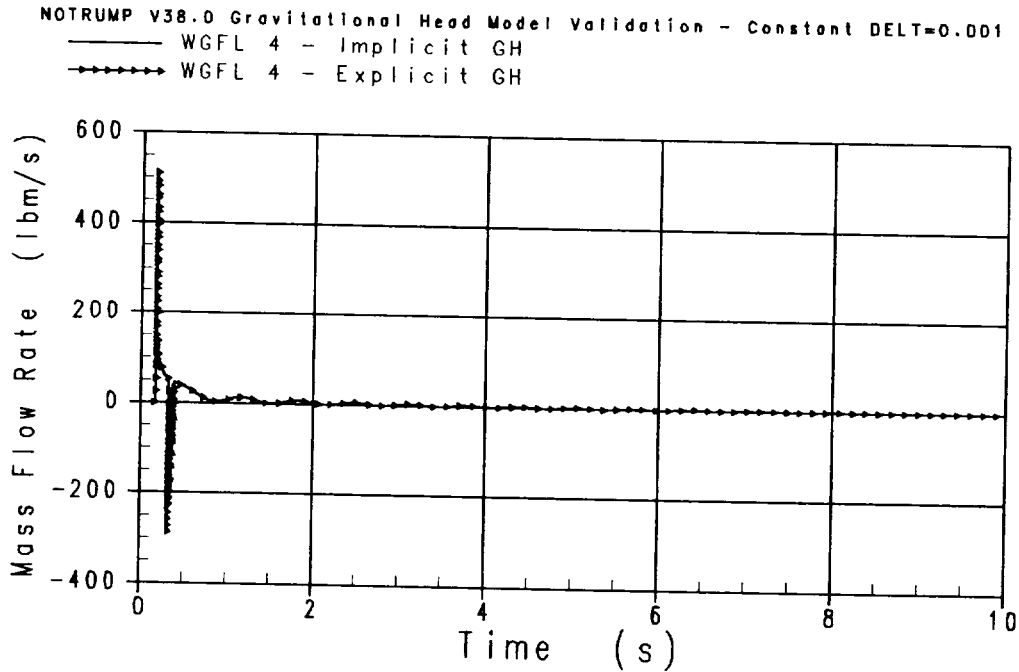


Figure 4.1.3-44 Implicit vs. Explicit GH (DELT=0.001): Flow Link 4 Vapor Mass Flow Rate WGFL 4 (Subcase 3)

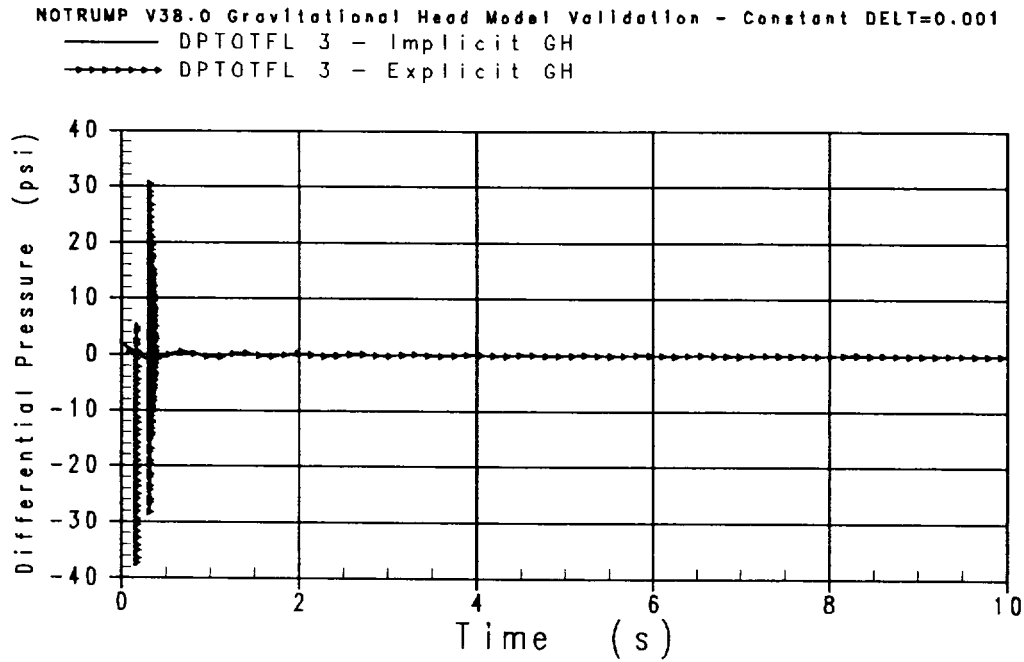


Figure 4.1.3-45 Implicit vs. Explicit GH (DELTA=0.001): Flow Link 3 Total Pressure Drop DPTOTFL 3 (Subcase 3)

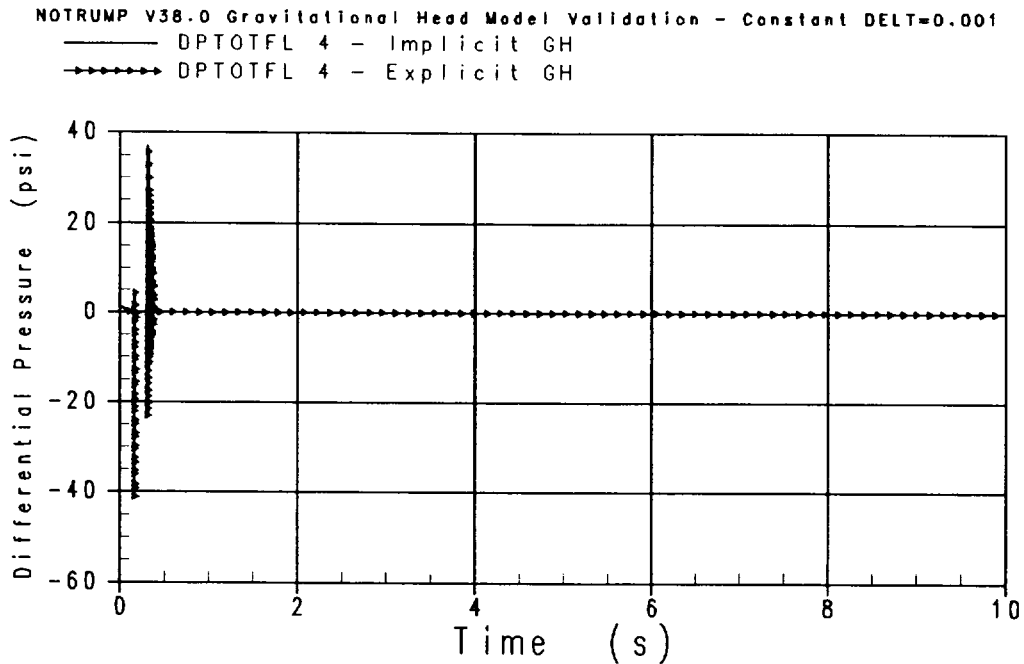


Figure 4.1.3-46 Implicit vs. Explicit GH (DELTA=0.001): Flow Link 4 Total Pressure Drop DPTOTFL 4 (Subcase 3)

4.1.4 Validation of Semi-implicit Metal Node Model

The purpose of this section is to validate NOTRUMP's semi-implicit method of solving metal node temperatures. As discussed in Section 2.4, the previous NOTRUMP Evaluation Model (EM) uses explicit treatment of interior metal node calculations. This test will also demonstrate the improvement of using semi-implicit treatment of metal node temperature calculations over the explicit metal node treatment currently used. To remain consistent with the implementation of the implicit model enhancements, the as coded semi-implicit method of solving metal node temperatures will be invoked during NOTRUMP's calculations. Recall from Section 2.4.3, that this semi-implicit treatment, refers to metal node temperature being linearized with respect to time in the metal node energy conservation equations within a given time step. However, the fluid node energy conservation equations hold metal node temperature change constant within the same time step.

To show that the semi-implicit treatment of metal node temperature is working correctly, several test cases were executed which exercise both the explicit and semi-implicit treatment of metal node temperatures. These cases varied time step size to demonstrate that the models are working correctly. Also, metal node mass and fluid node initial conditions were varied to further pronounce the differences between explicit vs. semi-implicit results. In each of these cases when the time step size is decreased the results of explicit vs. semi-implicit should converge. As a note, when referring to discussion of the metal node proper, the terms semi-implicit and implicit are interchangeable, that is they both are referring to the same numerical solution technique for solving metal node temperature.

4.1.4.1 NOTRUMP Simulation - Metal Node Model Description

The NOTRUMP model consists of four independent interior fluid nodes as shown in Figures 4.1.4-1 - 4.1.4-4, modeled as cylinders with a volume of 1.0 ft³ and a height of 1.0 foot. An interior metal node is modeled within each fluid node. Each metal node is connected to its respective fluid node via a non-critical heat link for exchange of heat transfer between the fluid and the metal in the node.

The following is a description of each node:

Node 1: Single region: superheated vapor, $h=1,700$ btu/lbm, $p=1,000$ psia, metal node temperature= 500°F , metal node mass= 0.1 lbm

Node 2: Single region: superheated vapor, $h=1,700$ btu/lbm, $p=1,000$ psia, metal node temperature= 500°F , metal node mass= 0.01 lbm

Node 3: Single region: subcooled liquid, $h=15$ btu/lbm, $p=1,000$ psia, metal node

temperature=500°F, metal node mass=0.01 lbm

Node 4: Two region: vapor region is superheated vapor, $h=1,700$ btu/lbm, mixture region is subcooled liquid, $h=15$ btu/lbm, $p=1,000$ psia, metal node temperature=500°F, metal node mass=0.01 lbm

Note that the fluid nodes 1 and 2 share the same initial conditions, while the conditions for fluid nodes 3 and 4 were varied. It should also be noted that the nodal pressures and enthalpies were arbitrarily chosen as they were judged to further magnify the effects of explicit vs. semi-implicit calculations.

As indicated above, metal node mass was varied by an order of magnitude between node 1 and the other three nodes; node 1 was modeled with a metal mass of 0.1 lbm, while nodes 2, 3 and 4 were modeled with a metal mass of 0.01 lbm. This was done to create a larger time rate of change on metal temperature, meaning, the smaller the mass, the higher the dT/dt should be for a given heat flux. As such, there should be a larger difference between explicit vs. semi-implicit for the smaller masses, because the explicit scheme holds the metal temperature central variable value constant for a given time step.

In conjunction with the metal mass variations discussed above, time step size was varied to verify that the semi-implicit model is working correctly. Because the explicit scheme holds the metal temperature central variable value constant for a given time step, if time step size is reduced, the differences in the metal temperature central variable between the beginning and the end of the time step will reduce accordingly and should approach the results of the semi-implicit cases.

The following sections detail the test cases performed and a comparison of the expected results with the results obtained.

4.1.4.1.1 Test Cases

The following four test cases were performed for this validation:

1. Explicit treatment of metal node calculations.
2. Semi-implicit treatment of metal node calculations.
3. Explicit treatment of metal node calculations with reduced time step size.
4. Semi-implicit treatment of metal node calculations with reduced time step size.

For Cases 1 and 2 the standard NOTRUMP EM time step sizes are used, where $\Delta t_{min} = 0.001$ and $\Delta t_{max} = 0.25$

For Cases 3 and 4 reduced time step sizes are used, where $\Delta t_{min} = 0.0001$ and

$\Delta t_{max}=0.001$.

The simulations are run for 10 seconds.

For consistency, other enhanced model features (described in Sections 2.1 and 2.2) are also activated for these test cases. They are:

1. Implicit bubble rise model.
2. Implicit droplet fall model.

4.1.4.2 Comparison of Test Results with Expected Results

To validate that the semi-implicit treatment of the metal node temperature model is implemented correctly, the results of the semi-implicit versus explicit treatments are compared to each other (using plot comparisons of key quantities). The expected result is that the semi-implicit and explicit solutions will converge as the time step size is reduced. Also, it is expected that by switching to the semi-implicit formulation, metal node temperature with respect to time will follow a smooth transition. As these particular test cases are simple thought problems developed for the purpose of demonstrating semi-implicit versus explicit features of metal node temperature, there is no intention here to validate results with experimental test data. All that is being assessed here is the relative performance of the explicit and semi-implicit treatments in providing results judged to be more reasonable or stable. The following sections detail the test cases performed, and a comparison of the expected results with the results obtained.

4.1.4.2.1 Explicit vs. Semi-implicit Metal Node Model with Standard EM Time Step Size

Plots of the results of the cases with the standard time step size (with both explicit and semi-implicit models) are compared in Figures 4.1.4-5 - 4.1.4-19. It is noted that the time scale is expanded on some of the plots in order to illustrate the differences/convergence between the explicit and semi-implicit models.

Figure 4.1.4-5 shows the time step sizes between the first two cases. It is interesting to note that when convergence values are approached, the semi-implicit scheme relaxes time step size, while the explicit scheme is still using relatively small steps. All of the figures plot a number of key variables with respect to time using both semi-implicit and explicit metal node temperature solutions for all four nodes. These variables include: metal node temperature, fluid node vapor temperature, heat link heat transfer rate and fluid node pressure. The majority of the plots are from node 2 as the differences between explicit and semi-implicit are the most pronounced. These plots indicate that the semi-implicit scheme is performing as expected, i.e., variable changes with respect to time are less abrupt.

Figures 4.1.4-15 - 4.1.4-19 are plots of the various quantities discussed above for node

4. Recall that this node contains both a liquid and vapor region. It is noted that there is little differences between the semi-implicit vs. explicit schemes. This is due to several factors. First, the vapor and metal masses are very small relative to the liquid mass, as such the vapor and metal temperatures will vary significantly with respect to time while liquid temperature will remain relatively constant. This is why the fluid node pressure converges to a value very close to 0 in Figures 4.1.4-19 and 4.1.4-33. Also, there is a fair amount of energy exchange between the upper and lower regions. Because metal node temperature remains constant along its entire axial length, the net heat transfer between the metal node and the two regions is essentially zero (see Figures 4.1.4-17 and 4.1.4-18). Therefore, the differences between semi-implicit vs. explicit results will be very small. However, this case proves that the use of the semi-implicit metal node solution has no adverse impacts on the fluid node calculations when two regions are present within the fluid node.

Another improvement to using the semi-implicit metal temperature scheme is that it reduces variability in metal node temperature that would normally be present over a series of time steps. When the resolution of Figure 4.1.4-15 is increased, as shown in Figure 4.1.4-16, it can be seen the semi-implicit scheme provides a much smoother calculation of metal temperature with respect to time. Whenever any behavior of this nature can be improved it is considered to be of overall benefit to the model.

4.1.4.2.2 Explicit vs. Semi-implicit Metal Node Model with Reduced Time Step Size

Figures 4.1.4-20 - 4.1.4-33 are essentially the same as those discussed above for the standard EM time step cases, as the same behavior is observed for the semi-implicit solutions. However, as expected the semi-implicit and explicit solutions converge as the time step size is reduced.

4.1.4.3 Additional Discussion

Further evidence that the semi-implicit vs. explicit scheme is working as intended can be seen in the plots of the fluid node quantities (temperature, pressure, etc.). This is evident in Figures 4.1.4-7, 4.1.4-9 and 4.1.4-13, as compared to Figures 4.1.4-22, 4.1.4-24 and 4.1.4-28. In each of these figures it can be seen that the values calculated with the explicit vs. semi-implicit metal node solution converge as the time step size is reduced. If the time step size was further reduced, these values would essentially become one in the same. Although it is not the focus of this discussion, it is worth noting that some of the same parameters calculated using the semi-implicit solution scheme, but with different time step sizes, converge to slightly different values. This can be seen in Figures 4.1.4-9 and 4.1.4-24. For example, fluid node 2 vapor temperature for the semi-implicit scheme (with EM time step inputs) in Figure 4.1.4-9 converges to a value of about 1342.5°F where as in Figure 4.1.4-24 (semi-implicit scheme with reduced time step size) it converges to a value of 1344.2°F. This is considered to be due to calculational

convergence within the fluid node coupled with numerical solution precision and the fact that metal node temperatures are still treated explicitly with respect to the fluid node energy conservation equations. The important point here is that the semi-implicit and explicit metal node temperature values converge as the time step size is reduced. This can be seen in any of the plots where metal node temperature is provided. This gives proof that the semi-implicit metal node temperature model is functioning as expected. In general, the results also show that regardless of region conditions (Nodes 1 & 2 - Vapor, Node 3 - Liquid, Node 4 - Liquid & Vapor) the semi-implicit calculation of metal node temperatures is performed in a consistent manner.

4.1.4.4 Semi-Implicit Metal Node Model Conclusions

Based on the results of both standard and reduced time step cases, the semi-implicit calculation of metal node temperature is functioning as expected, in all three fluid node states, Vapor, Liquid and Vapor/Liquid. The semi-implicit metal node temperature model provides smoother transitions to final values with less variability with respect to time. Therefore, the semi-implicit metal node model will be implemented in the new NOTRUMP EM beginning with code version 38.0.

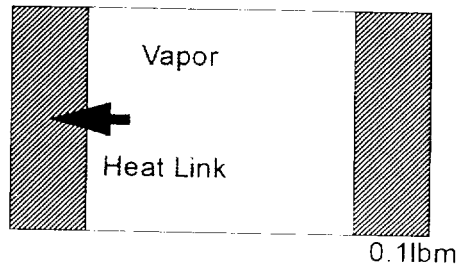


Figure 4.1.4-1 Node 1

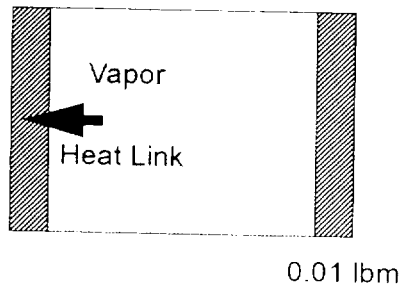


Figure 4.1.4-2 Node 2

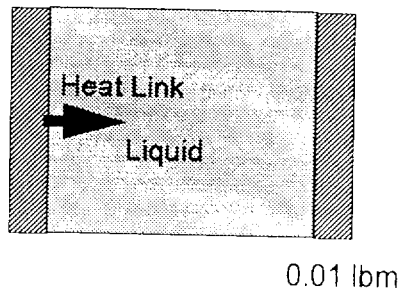


Figure 4.1.4-3 Node 3

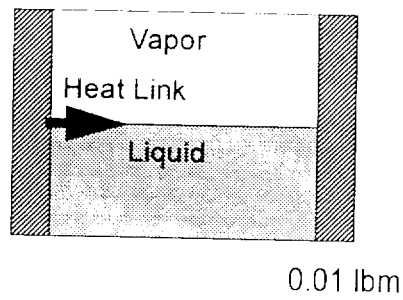


Figure 4.1.4-4 Node 4

WESTINGHOUSE ELECTRIC COMPANY LLC

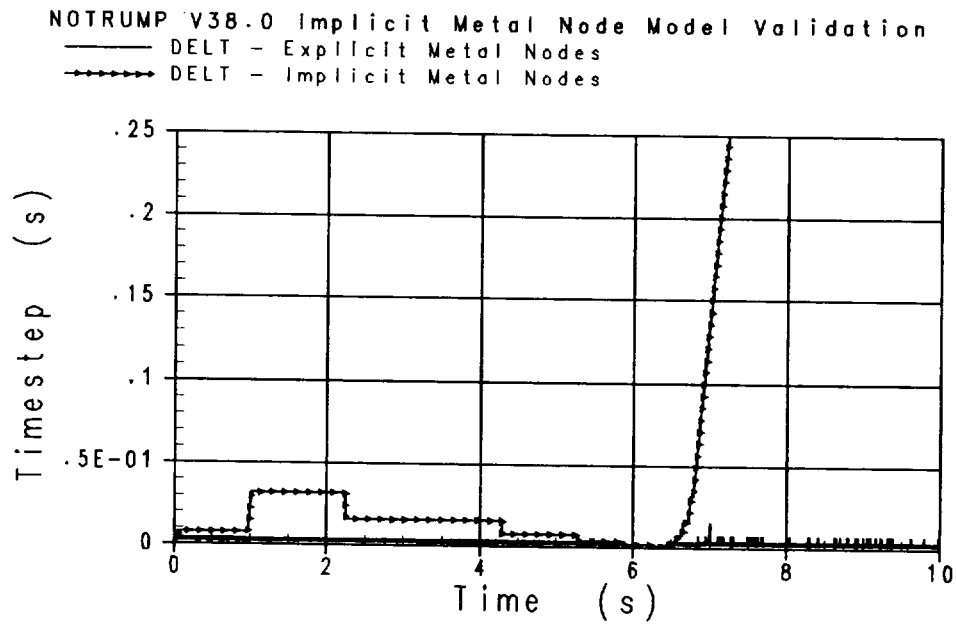


Figure 4.1.4-5 Standard EM Time Step Size

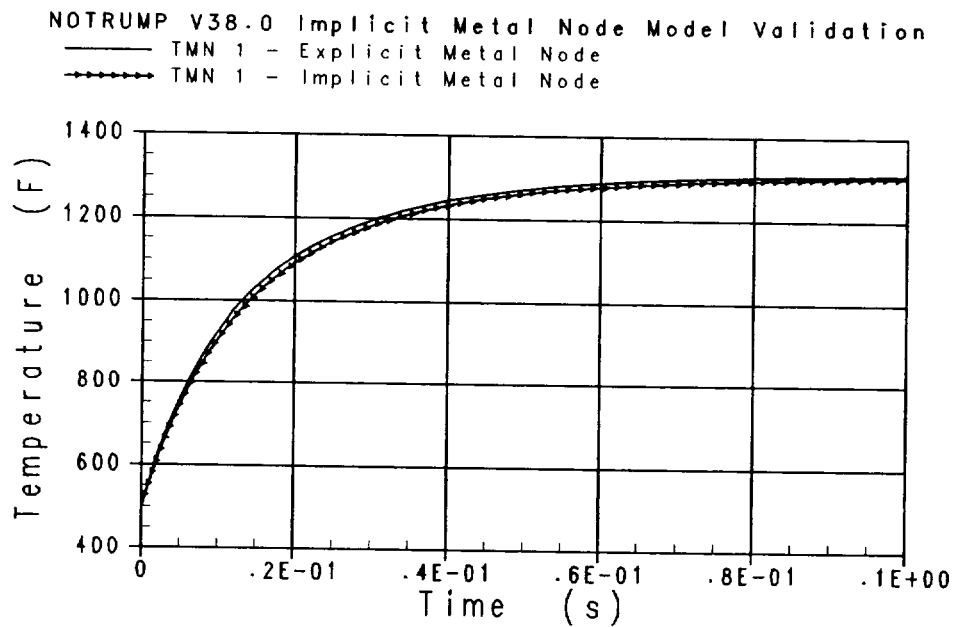


Figure 4.1.4-6 Node 1 - Metal Node Temperature, Standard EM Time Step Size

WESTINGHOUSE ELECTRIC COMPANY LLC

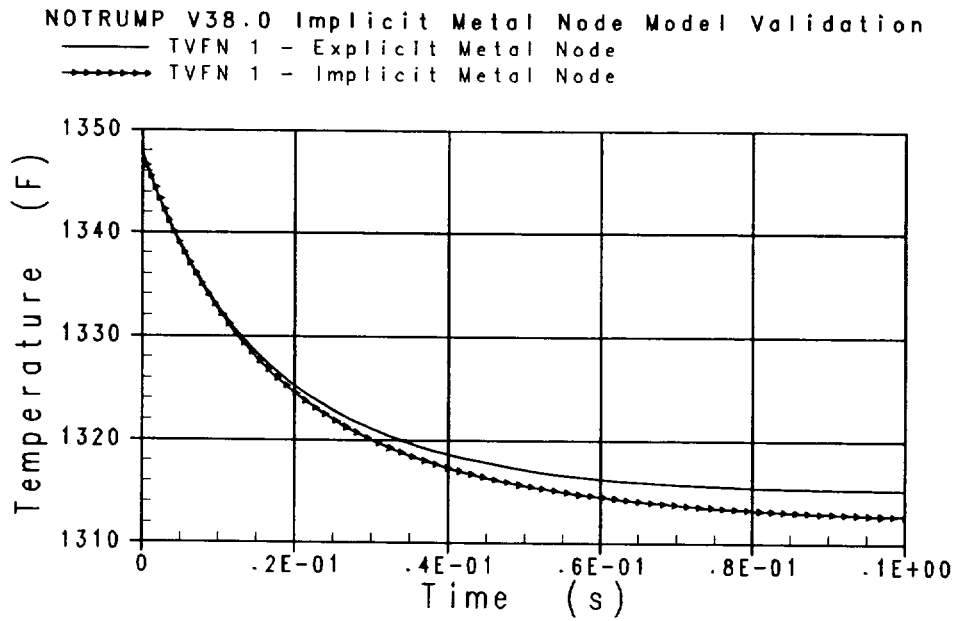


Figure 4.1.4-7 Node 1 - Fluid Node Vapor Temperature, Standard EM Time Step Size

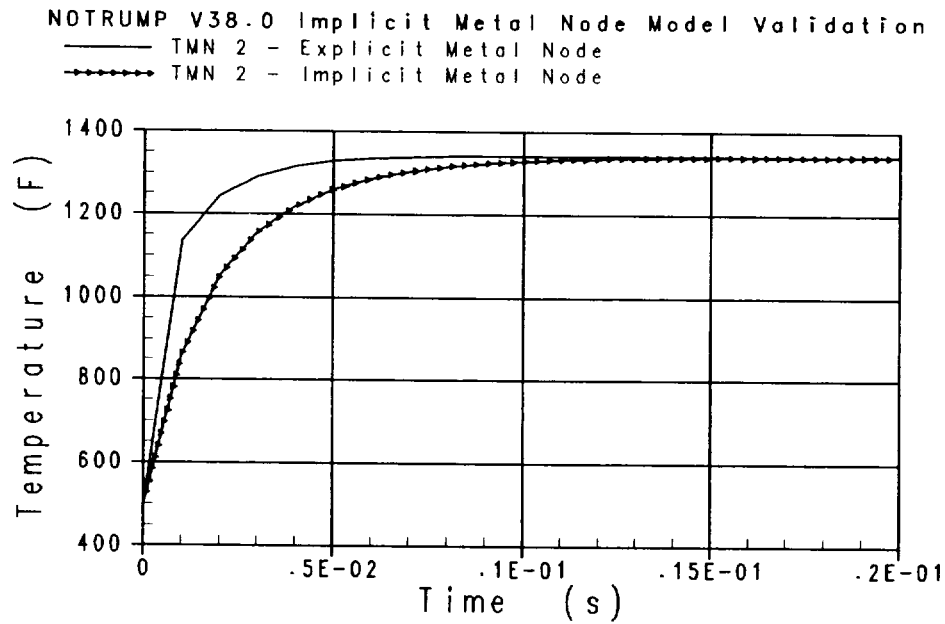


Figure 4.1.4-8 Node 2 - Metal Node Temperature, Standard EM Time Step Size

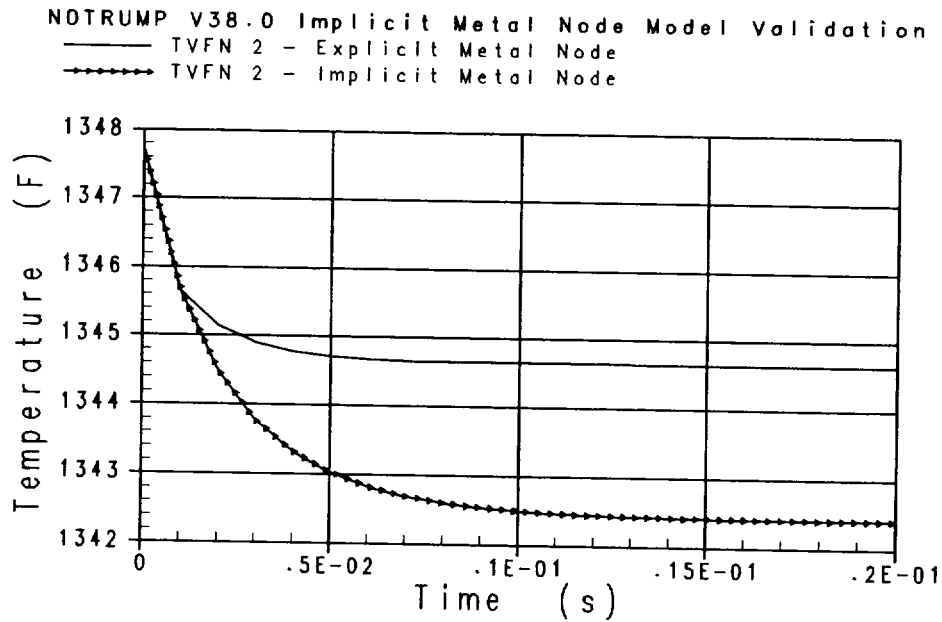


Figure 4.1.4-9 Node 2 - Fluid Node Vapor Temperature, Standard EM Time Step Size

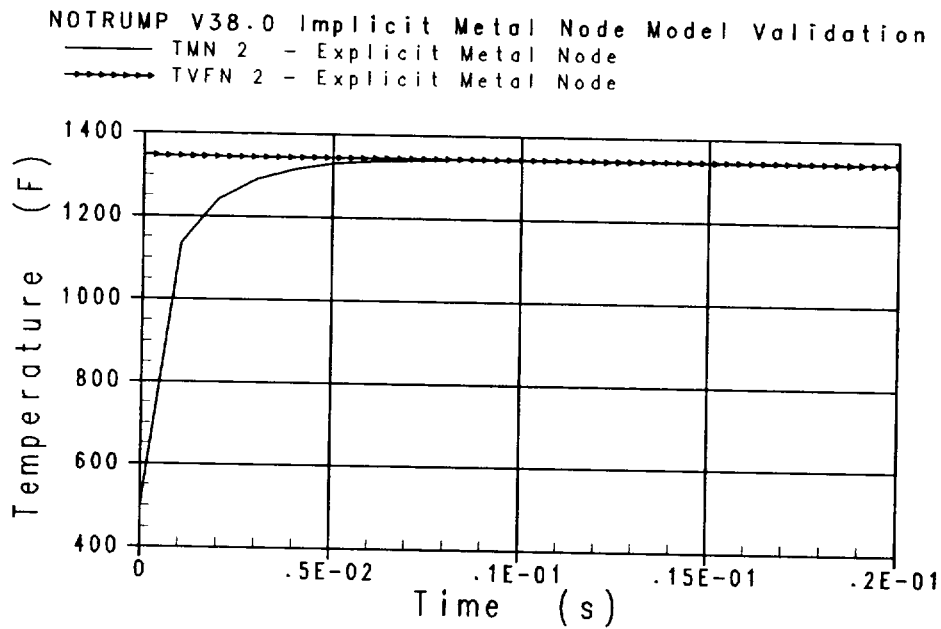


Figure 4.1.4-10 Node 2 - Explicit Fluid Node Vapor Temperature w/ Metal Node Temperature, Standard EM Time Step Size

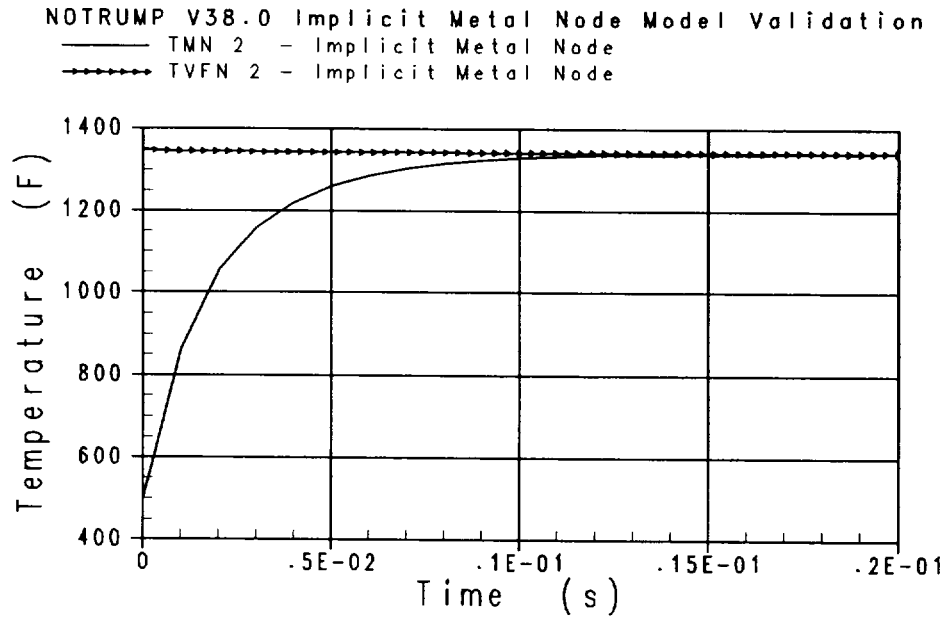


Figure 4.1.4-11 Node 2 - Semi-implicit Fluid Node Vapor Temperature w/ Metal Node Temperature, Standard EM Time Step Size

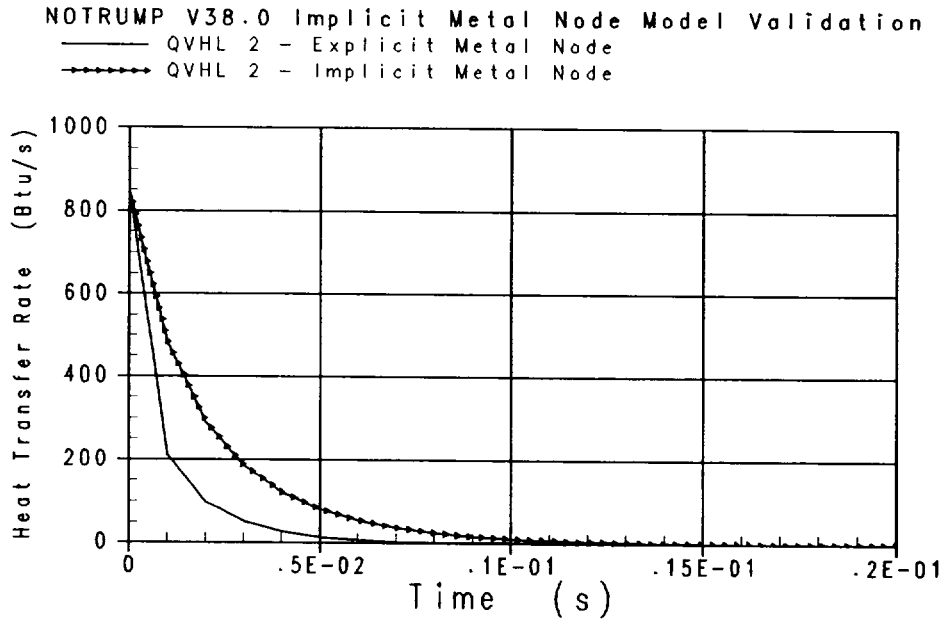


Figure 4.1.4-12 Node 2 - Vapor Region Heat Transfer Rate, Standard EM Time Step Size

WESTINGHOUSE ELECTRIC COMPANY LLC

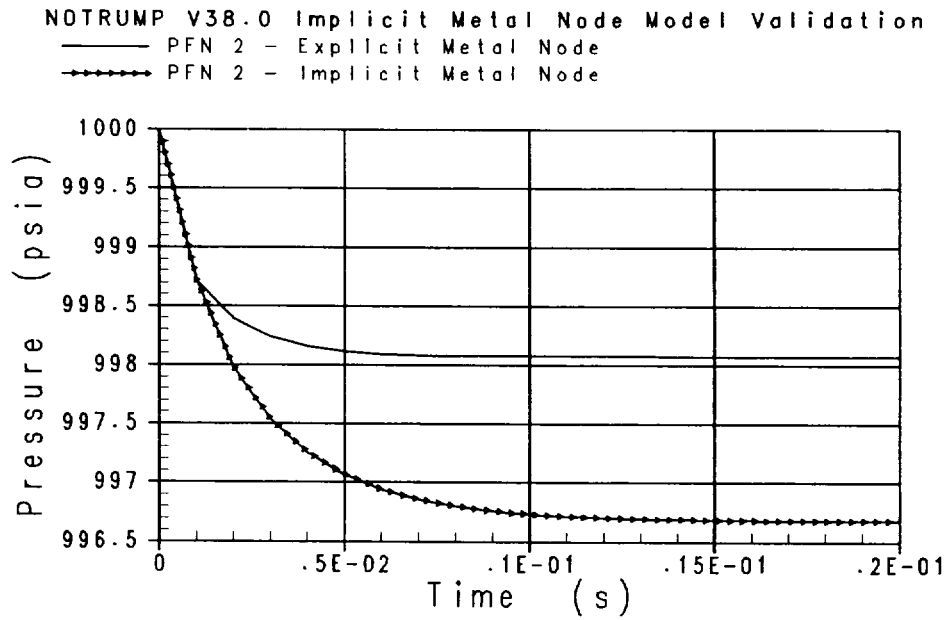


Figure 4.1.4-13 Node 2 - Fluid Node Pressure, Standard EM Time Step Size

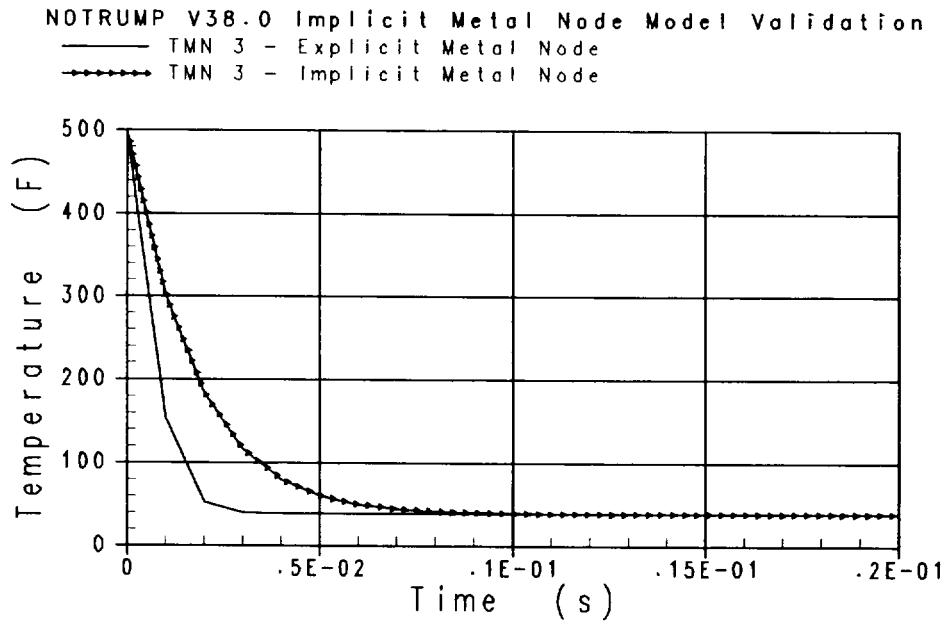


Figure 4.1.4-14 Node 3 - Metal Node Temperature, Standard EM Time Step Size

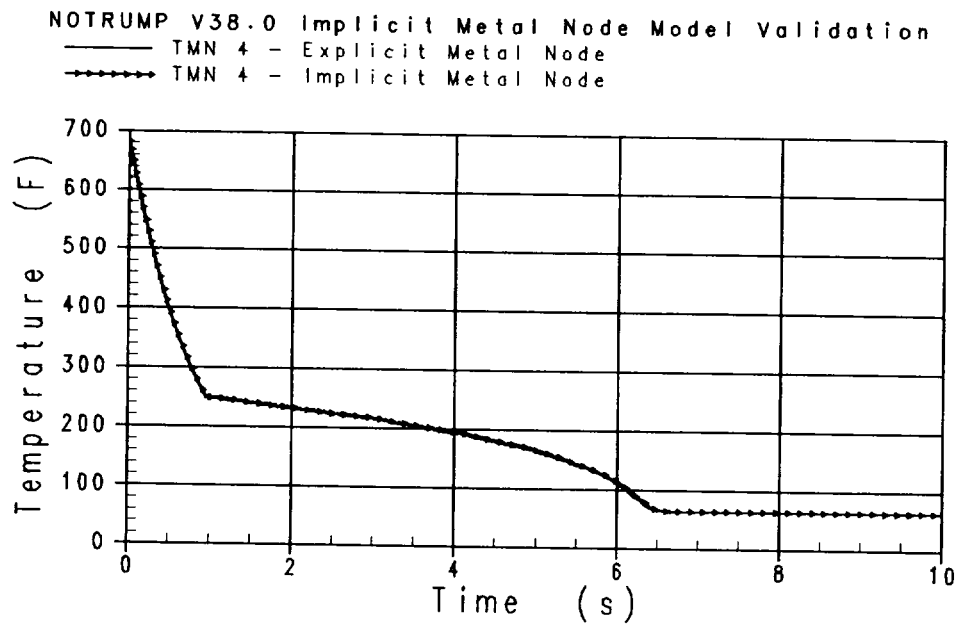


Figure 4.1.4-15 Node 4 - Metal Node Temperature, Standard EM Time Step Size

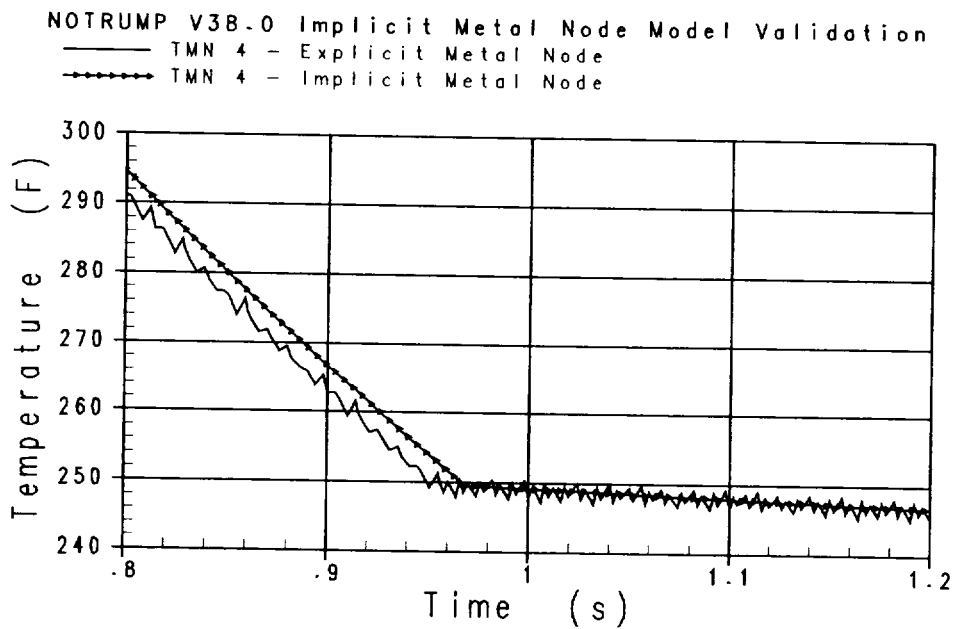


Figure 4.1.4-16 Node 4 - Metal Node Temperature - Expanded Resolution, Standard EM Time Step Size

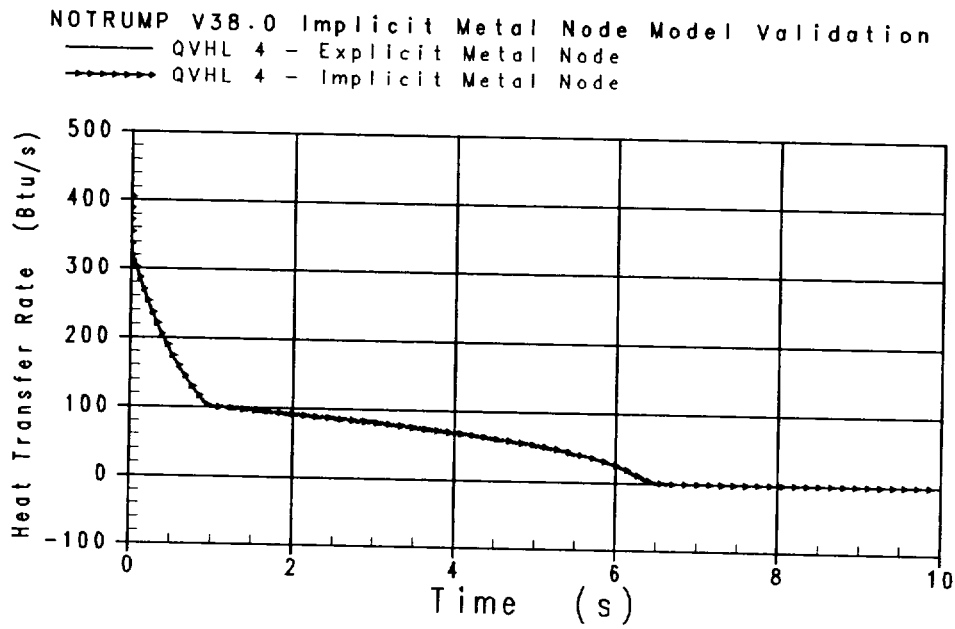


Figure 4.1.4-17 Node 4 - Vapor Region Heat Transfer Rate, Standard EM Time Step Size

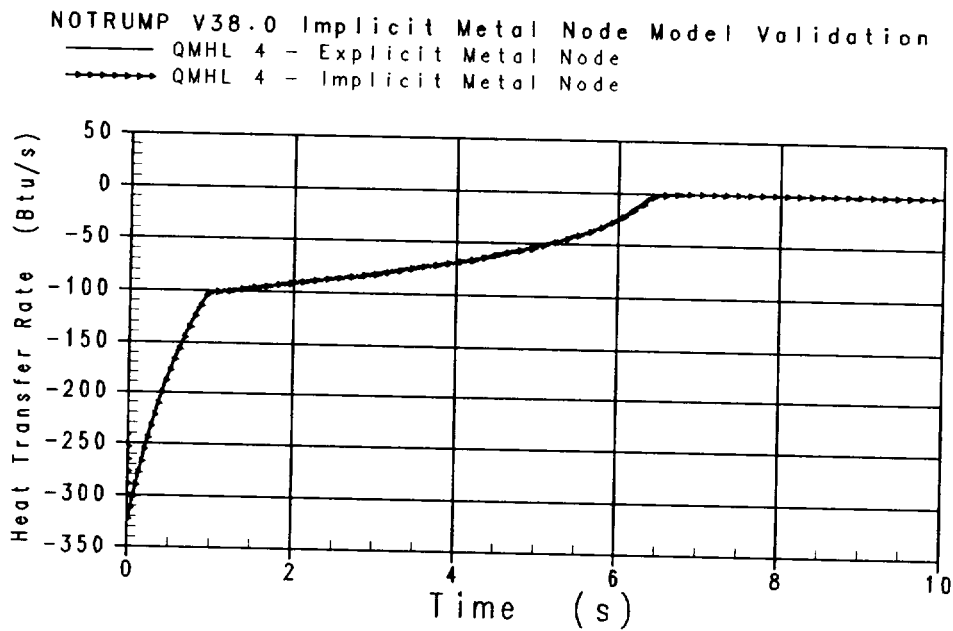


Figure 4.1.4-18 Node 4 - Mixture Region Heat Transfer Rate, Standard EM Time Step Size

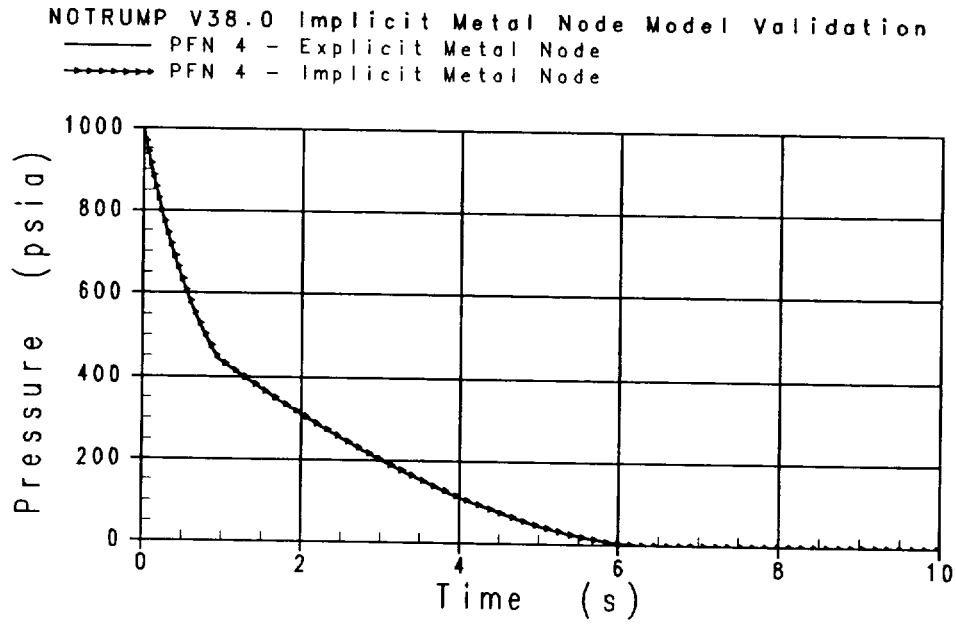


Figure 4.1.4-19 Node 4 - Fluid Node Pressure, Standard EM Time Step Size

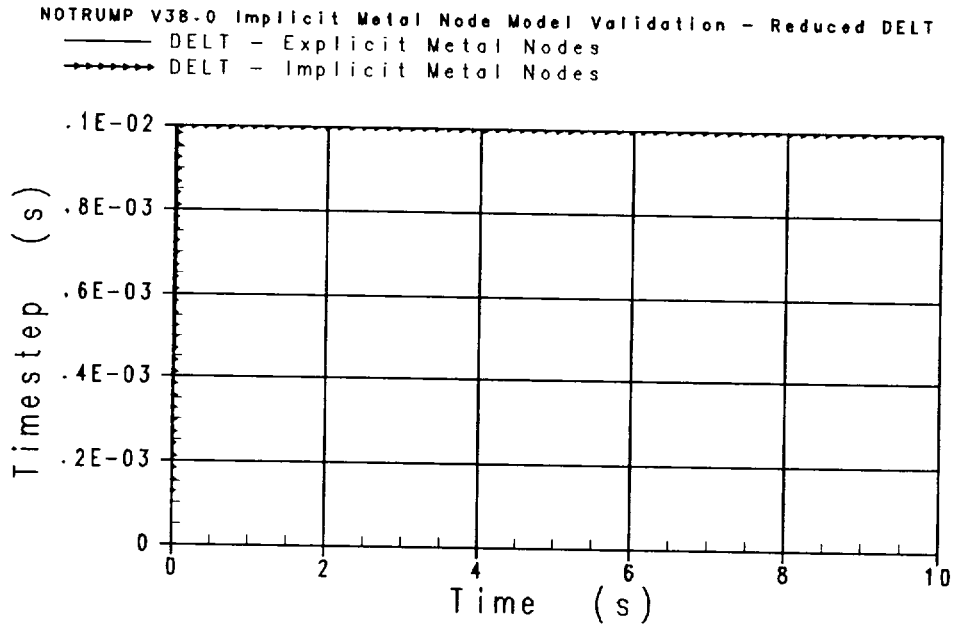


Figure 4.1.4-20 Reduced Time Step Size

WESTINGHOUSE ELECTRIC COMPANY LLC

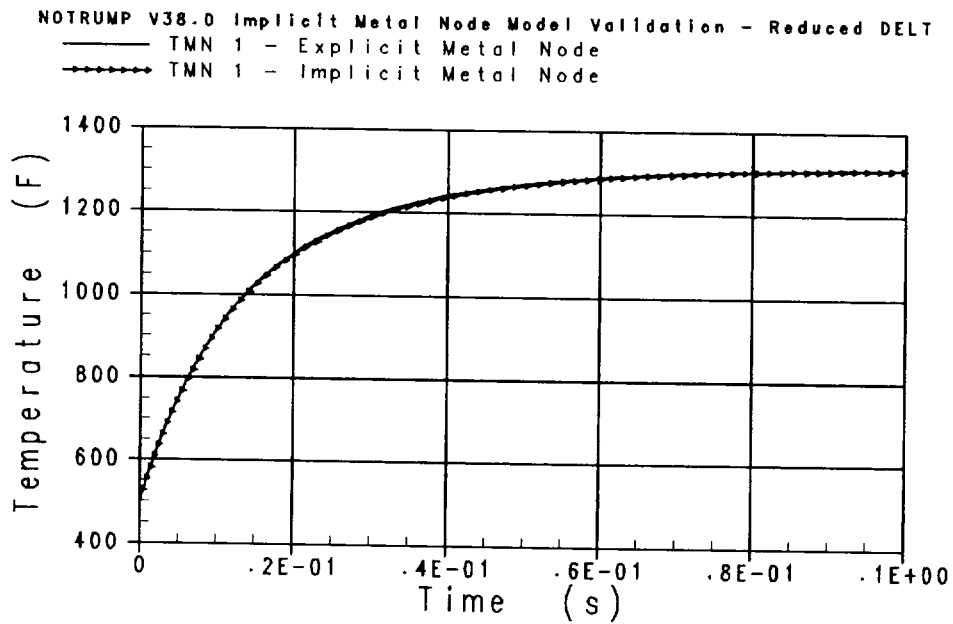


Figure 4.1.4-21 Node 1 - Metal Node Temperature, Reduced Time Step Size

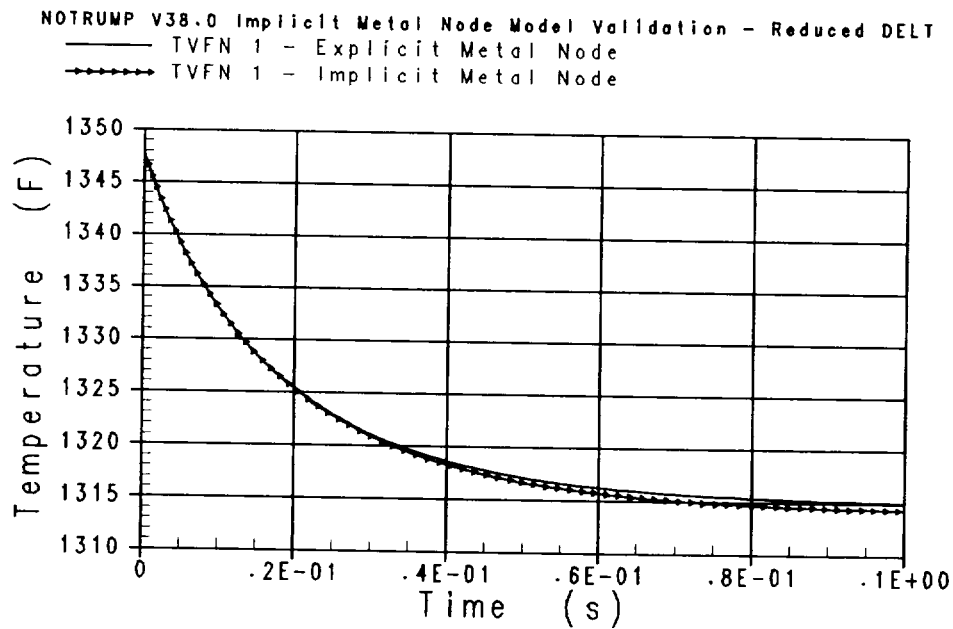


Figure 4.1.4-22 Node 1 - Fluid Node Vapor Temperature, Reduced Time Step Size

WESTINGHOUSE ELECTRIC COMPANY LLC

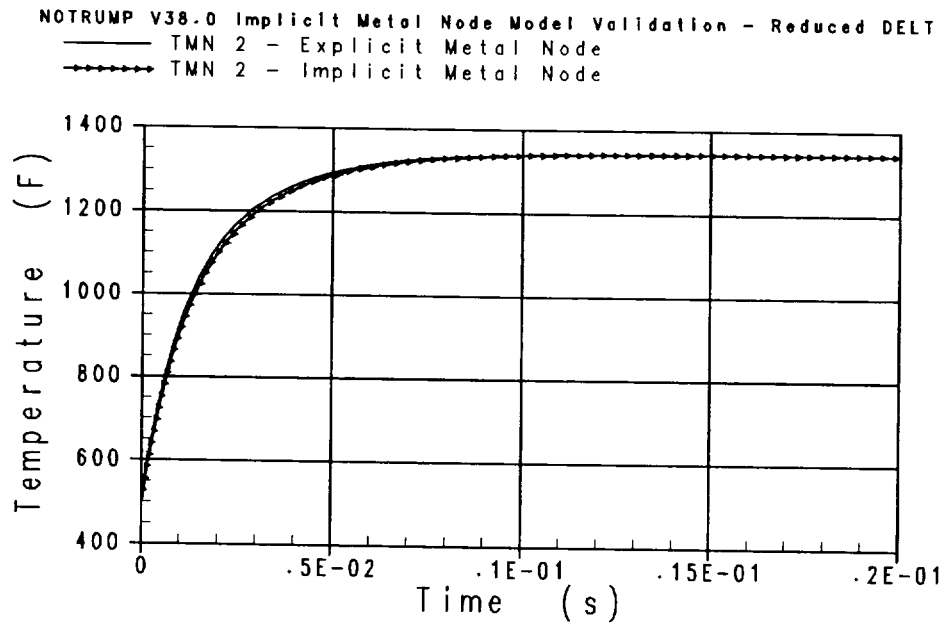


Figure 4.1.4-23 Node 2 - Metal Node Temperature, Reduced Time Step Size

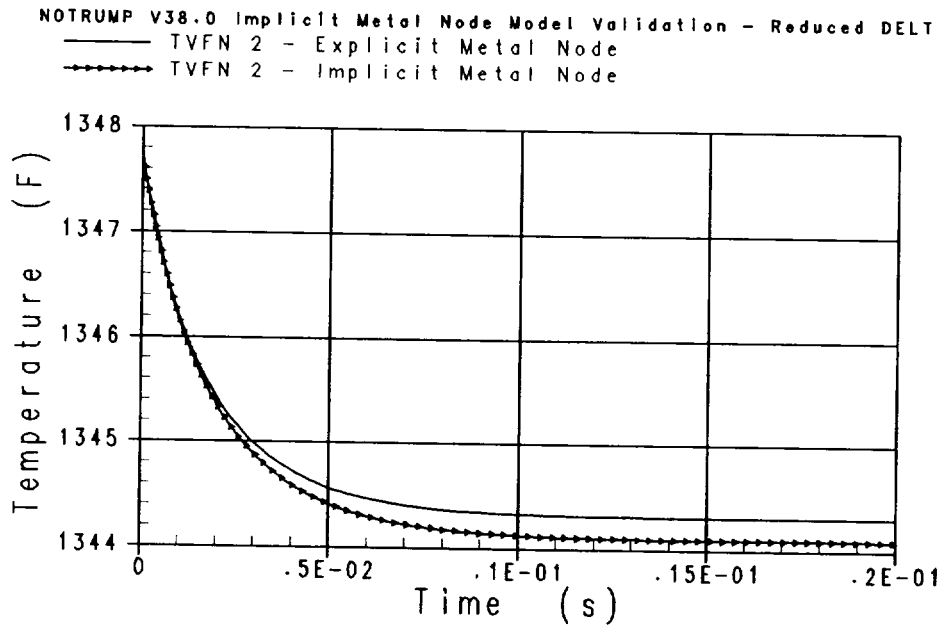


Figure 4.1.4-24 Node 2 - Fluid Node Vapor Temperature, Reduced Time Step Size

WESTINGHOUSE ELECTRIC COMPANY LLC

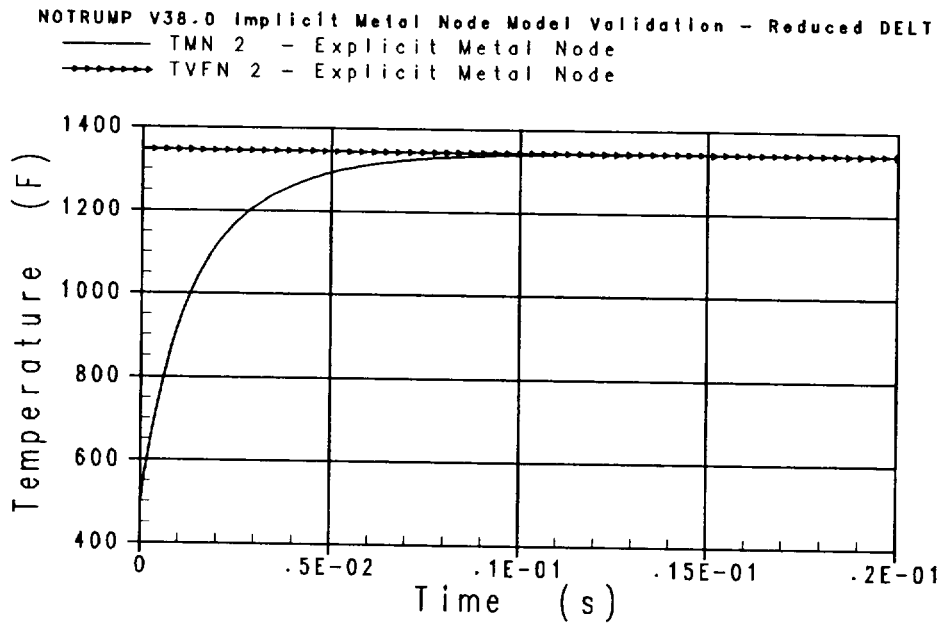


Figure 4.1.4-25 Node 2 - Explicit Fluid Node Vapor Temperature w/ Metal Node Temperature, Reduced Time Step Size

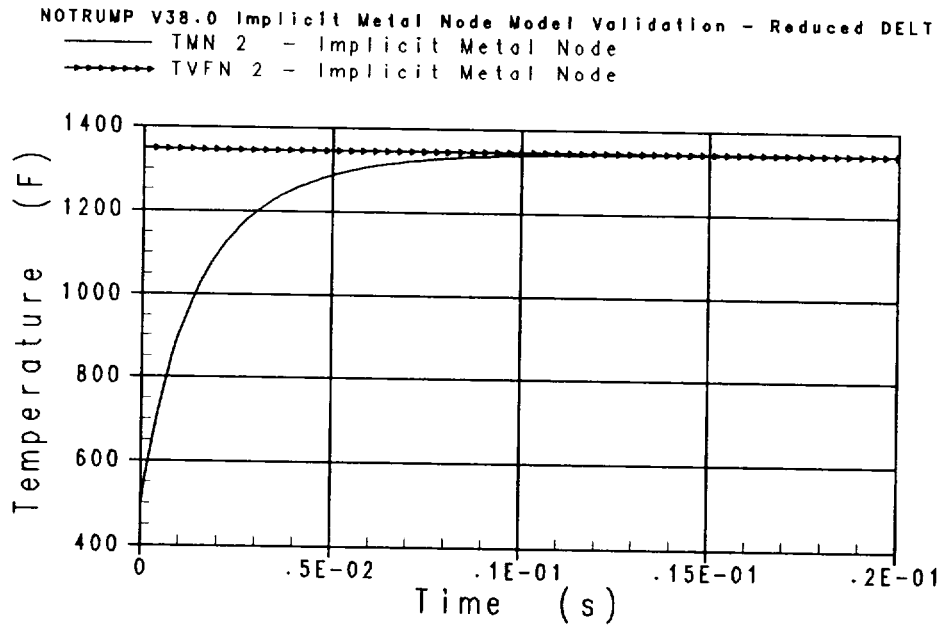


Figure 4.1.4-26 Node 2 - Semi-implicit Fluid Node Vapor Temperature w/ Metal Node Temperature, Reduced Time Step Size

WESTINGHOUSE ELECTRIC COMPANY LLC

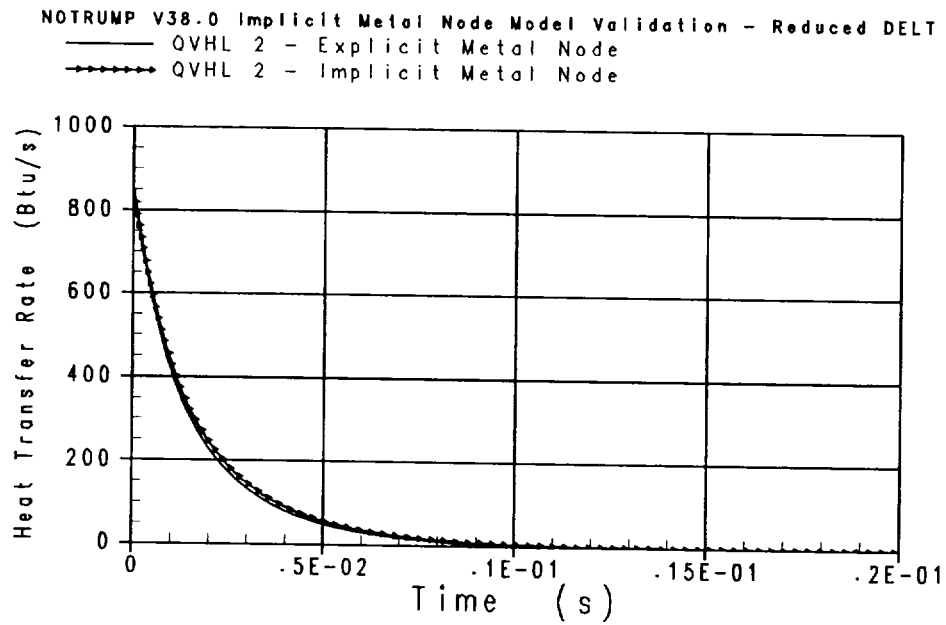


Figure 4.1.4-27 Node 2 - Vapor Region Heat Transfer Rate, Reduced Time Step Size

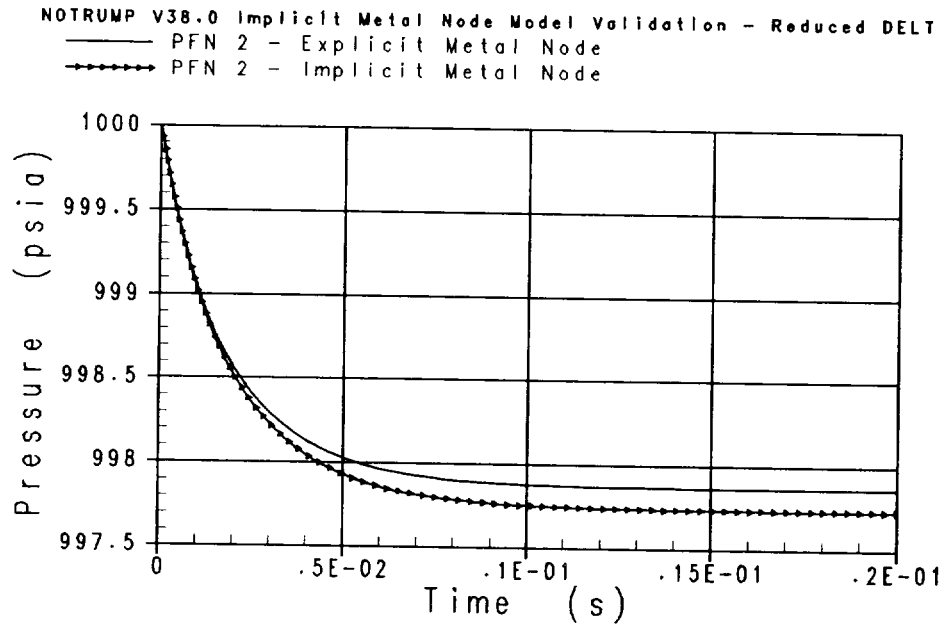


Figure 4.1.4-28 Node 2 - Fluid Node Pressure, Reduced Time Step Size

WESTINGHOUSE ELECTRIC COMPANY LLC

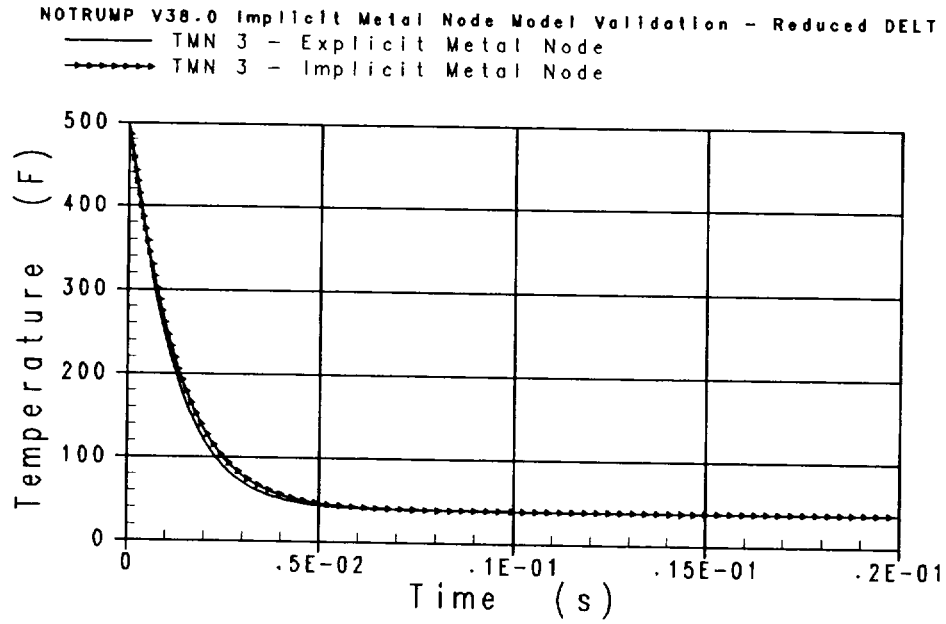


Figure 4.1.4-29 Node 3 - Metal Node Temperature, Reduced Time Step Size

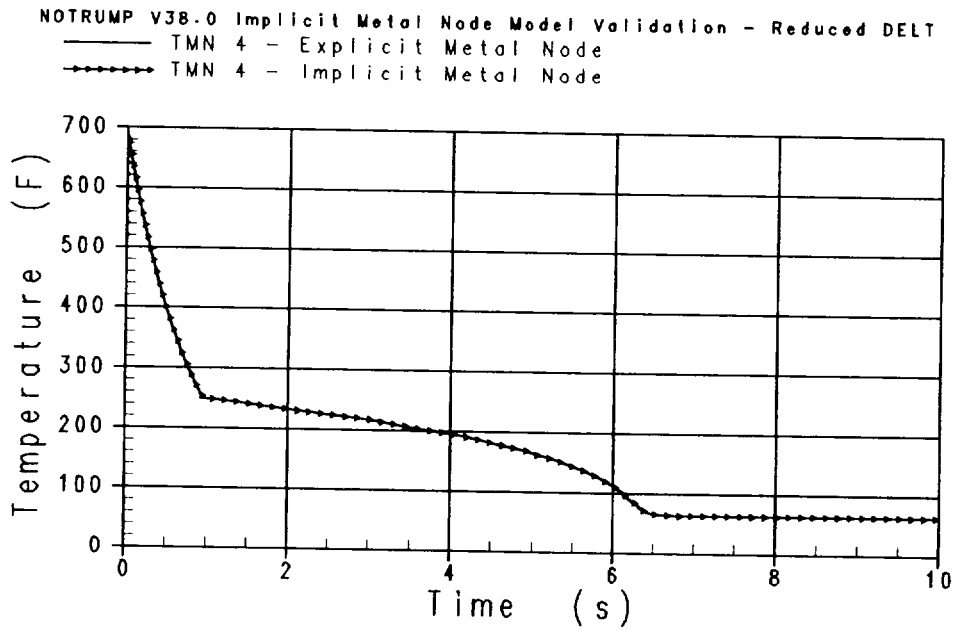


Figure 4.1.4-30 Node 4 - Metal Node Temperature, Reduced Time Step Size

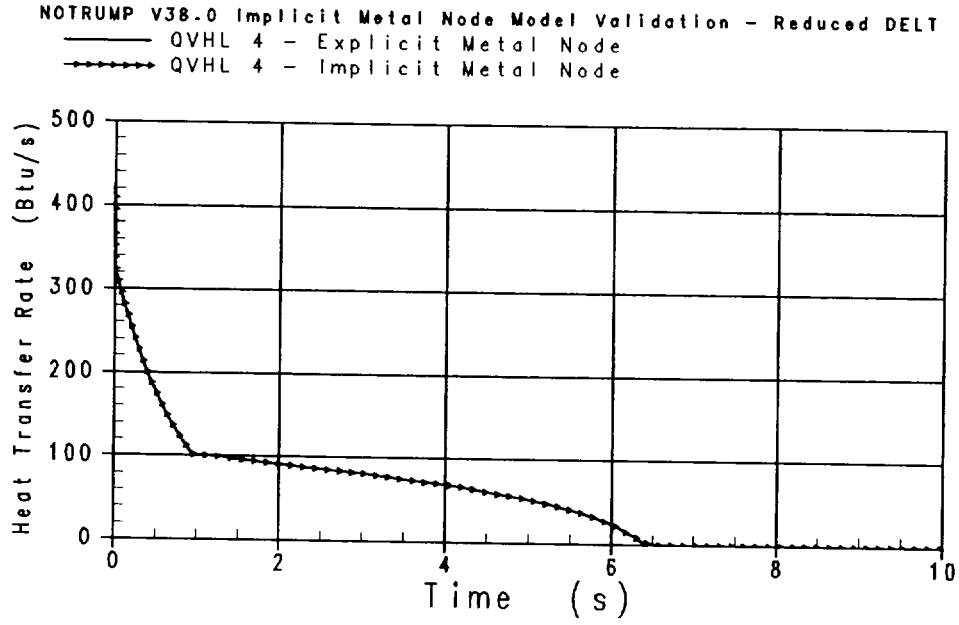


Figure 4.1.4-31 Node 4 - Vapor Region Heat Transfer Rate, Reduced Time Step Size

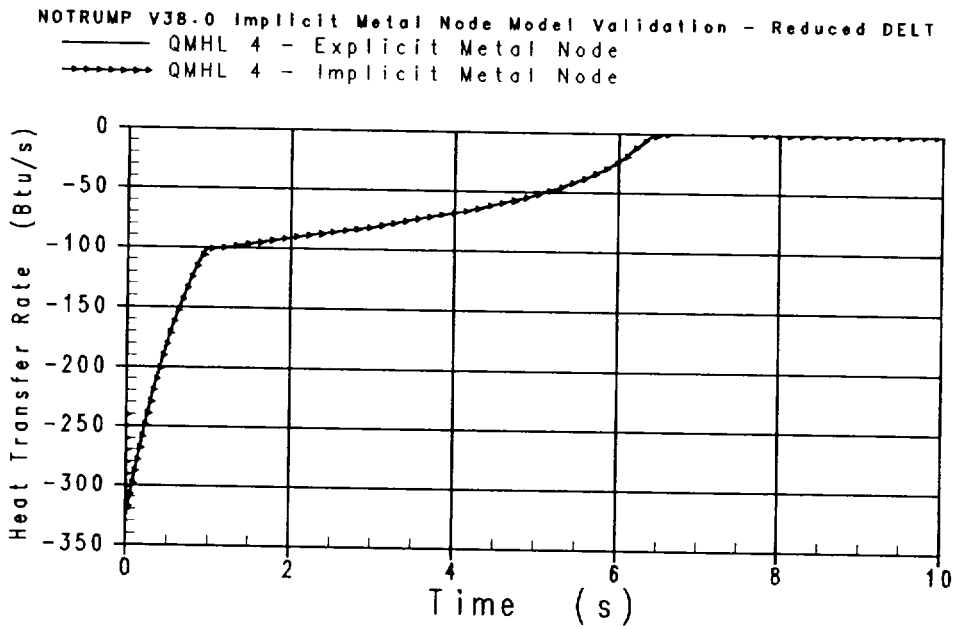


Figure 4.1.4-32 Node 4 - Mixture Region Heat Transfer Rate, Reduced Time Step Size

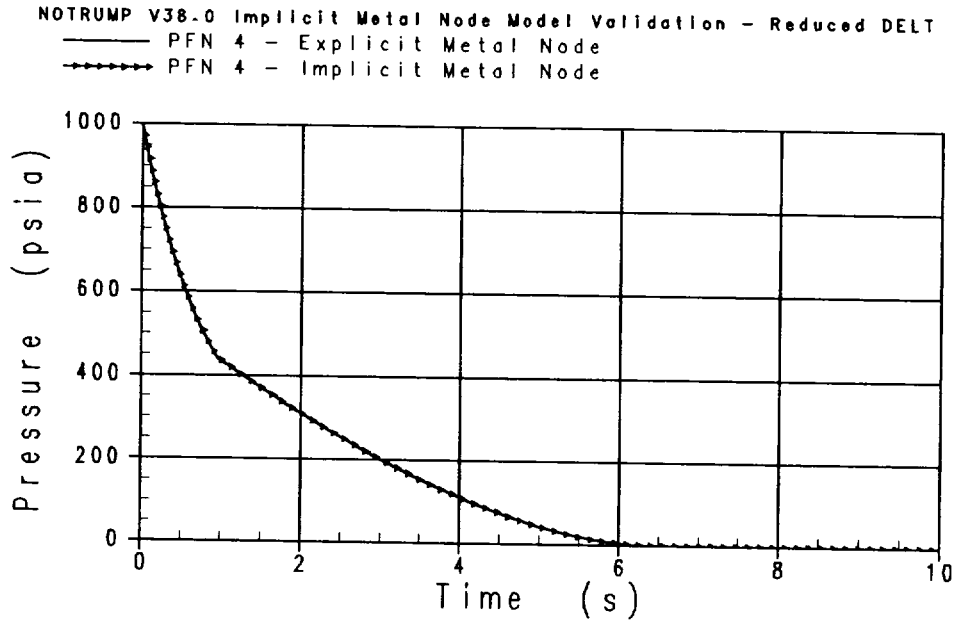


Figure 4.1.4-33 Node 4 - Fluid Node Pressure, Reduced Time Step Size

4.1.5 Validation of Improved Region Depletion Model

The purpose of this section is to validate the implementation of the improved region depletion model (i.e., the mixture level overshoot model) in the NOTRUMP Evaluation Model (EM) for interior fluid nodes within a stack. The previous NOTRUMP EM utilizes the original region depletion model for all interior fluid nodes, including those within a stack when the mixture level attempts to cross node boundaries. The derivations of the improved region depletion model, as well as a review of the original region depletion model, are provided in Section 2.5 of this report. The following subsections describe the test cases and the comparison of test results versus expected results for the validation of the improved region depletion model. The validation method employed is to compare the results of the test cases with the improved region depletion model to those with the original region depletion model, and show the difficulty that the original region depletion model has in passing the mixture level between interior fluid nodes within a stack.

4.1.5.1 Description of Test Cases

To validate the improved region depletion model, a manometer thought problem was developed. The NOTRUMP model for this test case is a 5 ft. high manometer, and the noding diagram is shown in Figure 4.1.5-1. One side of the manometer consists of a vertical column of four interior fluid nodes in a stack, and each fluid node is 1 ft. high and 1 ft.³ in volume. The other side of the manometer is a vertical column of equivalent size and consists of one interior fluid node that is 4 ft. high and 4 ft.³ in volume. The bottom of the manometer, which connects both vertical columns, consists of one interior fluid node that is 1 ft. high and 3 ft.³ in volume. The manometer is connected at the top to a constant-pressure boundary fluid node. Point contact non-critical flow links connect the fluid nodes, as depicted in Figure 4.1.5-1. Each flow link has a length of 1 ft. and an area of 1 ft.². A constant friction (fL/D) value of 0.02 is assigned to each flow link. The manometer is initialized to a non-equilibrium condition with a high (4.5 ft.) water level in the column containing the stack of four interior fluid nodes, and a low (1.5 ft.) water level in the column containing the one interior fluid node. The initial pressure in all fluid nodes is 14.696 psia. To maximize the piston-like behavior of the oscillating manometer, single-phase fluids are employed. The water is initialized subcooled with a specific enthalpy of 30 Btu/lbm, and the steam is initialized superheated with a specific enthalpy of 1300 Btu/lbm. The initial mass flowrate in all flow links is zero. The simulation is run for 5 seconds.

For the validation of the improved region depletion model, the following test cases (i.e., NOTRUMP runs) are performed:

1. Base Case, with the improved region depletion model, and the NOTRUMP EM maximum (0.25 seconds) and minimum (0.001 seconds) time step sizes.
2. Same as Case 1, but with the original region depletion model.

Due to the known difficulty that the original region depletion model has in passing the mixture level between interior fluid nodes within a stack, the method employed here is to perform as many attempts as necessary to enable this case to run to completion, reducing the minimum time step size each time. Case 2 failed to execute beyond the time when the mixture level attempted to cross the first node boundary that it encountered (which will be discussed in Section 4.1.5.2), thus it is necessary to rerun this case with a reduction in the minimum time step size, as follows:

3. Same as Case 2, but with a reduced minimum time step size of 0.0001 seconds.

Case 3 failed to execute beyond the time when the mixture level attempted to cross the second node boundary that it encountered (which will be discussed in Section 4.1.5.2), thus it is necessary to rerun this case again with a further reduction in the minimum time step size, as follows:

4. Same as Case 2, but with a reduced minimum time step size of 0.00001 seconds.

The results of Cases 2, 3, and 4 will be compared to each other, and the results of Case 1 will be compared to the results of Case 4, in Section 4.1.5.2.

All of the aforementioned test cases employ the other applicable enhanced model features that are being implemented in the new NOTRUMP EM, which are:

1. Implicit bubble rise model (described in Section 2.1).
2. Implicit droplet fall model (described in Section 2.2).
3. Implicit fluid node gravitational head model (described in Section 2.3).

Note that the semi-implicit metal node model does not apply here, since there are no metal nodes.

4.1.5.2 Comparison of Test Results with Expected Results

As stated in Section 4.1.5.1, Case 2 failed to execute beyond the time when the mixture level attempted to cross the first node boundary that it encountered. Specifically, this occurs at an elevation of 4 ft. at the boundary between interior fluid nodes 2 and 3, at transient time 0.234 seconds. The code aborted due to a non-positive vapor region mass and/or energy in interior fluid node 2. Recall from Section 2.5 that in the original region depletion model, when a region's mass and/or energy becomes non-positive (which triggers the region depletion logic), this non-positive mass and energy of the depleted region are added to the mass and energy, respectively, of the other region of the same interior fluid node, in conjunction with setting the depleted region's mass and energy to zero. This can result in a non-positive mass and/or energy in the other (non-depleted) region, or can lead to a non-physical temperature and/or pressure. This is exactly what

happened in Case 2: the mixture region was depleted in interior fluid node 2, and that node's vapor region mass and/or energy became non-positive.

Case 3, with the minimum time step size reduced to 0.0001 seconds, is able to execute past the first node boundary crossing, but fails to execute beyond the crossing of the second node boundary, at an elevation of 3 ft. between interior fluid nodes 3 and 4, at transient time 0.434 seconds. Note that even though this case executes past the first node boundary crossing, numerous high vapor temperature steam table warning messages are obtained in interior fluid nodes 2, 3, and 4, and several low pressure steam table warning messages are obtained in interior fluid node 3, during the time in which the mixture level is passing through interior fluid node 3. This is clearly undesirable behavior. The eventual code abort occurs in interior fluid node 2 with a non-positive vapor region mass and/or energy.

Case 4, with the minimum time step size reduced to 0.00001 seconds, is able to execute the entire transient to completion, and no steam table warning messages are obtained.

Plot comparisons of the stack mixture level from Cases 2, 3, and 4 are contained in Figure 4.1.5-2.

Plot comparisons of the stack mixture level from Case 1 with the improved region depletion model (and minimum time step size of 0.001 seconds) versus that from Case 4 with the original region depletion model (and minimum time step size of 0.00001 seconds) are contained in Figure 4.1.5-3. Note that the results of the two cases are in very close agreement.

4.1.5.3 Improved Region Depletion Model Conclusions

It has been demonstrated that the improved region depletion model (i.e., mixture level overshoot model) is capable of reliably and relatively smoothly allowing the mixture level to cross the interior fluid node boundaries in a stack, in both draining and filling situations. It does so at time step sizes that are not prohibitively small (i.e., at time step sizes that are within the range of the NOTRUMP EM minimum and maximum values), and behaves as expected. In contrast, it has been demonstrated that the original region depletion model is not capable of reliably allowing the mixture level to cross the interior fluid node boundaries in a stack, and in fact requires a prohibitively small minimum time step size in order to execute simulations to completion without aborting. Since there is no provision in the current NOTRUMP time step size controller that checks for region depletion, use of the original region depletion model requires intervention by the user to reduce the minimum time step size to obtain successful execution. Also, the original region depletion model, by its method of forcing the mixture level to stop exactly at the interior fluid node boundaries within a stack, is more likely to obtain unrealistic "level hangs".

WESTINGHOUSE ELECTRIC COMPANY LLC

In summary, the improved region depletion model has been adequately validated in NOTRUMP Version 38.0. The use of this model within interior fluid node stacks represents an improvement over the previous NOTRUMP EM's use of the original region depletion model within interior fluid node stacks. The improved region depletion model will be included as the default model in the new NOTRUMP EM beginning with NOTRUMP Version 38.0.

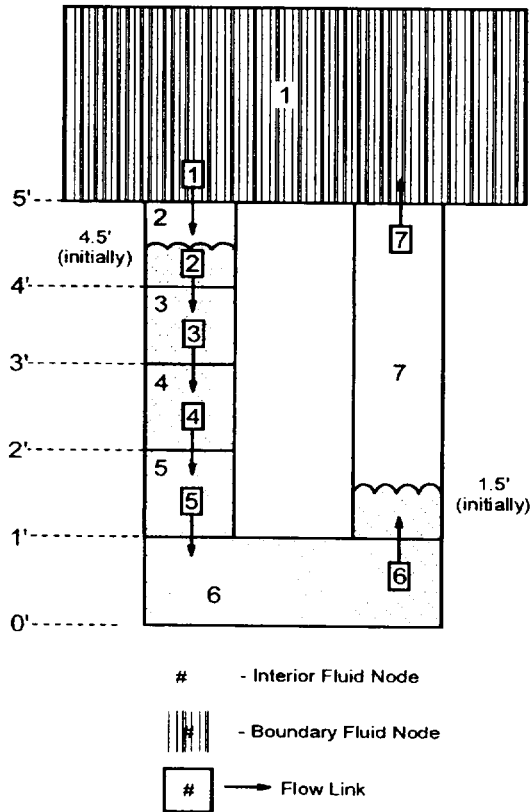


Figure 4.1.5-1 Manometer Noding Diagram

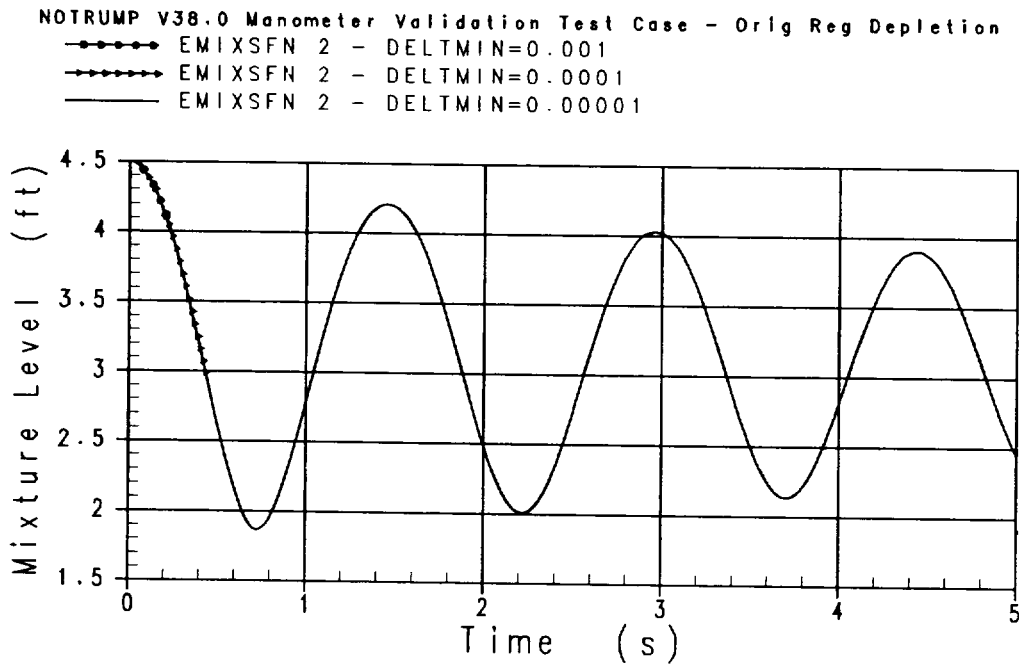


Figure 4.1.5-2 Original Region Depletion Model: Stack Mixture Level EMIXSFN 2

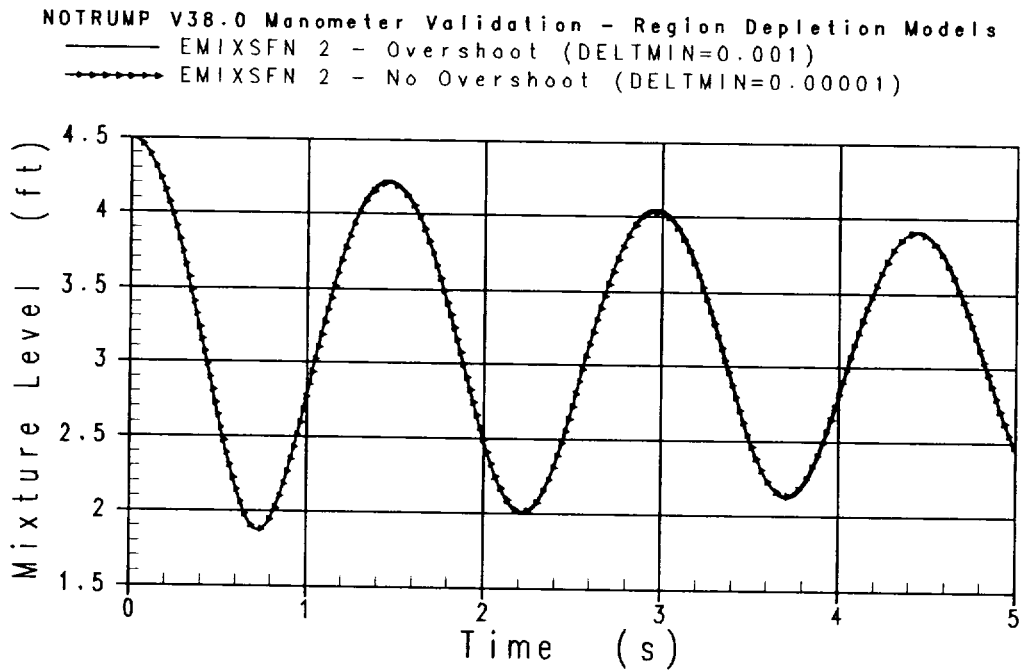


Figure 4.1.5-3 Improved (Overshoot) vs. Original (No Overshoot) Region Depletion: Stack Mixture Level EMIXSFN 2

4.2 Integral Effects Validation

The following section presents the results of an integral simulation performed in support of the validation of the new NOTRUMP Version 38.0 Evaluation Model (EM) features. It presents a comparison of the results obtained with and without the application of the new model features on a sample PWR calculation.

4.2.1 Sample Plant - Small Break LOCA Simulation

This section documents the simulation of a small break (SB) LOCA for a sample Westinghouse PWR, using the NOTRUMP Version 38.0 code. This simulation is performed as a part of the NOTRUMP validation effort; therefore no PCT calculations are included here. Cases with and without the enhanced model features are included in this simulation to demonstrate the effect of these features on the transient results.

4.2.1.1 Cases Analyzed

A 3 inch cold leg break with no auxiliary feed water (AFW) flow and a 6 inch cold leg break with 200 gpm AFW flow are simulated in this effort, using NOTRUMP Version 38.0. The 6 inch case (with 200 gpm AFW) was chosen because it was found to contain non-physical mixture level hangs, which resulted in extended core mixture level depression and level oscillations. It is expected that this case would demonstrate the effect of applying the enhanced model features on the calculated results, since the features being implemented are intended to improve mixture level behavior. The 3 inch break size with no AFW flow was chosen as a second test case for comparison to the 6 inch case. Each break is analyzed with and without activating the enhanced model features.

4.2.1.2 NOTRUMP Simulation

The standard Westinghouse NOTRUMP Evaluation Model (EM) noding scheme is used for this analysis.

The enhanced model features activated were:

1. Implicit bubble rise model.
2. Implicit droplet fall model.
3. Implicit fluid node gravitational head model.
4. Semi-Implicit metal node model.
5. Improved region depletion model.

4.2.1.3 Discussion of Results

4.2.1.3.1 6-inch Cold Leg Break, AFW=200 gpm

The results of the 6 inch break are presented in Figures 4.2.1-1 to 4.2.1-8. Figure 4.2.1-1 presents a comparison of the core mixture level response between the cases with and without the enhanced model features activated. As can be seen, the enhanced models eliminate the mixture level oscillations observed between 150 and 250 seconds in the transient. To better understand this behavior, Figure 4.2.1-2 is presented which is a multiplot of the mixture level and the vapor flow through flow link 17 (connecting the downstream side of the loop seal to the reactor coolant pump, See Figure 1-1 of Section 1.0) for the case without the enhanced model features. A similar plot is presented for the case with the enhanced model features (Figure 4.2.1-3). These plots focus on the time frame (170 to 200 seconds) when the core mixture level oscillations occur. Comparing the two figures it can be seen that the core mixture level oscillations observed for the case without the enhanced model features is directly related to the oscillatory vapor flow through flow link 17. Figure 4.2.1-3 shows that these flow oscillations have been eliminated with the implementation of the enhanced model features. From Figure 4.2.1-4, it can be seen that the erratic behavior of the vapor flow through link 17 occurs at the same time that mixture level hangs occur at the boundary between node 17 and node 18. This implies a manometric effect between the pump stack and the core, resulting in the core mixture level oscillations (Figure 4.2.1-2) at the same time. Figure 4.2.1-5 shows that the implementation of the enhanced model features results in a smoother vapor flow through flow link 17. This is directly related to the elimination of the mixture level hangs in the pump stack (resulting in a smoother core mixture level during refill as seen in Figure 4.2.1-3).

Figure 4.2.1-6 compares the broken loop steam generator upside mixture level for the cases with and without the enhanced model features. This figure shows oscillatory behavior in the mixture levels for both cases with and without the enhanced model features after 250 seconds in the transient. Figures 4.2.1-7 and 4.2.1-8 focus on the vapor flow through flow link 12 between 270 and 280 seconds in the transient. These figures show that the activation of the enhanced model features results in a smoother vapor flow through link 12 (from the bottom of the steam generator upside tubes to the top of the uphill tubes).

In addition, it was observed that the use of the enhanced model features resulted in reduced core vapor region temperature (plots not presented), which results in a lower calculated peak clad temperature (PCT).

In summary, the effects of implementing the enhanced model features for the sample plant 6 inch cold leg break simulation, are primarily seen in the mixture level and vapor flow behavior within the pump stack region. The resulting smoother core mixture level and the reduced core vapor region temperature will result in reduced peak clad

temperature as calculated by the small break LOCTA code.

4.2.1.3.2 3-inch Cold Leg Break, AFW=0 gpm

Figure 4.2.1-9 compares the core mixture level plots for the cases with and without the enhanced model features. No major differences are seen in these plots. However, a closer look at the plot between 540 and 560 seconds (Figure 4.2.1-10) shows that the calculated mixture region void fraction in the upper plenum (node 7) increases until the mixture level drops into the core region (20.437 ft.) for the case without the enhanced model features. The case with the enhanced model features results in a more realistic mixture region void fraction calculated in the upper plenum, since it stays at a near constant rate until the mixture level drops into the core region. This is directly related to the implementation of the implicit bubble rise model.

Figures 4.2.1-11 and 4.2.1-12 compare the mixture levels in the broken loop steam generator upside tubes and the pump stack, respectively, for the two cases. The steam generator mixture level behavior is similar to that seen for the 6 inch break. The pump mixture level shows virtually no effect due to the implementation of the enhanced model features in this region.

In summary, the effects of implementing the enhanced model features for the sample plant 3 inch cold leg break simulation, are minimal. However, the results do illustrate the effect of the implicit bubble rise model in the core when the mixture level drains from the upper plenum to the top of the core.

4.2.1.4 Conclusion

The effect of the combined activation of the enhanced model features has been studied using a sample plant Small Break LOCA Simulation. The 6 inch and 3 inch cold leg breaks were simulated for this study.

The results of the 6 inch cold leg break simulation clearly show the effects of implementing the enhanced model features in the pump stack region. In particular the elimination of the mixture level hangs in the pump stack results in smoother core mixture level (during core refill) and a smoother vapor flow rate through the pump. It was also observed that the use of the enhanced model features results in reduced core vapor temperature, which would result in a lower calculated PCT for the 6 inch case.

The results of the 3 inch cold leg break show minimal effect due to the implementation of the enhanced model features. One notable effect, due to the implicit bubble rise model, is seen for this case in the upper plenum mixture region void fraction calculation (during core drain). The implicit model eliminates the unrealistic increase in the upper plenum void fraction prior to the mixture level entering the core region.

WESTINGHOUSE ELECTRIC COMPANY LLC

In conclusion the combined effects of the enhanced model features on the small break LOCA Evaluation Model using NOTRUMP Version 38.0 have been illustrated by this study, and the results are consistent with the single effects validation efforts performed and discussed previously. These enhanced features will become the default EM features starting with NOTRUMP Version 38.0.

6-INCH Cold Leg Break NOTRUMP V38.0 SIMULATION

— Core Mixture Level (Previous EM)
 - - - Core Mixture Level (Enhanced EM)
 - - - Top of Node 5
 — Top of Node 6

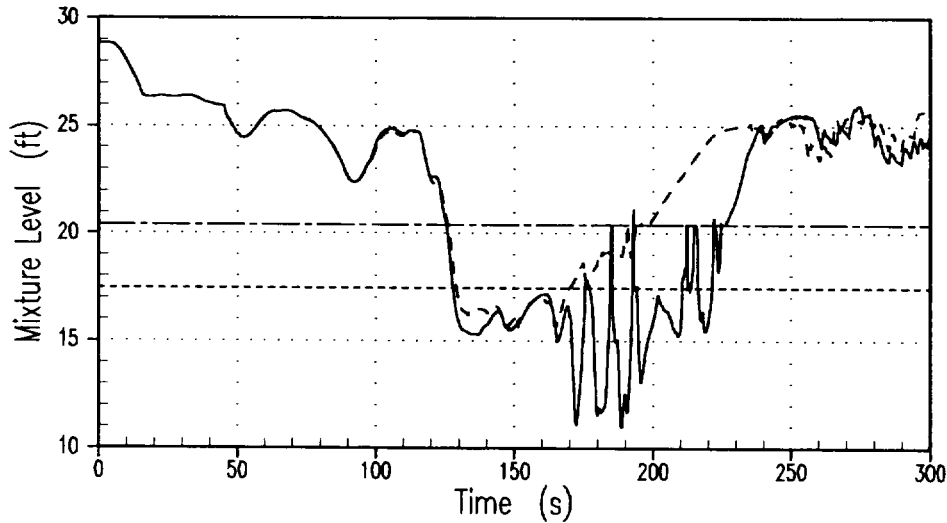


Figure 4.2.1-1

6-INCH Cold Leg Break NOTRUMP V38.0 SIMULATION

Mixture Level (ft)
 — Core Mixture Level (Previous EM)
 — Top of Node 5
 Mass Flow Rate (lbm/s)
 - - - Flow Link 17 Vapor Flow (Previous EM)

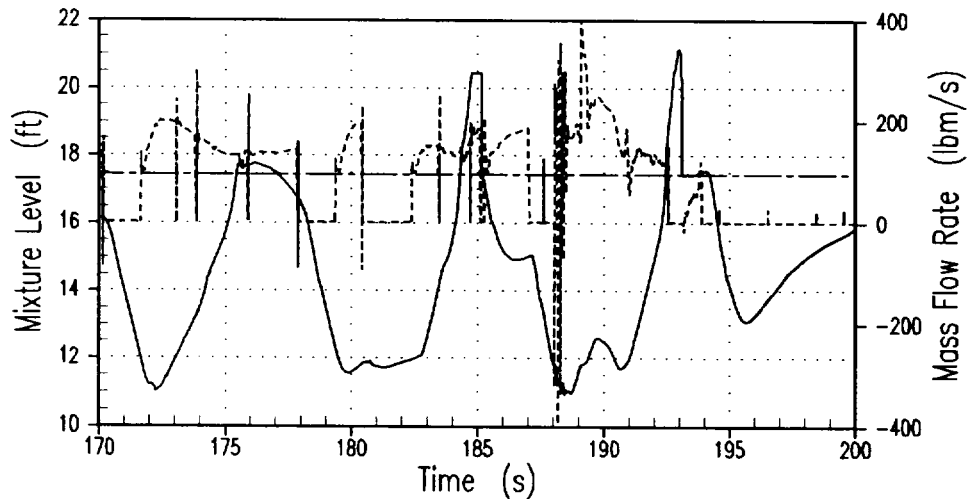


Figure 4.2.1-2

6-INCH Cold Leg Break NOTRUMP V38.0 SIMULATION

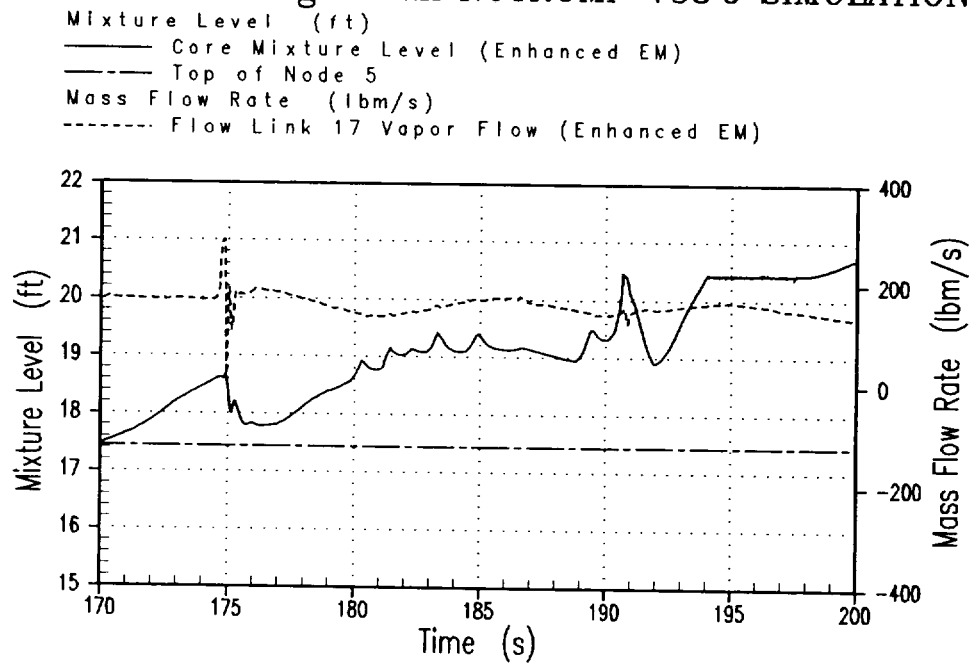


Figure 4.2.1-3

6-INCH Cold Leg Break NOTRUMP V38.0 SIMULATION

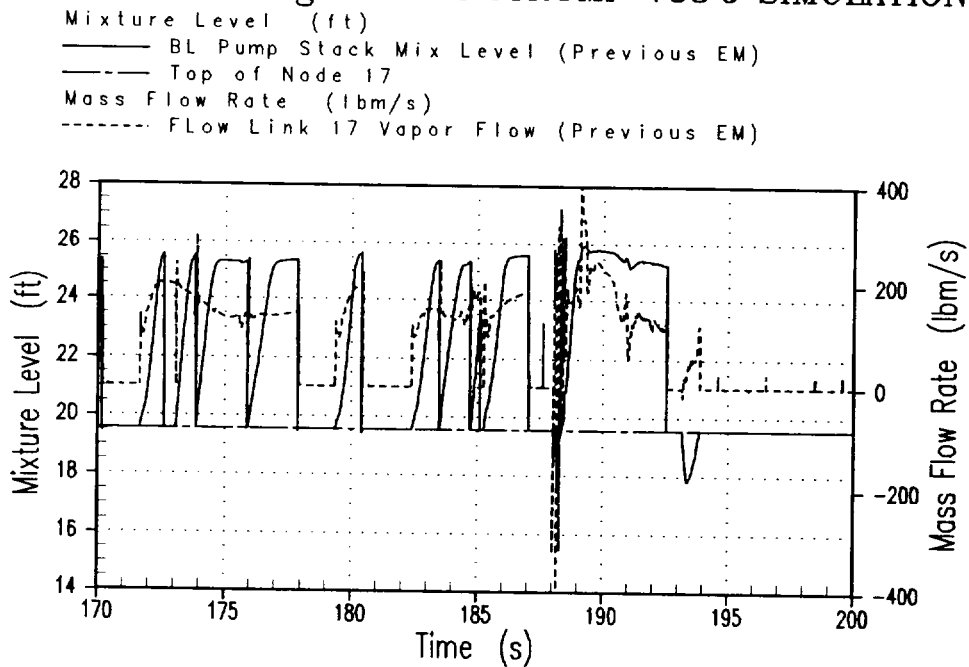


Figure 4.2.1-4

6-INCH Cold Leg Break NOTRUMP V38.0 SIMULATION

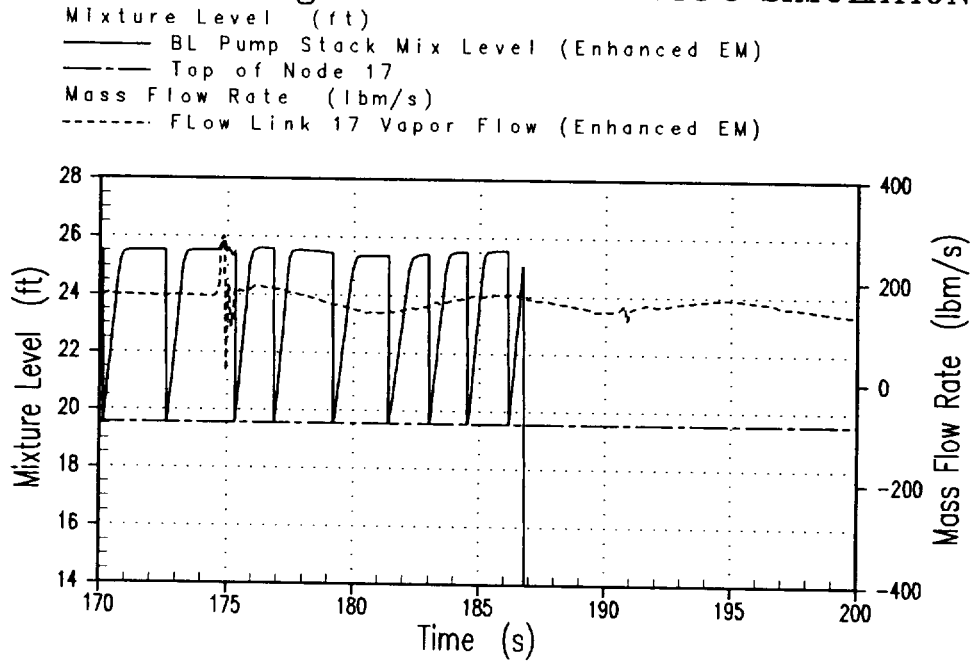


Figure 4.2.1-5

6-INCH Cold Leg Break NOTRUMP V38.0 SIMULATION

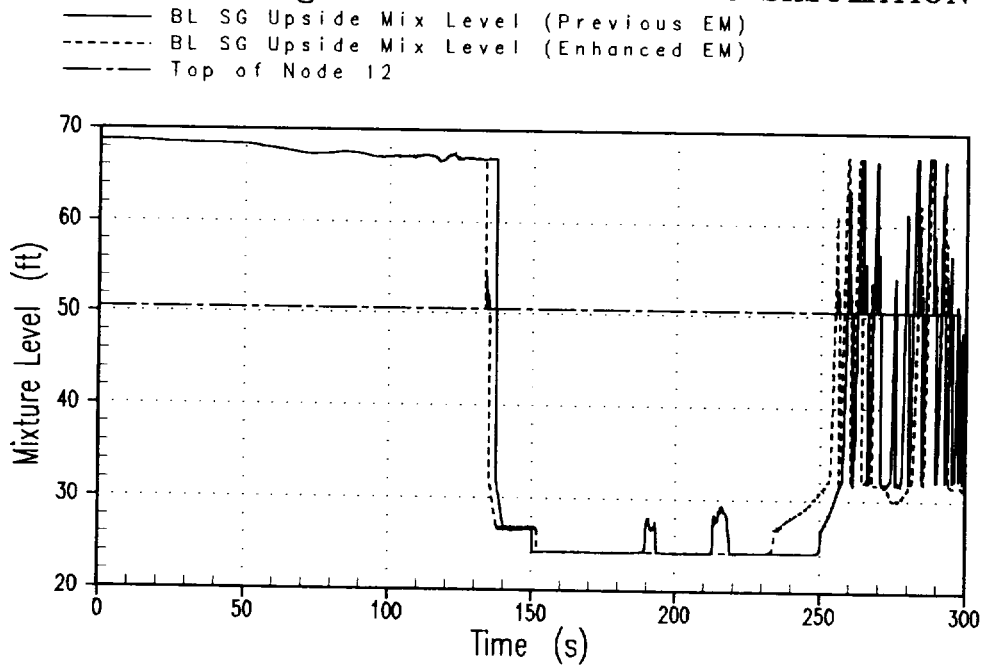


Figure 4.2.1-6

6-INCH Cold Leg Break NOTRUMP V38.0 SIMULATION

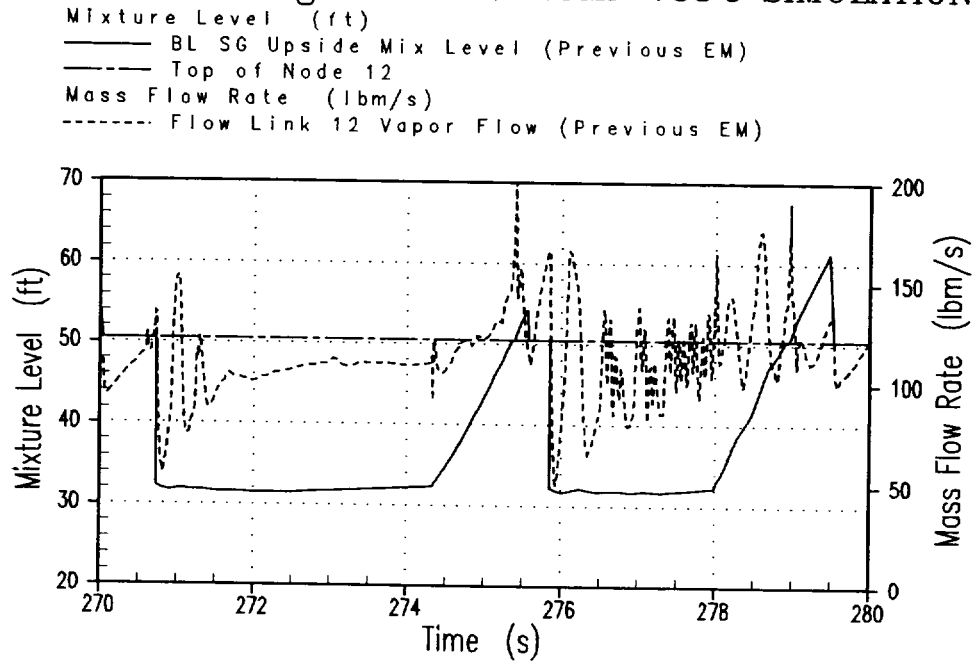


Figure 4.2.1-7

6-INCH Cold Leg Break NOTRUMP V38.0 SIMULATION

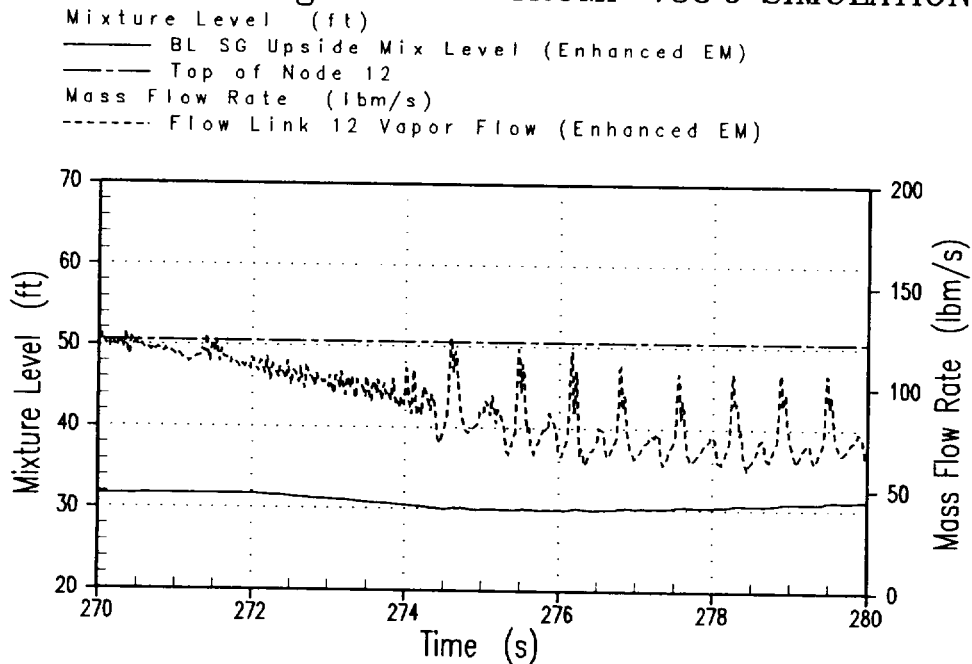


Figure 4.2.1-8

3-INCH Cold Leg Break NOTRUMP V38.0 SIMULATION

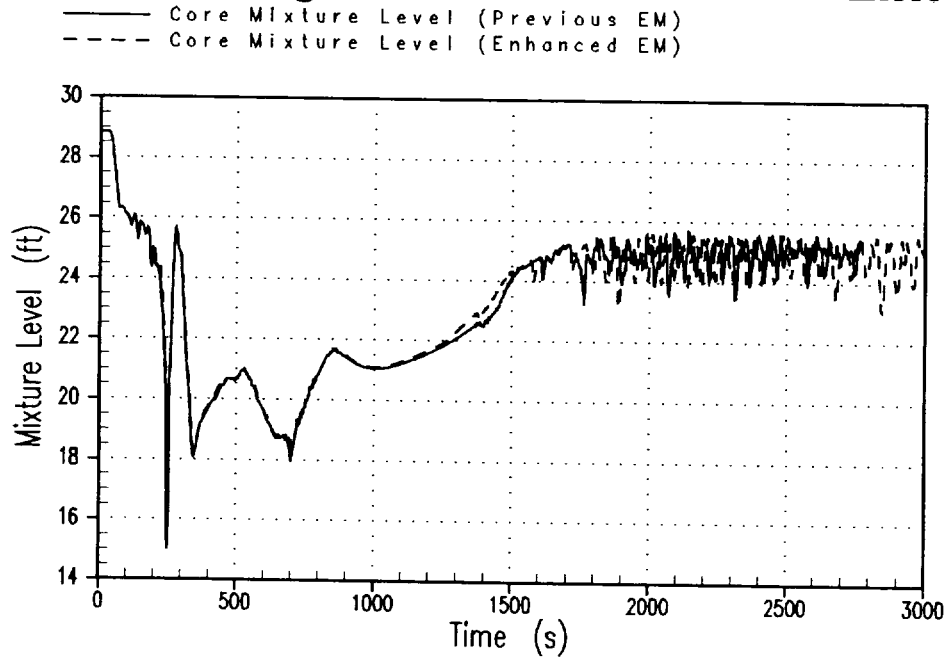


Figure 4.2.1-9

3-INCH Cold Leg Break NOTRUMP V38.0 SIMULATION

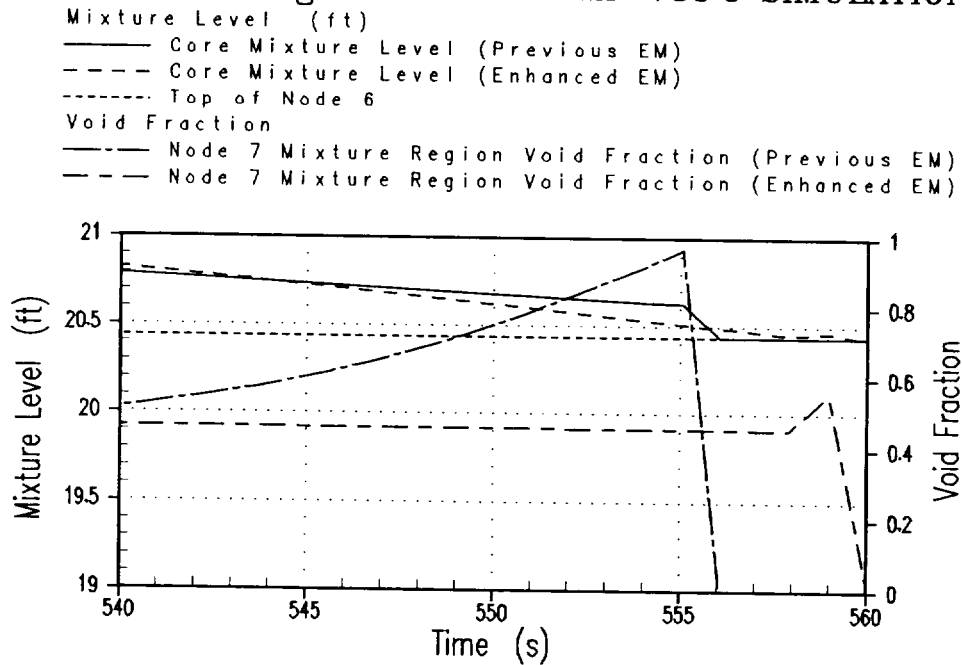


Figure 4.2.1-10

3-INCH Cold Leg Break NOTRUMP V38.0 SIMULATION

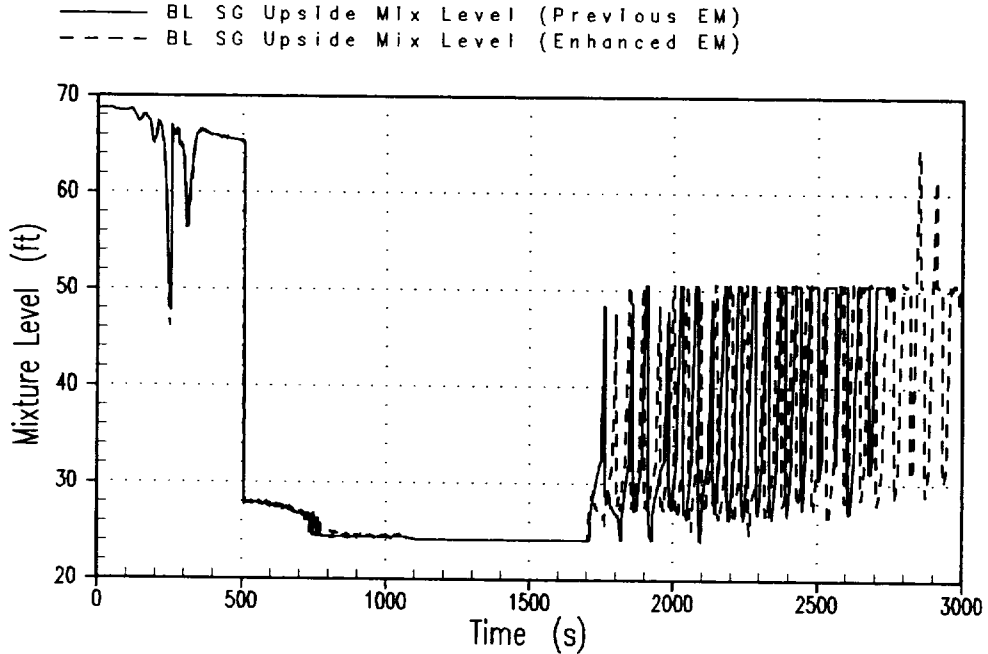


Figure 4.2.1-11

3-INCH Cold Leg Break NOTRUMP V38.0 SIMULATION

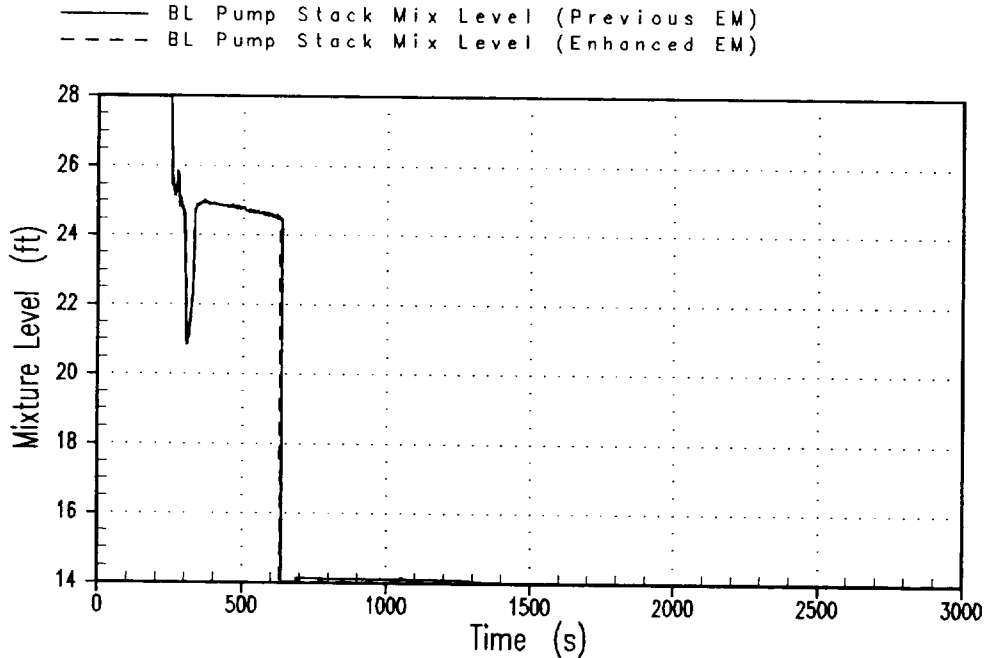


Figure 4.2.1-12

4.3 References

1. Meyer, P. E., "NOTRUMP: A Nodal Transient Small Break And General Network Code," WCAP-10079-P-A (Proprietary) WCAP-10080-A (Non-Proprietary), August 1985.